DEVELOPMENT OF 3D MULTI-PHYSICS SIMULATION TOOL FOR COUPLED NEUTRONICS - THERMAL-HYDRAULICS STUDIES OF SAFETY TRANSIENTS IN HIGH TEMPERATURE REACTORS

By

DEVENDRA KUMAR DWIVEDI

Enrolment No: PHYS01201404013

Bhabha Atomic Research Centre, Mumbai-400085

A thesis submitted to the

Board of Studies in Physical Sciences

In partial fulfillment of requirements

for the Degree of

DOCTOR OF PHILOSOPHY

of

HOMI BHABHA NATIONAL INSTITUTE

January, 2021

Homi Bhabha National Institute[1]

Recommendations of the Viva Voce Committee

As members of the Viva Voce Committee, we certify that we have read the dissertation prepared by **Devendra Kumar Dwivedi** entitled **"Development of 3D multi-physics simulation tool for coupled neutronics - thermal hydraulics studies of safety transients in High Temperature Reactors"** and recommend that it may be accepted as fulfilling the thesis requirement for the award of Degree of Doctor of Philosophy.

Chairman -**Prof. Umasankari Kannan**		**Date:** 21/09/2021
Guide / Convener - **Prof. Anurag Gupta**		**Date:** 21/09/2021
Examiner - **Prof. Suneet Singh**	Suneet Singh	**Date:** 21/09/2021
Member 1- **Prof. K. Devan**		**Date:** 21/09/2021
Member 2- **Prof. A.K. Nayak**		**Date:** 21/09/2021
Member 3- **Prof. K.P. Singh**		**Date:** 21/09/2021

Final approval and acceptance of this thesis is contingent upon the candidate's submission of the final copies of the thesis to HBNI.

I/We hereby certify that I/we have read this thesis prepared under my/our direction and recommend that it may be accepted as fulfilling the thesis requirement.

Date: 21/9/2021

Place: MUMBAI

Prof. Anurag Gupta

Guide

[1] This page is to be included only for final submission after successful completion of viva voce.

STATEMENT BY AUTHOR

This dissertation has been submitted in partial fulfillment of requirements for an advanced degree at Homi Bhabha National Institute (HBNI) and is deposited in the Library to be made available to borrowers under rules of the HBNI.

Brief quotations from this dissertation are allowable without special permission, provided that accurate acknowledgement of source is made. Requests for permission for extended quotation from or reproduction of this manuscript in whole or in part may be granted by the Competent Authority of HBNI when in his or her judgment the proposed use of the material is in the interests of scholarship. In all other instances, however, permission must be obtained from the author.

Devendra Kumar Dwivedi

DECLARATION

I, hereby declare that the investigation presented in the thesis has been carried out by me. The work is original and has not been submitted earlier as a whole or in part for a degree / diploma at this or any other Institution / University.

Dwivedi

Devendra Kumar Dwivedi

List of publications arising out of the research work

Journals

1. "Analysis of unprotected loss of heat sink accident in compact high temperature reactor cooled under natural circulation of LBE coolant", **D.K. Dwivedi**, Anurag Gupta and Umasankari K., *Nuclear Engineering and Design*, **2020**, *370*, 110881.

2. "3D space-time analysis of ATWS in compact high temperature reactor with integrated thermal-hydraulic model in code ARCH-TH", **D.K. Dwivedi**, Anurag Gupta and Umasankari Kannan, *Annals of Nuclear Energy*, **2017**, *110*, pp. 306-316.

3. "Development of adiabatic Doppler feedback model in 3D space time analysis code ARCH", **D.K. Dwivedi** and Anurag Gupta, *Life Cycle Reliability and Safety Engineering*, **2015**, *4(4)*, pp. 22-28.

Chapter in book

1. "3D space time analysis of anticipated transient analyses in CHTR with Fuel Temperature feedback", **D.K. Dwivedi**, A. Gupta, P.D. Krishnani, *In: Nayak A., Sehgal B. (eds) Thorium—Energy for the Future. Springer, Singapore, **2019*** https://doi.org/10.1007/978-981-13-2658-5_31

Conferences

1. **D.K. Dwivedi**, Anurag Gupta, Umasankari K., "Transient simulation of LBE cooled CHTR under natural circulation with 3D multi-physics code ARCH", *IUSSTF, Nuclear Safety Symposium, at IITB, Mumbai, December 15-19,* **2018**. https://newprairiepress.org/asemot/2018/fullprogram/20/

2. **D.K. Dwivedi**, Anurag Gupta, Umasankari K., "Analysis of coolant blockage in Compact High Temperature Reactor with 3D space-time code ARCH-TH'; *Proceedings of DAE-BRNS National Symposium on 'Advances in Reactor Physics'*, page 275-278, Mumbai, December 06-09, **2017**

3. **D. K. Dwivedi**, A. Gupta, P. D. Krishnani; "Development of coupled Neutronics - Thermal-Hydraulics capability for the reactivity initiated transient analysis in Compact High Temperature Reactor (CHTR)"; *Proceedings of '36th Annual Conference of the Canadian Nuclear Society and 40th Annual CNS/CNA Student Conference',* vol-2, pp-1170-1177, Toronto, ON, Canada, June 19-22, **2016**. ISBN: 978-1-5108-3649-5

4. **D.K. Dwivedi**, Anurag Gupta and P.D. Krishnani, “3D space time analysis of anticipated transient analyses in CHTR with Fuel Temperature feedback”, *International Thorium Energy Conference 2015- ThEC15', Mumbai, India, October 12-15,* **2015**.

5. **D.K. Dwivedi**, Anurag Gupta, P.D. Krishnani, "Significance of moderator temperature feedback in 3D space time safety analysis of Compact High Temperature Reactor (CHTR)", *Proceedings of CANSAS - 2015 (CANDU Safety Association for Sustainability) & NRTHS - 2015 (New Horizons in Nuclear Reactor Thermal-Hydraulics and Safety), Mumbai, Dec. 8 - 11,* **2015**[b].

Dwivedi

Devendra Kumar Dwivedi

Dedicated

To

My Parents

ACKNOWLEDGEMENTS

I wish to express my heartfelt gratitude to **Dr. Anurag Gupta**, Head Reactor Physics Analysis Section, RPDD, Bhabha Atomic Research Centre (BARC), Mumbai, for his enriching guidance, encouragement and constant support throughout this research. I am indebted to him for giving me proper direction and adequate time to pursue this endeavour.

I am truly grateful to **Dr. Umasankari Kannan**, Head RPDD, for her motivational encouragement and enlightening discussions during my research work.

I wish to express my special thanks to the members of my Doctoral Committee, **Dr. K. Devan** (RND, IGCAR), **Dr. A.K. Nayak** (RED, BARC) and **Dr. K.P. Singh** (RPDD, BARC) for their precious advice and support during this research work.

I am sincerely thankful to **Dr. A. Borgohain** (RED, BARC) for enriching discussions and providing generous help during the present research work.

I am thankful to **Dr. P.D. Krishnani** (Ex. RPDD, BARC) for his guidance and encouragement during initial periods of the present research work.

I am thankful to **Dr. S.B. Degweker** (Ex. MP&RThS, BARC), **Dr. H.P. Gupta** (Ex. ThPD, BARC) and **Dr. Amar Sinha** (Ex. BARC) for their pieces of advice and guidance.

I gratefully acknowledge **Dr. Francesco D'Auria**, University of Pisa, Italy, for his critical suggestions to the safety analysis of CHTR reported in the present thesis.

I would like to thank **Dr. P.K. Vijayan** (Ex. BARC), **Dr. N.K. Maheshwari** (HWRD, BARC) and **Shri I.V. Dulera** (HTRS, BARC) for fruitful discussions.

I am thankful to all my colleagues at RPDD, BARC for their encouragement and support during this research wok.

I am grateful to Director RD&DG, BARC, for his encouragement and support.

I wish to express my gratefulness to the authorities of BARC, Mumbai, for providing a very conducive atmosphere for carrying this research.

I express my special gratitude to my family members and relatives whose blessings and love made me up to this level. Above all, I am thankful to my adorable wife **Rashmi** and my cheerful daughter **Ishi** for their profound love and care for me. Their prayers for me was what sustained me during this challenging time.

Thank you everyone.

CONTENTS

SYNOPSIS

In the present era of Generation-IV reactor design, the High-Temperature Reactor (HTR) is one of the promising concepts to meet a variety of goals including improved safety, sustainability, efficiency and cost of nuclear energy (Pioro and Duffey, 2018). A comprehensive high-temperature reactor programme has been initiated in India to fulfil the country need for process heat applications utilising thorium fuel cycle (Dwivedi, 2010; Sinha et al., 2016). As the future need of the environmentally benign fuel, hydrogen production through the thermo-chemical splitting of water is the primary aim of the programme. The efficient Iodine-Sulphur cycle for the thermo-chemical process requires heat at more than 850^{o}C for hydrogen production. Therefore, a challenging goal for the high temperature reactors technology development in India is to achieve coolant temperature of 1000^{o}C (Sinha et al., 2016). As a key first step, a prototype Compact High Temperature Reactor (CHTR) is being developed as a technology demonstrator and critical facility for Indian HTRs (Dwivedi et al., 2010).

Nuclear fission reactors are archetypal multi-scale, multi-physics systems necessitating high-fidelity tools to study the science of nuclear fission power. In case of HTRs, as very limited experiments could be performed, the numerical simulation capability to realistically model the core for neutronics physics studies is the state-of-the-art. The high-temperature reactor cores consist of ceramic-based moderator & reflector materials, single-phase coolant and multi-layered coated fuel particles. In the HTRs, the nuclear fissions in the tiny kernels of the TRISO fuel particles are the primary heat source. The design of high temperature cores that rely on natural circulation (NC) for passive safety features is also challenging. In these cases, the temperature distribution and the mass flow rate are tightly-coupled. The multi-physics modelling and simulation tools are required for improved understanding and more realistic predictions of coupled neutronics - thermal-hydraulics (N-TH) phenomena in such advance reactors. The present research aims to develop 3D multi-physics capability for simulations of coupled neutronics - thermal-hydraulics during safety transients in HTRs. In the present thesis, CHTR is considered as a representative core for the investigations of safety transients in the high-temperature reactor.

The 100 kWth CHTR core consists of Th-^{233}U based TRi-structural ISOtropic (TRISO) coated fuel, beryllium oxide (BeO) moderator and lead-bismuth eutectic (LBE) as coolant. The reactor core is being designed with 19 prismatic fuel assemblies to attain the outlet temperature of 1000^{o}C for 15 effective full power years without refuelling and reshuffling (Dwivedi et al., 2010). The proliferation-resistant thorium-based TRISO fuel particles have leak-tightness limit of about 1600^{o}C to ensure safe operation at high temperature with deep burn-up. The BeO is used as the moderator and reflector for a high-temperature core with compact size. The neutron transparent LBE is a better choice of liquid metal coolant as it is inert to water and suitable for natural circulation. Also, the high boiling point (1670°C) of the LBE ensures that the core can be operated at a wider range of temperatures without the risk of the coolant boiling even at the atmospheric pressure. The design incorporates several passive safety features such as the negative reactivity coefficients of the fuel and moderator temperatures, core heat removal by natural circulation of LBE, passive rejection of decay heat under accidental conditions to the atmosphere using a set of heat pipes etc..

Design of a high-temperature core with desired long refuelling intervals imposes several challenges such as reactivity management, control and safety during operation and materials compatibility. For material related studies and natural circulation experiments, a high-temperature LBE based Kilo Temperature Loop (KTL) has been installed and is being operated at BARC (Borgohain et al., 2016). For the Indian HTR programme, the development of high-temperature materials such as TRISO fuel, reactor-grade graphite and BeO blocks, reactor vessel and tantalum-tungsten based alloy is also in progress (Mollick et al., 2015;

Mirji et al., 2016; Sinha et al., 2010 and Majumdar et al., 2020). In the era of Generation-IV reactor design with intrinsic safety features (Sinha et al., 2016), extensive safety analyses of the new concept like CHTR is an essential aspect of R&D studies. During operational or accidental transients in the prototype high-temperature core, any misbalances between heat generation by fission and heat removal under the natural circulation of coolant could consequently lead to a further rise in temperatures of the core materials. In these scenarios, negative reactivity coefficients of thermal-hydraulics (TH) feedbacks could arrest the increase in the power/ temperatures and could be vital to ensure the safety of the core. Thus the TH feedbacks can play a crucial role as the passive safety feature of the designed core and need to be investigated thoroughly. Hence, an effort has been led to develop an in-house 3D space-time neutronics capability with integrated thermal-hydraulics for feedbacks. The aim of the TH development was focussed on the core design evaluations rather than detailed analyses of system thermal-hydraulics. In this thesis, the indigenous development and validation of 3D multi-physics code ARCH-TH (code for Analysis of Reactor transients in Cartesian and Hexagonal geometries with Thermal- Hydraulics feedbacks), and its application to investigate the safety transients such as postulated loss of regulation accident (LORA), anticipated transient without scram (ATWS), loss of flow accident (LOFA) and unprotected loss of heat sink accident (ULOHSA) in the core are discussed. The developed code can simulate the integrated core N-TH phenomena during operation and anticipated transients in high-temperature reactors (Dwivedi et al., 2013; 2017; Gupta and Kannan, 2017; Dwivedi et al., 2018).

The in-house code ARCH (Gupta, 2017) has been used for 3D space-time neutronics analyses of CHTR. For lattice physics analyses of each type of fuel and reflector cells, an integral neutron transport theory based in-house code ITRAN (Krishnani, 1982) is used to compute the homogenised, condensed few group cross-sections and delayed neutron parameters of the core. Using these lattice homogenised parameters, a detailed 3D space-time analyses with TH feedbacks are done with ARCH code. For the efficient analyses of the reactor transients, a flux factorisation scheme based Improved Quasi-Static (IQS) module has also been developed in the code ARCH (Ott and Minely, 1969; Dwivedi et al., 2013). The predictions of the code with the IQS module has been qualified for the reactor transient without feedback, e.g. AER-Dyn001 (Dwivedi et al., 2017). The code is also benchmarked for the transient with fuel temperature feedback using the model for adiabatic heating of the fuel (Dwivedi et al., 2015 and 2017).

The code ARCH is integrated with thermal-hydraulics (TH) modules for multi-physics simulation of the core transients as ARCH-TH (Dwivedi et al., 2015, 2017 and 2018). The developed TH modules in the code are mainly based on the following three types of heating model of the core:

(i) Adiabatic heating of the fuel during the transients

(ii) 1D-radial heat conduction with given inlet mass flow rate in the multi-channel

(iii) TH model for natural circulation in the coupled multi-channel of close loop system

In the first case of adiabatic heating of fuel, the model is capable of computing the changes in temperature of all the fuel meshes in the core for reactivity feedback during transients but requires initial fuel temperature profile as input (Grundmann and Rossendorf, 2000). The model is simple and requires only thermo-physical parameters of the fuel. It provides a better insight into fuel temperature variation over the point kinetics analysis with lumped TH model but predicts more conservative results during slow transients. It has been observed that the model is mostly applicable in case of large reactivity transients of short duration, i.e. unprotected LORA during the approach to criticality. The adiabatic fuel heating based TH module in the code is validated with AER-Dyn002 benchmark problem and predictions are found to be in good agreement with the reference results (Dwivedi et al., 2015 and 2017). The postulated case of inadvertent withdrawal of control rod in CHTR during the first approach to criticality has been studied using the adiabatic heating model (Dwivedi et al., 2015). The finding indicates that the peak temperature of the fuel stays within the safety limit even in case of a conservative approach where only the fuel temperature feedback is considered.

In the second model, the 1D-radial heat conduction (Jain, 1989) based TH module has been developed and incorporated in code ARCH-TH. The module computes the radial as well as axial temperature profiles in the channels during steady-state as well as the transients with given inlet mass flow rate of the coolant. The TH module has also the capability to be coupled with point kinetics. The predictions of the module have been validated with benchmarks based on beam trip transients in MOX fuelled, and LBE cooled ADS designs (D'Angelo and Gabrielli, 2003 and 2004). The predictions are compared and found to be in good agreement with the benchmark results (Dwivedi et al., 2017 and 2020). As the TH module requires inlet mass flow rate for the transient simulation, the core average mass flow rate is estimated under the steady-state operation of CHTR at full power (Dwivedi et al., 2018). The ATWS has been investigated to assess the safety of CHTR at full power with the given flow rates in the channels. The transient has been simulated with only fuel temperature feedback (Dwivedi et al., 2015 and 2019), including the moderator temperature feedback (Dwivedi et al., 2015[b]) and also in the case of combined feedbacks from fuel, moderator and coolant temperatures in the core (Dwivedi et 2016). As CHTR being a low power reactor, it has also been observed that the effect of these feedbacks is almost insignificant in case of protected overpower transient, i.e. scram actuated at 110% of the core power level with small time delay. Therefore, the postulated transients without scram in CHTR are the major concerns for the design and safety assessment. The research led to an outcome that the thermally coupled BeO moderator in the high-temperature core can play a very crucial role to limit the rise in power and temperatures during ATWS (Dwivedi et al., 2015[b] and 2017). Whereas, the temperature feedback from the LBE coolant does not show considerable effect (Dwivedi et al., 2016). In these studies, the mass flow rates in the channels under natural circulation condition are expected to increase but considered to be unchanged during the transients conservatively. However, the peak temperature of the fuel and coolant are found to be varying much below the safety limits of leak-tightness of TRISO particles (1600^{o}C) and the boiling point of the LBE (1670^{o}C) (Dwivedi et al., 2017).

The passive core heat removal in CHTR is based on the natural circulation of the LBE coolant in vertical multi-channel between the two plenums. Therefore, the TH capability for natural circulation in the coupled multi-channel of close loop system has also been developed in the code ARCH-TH. In this model, the TH module solves the mass, energy and momentum conservation equations in all the coupled multi-channel for natural circulation of single-phase coolant (Todreas and Kazimi, 2012). The case of ATWS has been re-assessed under the natural circulation of the coolant in the coupled multi-channel of CHTR (Dwivedi et al., 2018). The research shows that the mass flow rates in the channels increase during the ATWS as the driving force of natural circulation enhances due to more heating in the channels. Thus the core outlet power increases, and the reactor is observed to be stabilising at a higher power level and temperature profile in the core. However, the rise in peak fuel and coolant temperatures are found to be lesser as compared to the earlier investigation with invariable mass flow rate during the transient (Dwivedi et al., 2018). The capability to simulate natural circulation with the TH model in ARCH-TH has also been successfully validated and compared with experimental results obtained from the thermal-hydraulics study in KTL (Borgohain et al., 2016; Dwivedi et al., 2020). However, The present capability of the TH module is limited to solve the energy conservation at the primary side only, hence, the outlet temperature of the PHX is considered as a given boundary condition in the simulation of NC in KTL.

In the envisaged design of CHTR, a set of sodium heat pipes placed in the downcomers at the upper plenum, passively transfer core heat to the secondary side (Panda et al., 2017 and Dulera et al., 2017). Durability, reliability and robust functioning of these heat pipes are essential for the safe and efficient operation of the reactor (Mylavarapu et al., 2012). The failure of these pipes disrupts the core heat transfer to the secondary side and result in the loss of heat sink accident. Therefore, the scenario of unprotected loss of heat sink accident (ULOHSA) in CHTR at full power during the initial core life cycle has been investigated with the newly developed and benchmarked code ARCH-TH. The study shows that the core is being shutdown passively due to negative reactivity feedbacks. Since the loss of heat sink drastically reduces the natural circulation of LBE, the phenomena of flow reversal in low powered channels during transient are also predicted. The study indicates that the low powered channels could also act as downcomers during such transients. This phenomenon has been the first observed in LBE cooled high-temperature core design and reported in the literature (Dwivedi et al., 2020). Even though the peak temperatures of the fuel and the coolant are varying much below the safety limits; the design modifications in the core have also been investigated and suggested based on the analysis to suppress the predicted flow reversals during such transients. The research shows that phenomena of flow reversals in couple multi-channel core can arise during ULOHSA due to asymmetric heating and hydraulic conditions in the channels. The modelling of several complex TH phenomena in HTRs has been carried out and successfully incorporated for the first time in an indigenous 3D neutron kinetics code.

The thesis is organized in following chapters as briefly described below.

Chapter 1 briefly introduces the design of conventional nuclear reactors in operation, fast spectrum PFBR, advanced reactor design AHWR, Generation-IV reactor concepts and more particularly a discussion on the general design features of HTRs available in the literature. A brief discussion on the advantages and challenges of HTR concepts over the conventional power reactors followed by a short overview of carbon-free methods for hydrogen production are also presented. A brief on the Indian high-temperature reactor programme followed by a core description of CHTR relevant to this thesis is presented.

Chapter 2 discusses the methodology used in the neutronics calculation of the reactor transients, particularly the diffusion theory based 3D space-time neutron kinetics. The direct and indirect methods to solve the time-dependent 3D multi-group neutron diffusion equations with multi-group delayed neutron precursors, especially the flux factorization based IQS method are presented in this chapter of the thesis. The 3D space-time code ARCH with IQS module and in-house lattice analysis code ITRAN are also briefly described here.

Chapter 3 describes the new developments and the TH models integrated with code ARCH and the advanced version has been called ARCH-TH. The theory and the implementation of mass, energy and momentum conservation equations for natural circulation in the close loop system of coupled multi-channel are discussed. The considerations of temperature-dependent thermo-physical properties of the core materials, i.e. LBE coolant, BeO moderator/ reflector, fuel compacts embedded with TRISO particles are also described in the chapter. The algorithm of integrated neutronics thermal-hydraulics in code ARCH-TH followed by a short overview of other well known coupled neutronics- thermal-hydraulics (N-TH) codes reported in the literature are also discussed.

Chapter 4 presents the validation of the neutronics and thermal-hydraulics models developed for 3D multi-physics capability in code ARCH-TH. The reactor kinetics benchmark problems considered for neutronics validations of the code and the predicted results are discussed. The developed 1D-radial heat conduction based TH module has been validated with beam trip transients in ADS designs cooled with LBE. The predictions of the TH module are presented and compared with the reference results. The TH capability of simulating natural circulation in the code is also validated with the data obtained from the experiments carried out in kilo temperature loop (KTL) and discussed in this chapter.

Chapter 5 discusses the analyses carried out for the reactivity initiated transients, i.e. LORA during an approach to criticality, protected LORA and ATWS in CHTR at full power configuration. These studies have been performed using different TH models in ARCH-TH and results are presented and described. The outcome of the studies indicates that the temperature feedback from thermally coupled BeO moderator in CHTR is vital and contributes significant passive safety during such transients. The analysis of the postulated LOFA in the core is also presented in brief.

In chapter 6, a new investigation of the unprotected loss of heat sink accident (ULOHSA) in CHTR core cooled under natural circulation is discussed. The study shows that the transient led to the interruption in natural circulation in the core and flow reversal in the low powered channels of CHTR. Even though the fuel and coolant temperatures stay within the safety limits during the transient; some core design modifications are also investigated and suggested to suppress the condition of flow reversal and improve the safety features. These results are discussed in detail.

Chapter 7 briefly summarizes all the present research studies performed in the thesis. This chapter also presents the main conclusions drawn and scope for future development in code ARCH-TH and the safety investigations of CHTR.

The new work and findings in the present thesis can be summarized as follows:

1. The development of a high fidelity simulation capability to study the physics of nuclear fission power in high temperature reactors.
2. The thermally coupled BeO moderator, if used in the high temperature reactor, can provide vital temperature feedback during unprotected transients in the core.

3. The possibility of flow reversal in the natural circulation (NC) cooled high-temperature core is investigated for the first time and predicted using an indigenously developed multi-physics simulation tool.
4. The scope of design modifications in NC cooled high temperature core to suppress the condition of flow reversal are evaluated for the first time. The research asserts that the flow reversal during the ULOHSA occurs due to asymmetrical thermal-hydraulic conditions in the coupled multi-channel system.
5. The multi-physics analyses of transients in the new high-temperature concept are carried out to predict and prove the passive safety feature of the designed core.
6. The thesis includes the new development of 3D multi-physics code ARCH-TH for transient simulations of NC cooled high-temperature reactors. The code is validated with benchmarks to demonstrate its validity and use for safety analyses of any such future HTR designs.

Future Work:

It is planned to enhance the heat transfer model of the developed TH module to simulate even more complex heating in the high-temperature core of prismatic HTRs. The TH capability in code ARCH-TH is also intended to extend for pebble bed HTRs as well as water and molten salt cooled Indian concepts of the advance reactors.

References:

Borgohain et al., (2016). Natural circulation studies in a LBE loop for a wide range of temperature. Nuclear Engineering and Design, vol. 300, pp. 358–375.

D'Angelo, A. and Gabrielli, F., (2003). Benchmark on Beam Interruptions in an Accelerator-driven System – Final Report on Phase I Calculations, OECD Nuclear Energy Agency, NEA/NSC/DOC(2003)17, ISBN 92-64-02138-8.

D'Angelo, A. and Gabrielli, F., (2004). Benchmark on Beam Interruptions in an Accelerator-driven System – Final Report on Phase II Calculations, OECD Nuclear Energy Agency, NEA/NSC/DOC(2004)7, ISBN 92-64-02072-1.

Dulera, I.V., Sinha, R.K., Rama Rao, A., Patel, R.J., (2017). High temperature reactor technology development in India. Progress in Nuclear Energy, 101, pp.82-99.

Dwivedi, D.K., Gupta, A., Krishnani, P.D., (2010). Challenges in core reactivity management and control optimization in physics design of Compact High Temperature Reactor. BARC Newsletter 317, 22–28.

Dwivedi, D.K., Gupta, A., Srivastava, A.K., Krishnani, P.D., (2013). Incorporation of Improved Quasi Static (IQS) scheme module in 3-D space-time analysis code ARCH. Proceedings of ARP-2013, Mumbai, India, October 23–25.

Gupta, Anurag, (2017). ARCH- A 3-D core simulations tool. Proceedings of 3rd DAE-BRNS Symposium on Advances in Reactor Physics, India, Dec 06-09, 2017.

Gupta, A., Kannan, U., (2017). An overview on neutronic simulation schemes for reactor transient and safety analysis. Life Cycle Rel. and Safety Engg. 6, pp. 83–98.

Grundmann, U., Rossendorf, FZ, (2000). AER Benchmark Specification Sheet- Test ID:AER-DYN-002. http://aerbench.kfki.hu/aerbench/Dyn002.pdf.

Jain, V.K., (1989). Point-kinetics model with one-dimensional (radial) heat conduction formalism. Report no. BARC-1452

Krishnani, P.D., (1982). CLUB-A multi group integral transport theory code for analysis of cluster lattices. Annals of Nuclear Energy, vol. 9, pp. 255–260.

Majumdar et al., (2020). Preparation and Characterization of Nb-1Zr-0.1C Alloy Suitable for Liquid Metal Coolant Channels of High Temperature Reactors. ASME J of Nuclear Rad Sci. doi: https://doi.org/10.1115/1.4047919

Mirji et al., (2016). Technological Challenges in Extractive Metallurgy and Refining of Nb, Ta and Preparation of their Compounds & Alloys. Mat. Today: Proc.3, 3151.

Mollick et al., (2015). Deposition of diversely textured buffer pyrolytic carbon layerin TRISO coated particle by controlled manipulation of spouted bed hydrodynamics. Chemical Engineering Science, vol. 128, pp. 44–53.

Mylavarapu et al., (2012). Fabrication and design aspects of high-temperature compact diffusion bonded heat exchangers. Nuc. Engg. and Des., vol.249, pp. 49– 56.

Ott, K.O., Meneley, D.A., (1969). Accuracy of the quasistatic treatment of spatial reactor kinetics. Nuclear Science and Engineering 36, 402–411.

Panda, K.K., Dulera, I.V., Basak, A., (2017). Numerical simulation of high temperature sodium heat pipe for passive heat removal in nuclear reactors. Nuclear Engineering and Design, vol. 323, pp. 376-385.

Pioro, I., Duffey, R., (2018), "Current and future nuclear-power reactors and plants. In: Letcher, T.(Ed.), Chapter 4 in Book: Managing Global Warming, an Interface of Technology and Human Issues. Elsevier–Ac. Press, UK, pp.117–197. 820 pages.

Sinha, R.K., Dulera, I.V., (2010). Carbon based materials – applications in high temperature nuclear reactors. Indian Journal of Engg & Material Sci. 17, pp. 321-326

Sinha et al., (2016). Generation-IV Concepts: India, Handbook of Generation IV Nuclear Reactors. Woodhead Publishing Series in Energy, pp. 413-452.

Todreas, N.E., Kazimi, M.S., (2012). Nuclear Systems, Vol-1: Thermal Hydraulic Fundamental. CRC Press, Taylor & Francis Group.

LIST OF FIGURES

LIST OF TABLES

NOMENCLATURE

A	area of coolant flow (m^2)
A_s	surface area of channel wall and coolant interface (m^2)
C	delayed neutron precursor density
c_p	isobaric specific heat (J/kg/ ^oC)
D	diffusion coefficient for neutron
D_h	equivalent hydraulic diameter (m)
f	friction factor (dimensionless)
g	acceleration due to gravity (m/s^2)
h	heat transfer coefficient ($W/m^2\,^oC$)
k	thermal conductivity (W/m ^oC)
K	local loss coefficient (dimensionless)
p	pressure (N/m^2)
q'''	power density (W/m^3)
r	Position/ radial position (m)
R_e	Reynolds number
t	time (s)
T	temperature (^oC)
T_c	temperature of coolant (^oC)
T_w	channel wall temperature ^oC
u	velocity (m/s)
v	Speed of neutron
V	volume (m^3)
W	coolant mass flow rate (kg/s)
x	length wise distance/ height (m)

Greek letters

β	Delayed neutron fraction
ϵ	wall roughness (m)
ϕ	Neutron flux (number $/m^2/s$)
ρ	coolant density (kg/m^3)
ρ_m	material density (kg/m^3)
Σ	macroscopic interaction cross-section
θ	inclination angle (dimensionless)
Δp	pressure drop (N/m^2)
Δt	time interval (s)
Δx	length difference (m)

Subscripts/ superscripts

d	delayed neutron group
dc	downcomer
g	for g^{th} energy group of neutron
i	i^{th} mesh/ node
j	j^{th} inlet
n	n^{th} channel
t	at time t or time dependence

ACRONYMS

ADS	Accelerator-Driven System
AGR	Advanced Gas-cooled Reactor
AHWR	Advanced Heavy Water Reactor
ARCH	Analysis of Reactor transients in Hexagonal and Cartesian geometry code
ATWS	Anticipated Transient without Scram
BWR	Boiling Water Reactor
CANDU	Canada Deuterium Uranium (reactor)
CHTR	Compact High Temperature Reactor
CP1	Chicago Pile-1
CR	Control Rod
DC	Down-comer
ETC	Effective Thermal Conductivity
FA	Fuel Assembly
FBTR	Fast Breeder Test Reactor
FDM	Finite Difference Method
FHR	Fluoride salt cooled High-temperature Reactor
GFR	Gas-cooled Fast Reactor
GIF	Generation-IV International Forum
HTR	High Temperature Reactor
HTTR	High Temperature engineering Test Reactor
HX	Heat Exchanger
IAEA	International Atomic Energy Agency
IHTR	Innovative High Temperature Reactor

IQS	Improved Quasi-Static
KTL	Kilo Temperature Loop
LBE	Lead Bismuth Eutectic
LEU	Low Enriched Uranium
LFR	Lead-cooled Fast Reactor
LOCA	Loss of Coolant Accident
LOHS	Loss of Heat Sink
LOHSA	Loss of Heat Sink Accident
LWR	Light Water Reactor
MHTGR	Modular High Temperature Gas-cooled Reactor
MSR	Molten Salt Reactor
MTR	Material Test Reactor
MYRRHA	Multi-purpose hYbrid Research Reactor for High-tech Applications
NC	Natural Circulation
N-TH	Neutronics - Thermal Hydraulics
OECD	Organization for Economic Co-operation and Development
OS	Operator Split (coupling scheme)
PBWFR	Pb-Bi cooled direct-contact-Boiling Water Fast Reactor
PFBR	Proto-type Fast Breeder Reactor
PHX	Primary Heat Exchanger
PHWR	Pressurized Heavy Water Reactor
PWR	Pressurized Water Reactor
RBMK	(Reaktor Bolshoy Moshchnosty Kanalny) High-Power Channel Reactor
R&D	Research and Development
SCWR	Supercritical Water-cooled Reactor

SDS	Shut-Down System
SFR	Sodium-cooled Fast Reactor
TH	Thermal Hydraulics
TRISO	TRi-structural ISOtropic
ULOHS	Unprotected Loss of Heat Sink
ULOHSA	Unprotected Loss of Heat Sink Accident
VHTR	Very High Temperature Reactor
VVER	Voda Voda Energo Reactor
WNA	World Nuclear Association
WPPT	Working Party on scientific issues in Partitioning and Transmutation
XADS	eXperimetal Accelerator-Driven System

CHAPTER 1

INTRODUCTION

1.1. Nuclear Reactor and Power

After the discovery of nuclear fission in 1938, the first nuclear reactor, CP1 was designed and demonstrated for the self-sustaining chain reaction in 1942 at the University of Chicago (Fermi, 1946). A nuclear reactor is a device which produces energy and neutrons during induced fission of heavy atomic nuclides such as uranium-235 and plutonium-239 in the self-sustenance and controlled manner. The energy production in the form of heat in the power reactor core is continuously extracted during the operation by the circulation of coolant fluid to generate steam. The nuclear-generated steam can be used for electricity generation, submarine propulsion and also for industrial process heat application, district heating and desalination. Some reactors are utilised for neutron scattering research, radiography, material irradiation, transmutation, isotope production for medical and industrial uses, teaching and training; and these are commonly known as research reactors. As per the IAEA reports, worldwide 443 nuclear power reactors and 224 research reactors are in operation as of the end of 2019 (IAEA, 2020).

Nuclear power plants are the clean and green sources of energy as nuclear fissions do not release greenhouse gases such as carbon-dioxide unlike in combustion of fossil fuels. The complete fission of 1 g of uranium or plutonium fissile atoms produce approximately 1 MW day of thermal energy, which is equivalent to burning of almost 3 tons of coal or about 600 gallons of fuel oil (Glasstone and Sesonske, 1994). The nuclear power plants are operated with much higher capacity factor as compared to renewable sources such as solar and wind (Banerjee and Gupta, 2017); and also their operations are practically unaffected by the condition of weather. The growing world's population, economy, rapid urbanisation and higher living standards of people are the factors, which will result in a surging demand of energy over the coming years (WNA, 2020). The resources of fossil fuels are limited, and also their faster consumptions are resulting in the acute release of greenhouse gases, which is concern for climate change and global warming. Nuclear power accounted for around 10% of electricity production over the world in 2019 (Pioro et al., 2019). The design and operation of nuclear reactors are based on the approach of 'Defence-in-Depth'. In the approach multilayer of physical barriers, redundancy and independence of diverse control & protection systems and emergency response measures are implemented to prevent the radiation hazards and its leakage below the safety limits. The worldwide experiences of reactor operations equivalent to several thousand-years establish a high level of maturity in reactor technology. The nuclear reactor technology is the energy source, which is capable of delivering the enormous quantities of energy in a clean, safe, reliable and sustainable way (Brook et al., 2014).

1.2. Types of nuclear power reactors

In each of the nuclear fission reactions, there are about 2 to 3 neutrons generated with the average kinetic energy of about 1-2 MeV (Glasstone and Sesonske, 1994). These fission neutrons cause further fission of the fissile nuclides in the fuel for the self-sustenance of chain reactions in a reactor core. From the physics viewpoint of nuclear fission, nuclear reactors are of two types: thermal reactors and fast reactors. The classification corresponds to the energy of neutrons or more specifically, their spectrum in the core, which causes the bulk of the fissions (Stacy, 2007). In the thermal reactors, majority of the fissions induced by thermal-energy neutrons ($E \leq 1$ eV), i.e. neutrons which are in thermal equilibrium with the atoms in the system/ core. Whereas, in fast reactors, most of the fissions are by fast-energy neutrons ($E > 1$keV).

Almost all the reactors which have been built and operated, are of the thermal type because these are easier to make critical, i.e. attaining and maintaining of the self-sustenance in fission chain reactions with small amount of fissile material as compare to fast reactors. It is because of the higher chance of fissions with thermal neutrons after absorption in fissile nuclides in the fuel (Stacy, 2007). But thermal reactors require moderator material such as water, heavy water, graphite etc. to moderate and thermalize the energy of neutrons generated after every fission.

The probability of liberation of neutrons in each fission is higher if it caused by fast neutrons (Stacy, 2007). On an average, at least about one neutron from each fission needed for the further fission, i.e. self-sustenance of the chain reactions. Therefore, the extra neutrons generated after each fission can be absorbed in the materials other than the fissile. The nuclides uranium-238 and thorium-232 can be converted to plutonium-239 and uranium-233 respectively after capturing neutrons in the operating reactor core and therefore called as fertile. The converted nuclides are the fissile materials (whose fission is possible by neutrons of any energy) and can be extracted/ reprocessed and further utilize as the fuel in reactors. If the net conversion rate of fertile to fissile is more than the depletion rate of the fissile material in a core, the process is termed as breeding, and such reactor system is known as a breeder (Stacy, 2007). As the more neutrons are available for producing fissile in fast neutron-induced fissions, especially of plutonium-239; the fast reactors are purposely made for the breeding of fissile fuel and power generation simultaneously. These reactors also generate less nuclear waste and can be used for the incineration of minor actinides. The fast reactors are also compact as these are built evading the materials which could moderate the energy of fission neutrons.

The thermal reactors are further classified according to the coolant and moderator material used in their core. The heat transport system is a major engineering aspect of a nuclear reactor. The water-cooled reactors such as the pressurized water reactors (PWRs/ VVERs) and boiling water reactors (BWRs), which use light-water as coolant and moderator, and the pressurized heavy water reactors (PHWRs), which use the heavy-water as coolant and moderator, are thermal-spectrum reactors. It is due to the excellent moderating properties of hydrogen (Stacy, 2007). As per the IAEA (2020), the world over about 89.2% of the operational nuclear power capacity comprised of PWRs (304 units) and BWRs (72 units). Whereas 6.1% are of PHWRs (i.e. 49, also called CANDU types); 2.4% are light water-cooled and graphite-moderated reactors (i.e. 14 units of RBMK reactors), while the remaining 2.0% are of gas-cooled reactor types (i.e. 14 units of AGR types). These also include three liquid metal cooled fast reactors. In India, the majority of the operating reactors are PHWRs because of the country's nuclear programme based on the available natural resources of the fuel and infrastructure, which is briefly discussed in the next section.

1.3. Indian three-stage nuclear programme and power reactors

In 1969, the first two power reactors commissioned in India were Boiling Water Reactors (BWRs) as Tarapur Atomic Power Stations (TAPS-1&2) near Mumbai (Katiyar and Bajaj, 2006). However, considering the advantage of using natural uranium as the fuel, India opted for the Pressurized Heavy Water Reactor (PHWR) technology. These heavy-water cooled and moderated pressure tube type horizontal reactors also make the best use of mined uranium. A modest uranium resource and a vast thorium reserve of nuclear fuel prompted the country to adopt the closed fuel cycle and a three-stage nuclear programme (Bhabha and Prasad, 1958; Banerjee and Gupta, 2017). These stages are in brief as follows: (1) the first stage with thermal reactors, i.e. PHWRs for power generation using natural uranium fuel and simultaneous production of reactor-grade plutonium through reprocessing of their spent fuel, then (2) plutonium-based fast breeders to enhance the nuclear power capacity and breeding of ^{233}U from thorium in the second stage, and (3) in the third stage ^{233}U-thorium based breeders (Bajaj and Gore, 2006).

In India, Nuclear Power Corporation of India Limited (NPCIL) is responsible for the construction, operation and maintenance of nuclear power reactors. NPCIL is presently operating 22 commercial nuclear power plants with an installed capacity of 6780 MWe (NPCIL, 2017). The reactor fleet comprises 18 PHWRs (including 540 MWe TAPS-3&4), 2 BWRs (TAPS-1&2), and 2 unit of 1000 MWe VVER reactors. The VVERs are in operation at Kudankulam, Tamilnadu, in collaboration with Russian organization(Agrawal et al., 2006).

India has also an enriched experience of the fast reactor with the three-decade-long successful operation of 40 MWt FBTR (Banerjee and Gupta, 2017). The design of sodium-cooled and MOX fuelled prototype fast breeder reactor (PFBR) with 1250MWt power was initiated for the second stage of the nuclear programme, and the reactor is now at an advanced stage of commissioning (Puthiyavinayagam et al., 2017). PFBR is designed as a pool-type reactor with inlet and outlet temperature of sodium coolant about 397 and 547ºC respectively at the nominal power (Chetal et al., 2006).

The sufficient production of ^{233}U from thorium in the blanket of fast reactors like PFBR will enable India to begin the third stage (Banerjee and Gupta, 2017). Hence, to demonstrate the thorium fuel cycle for the third stage, India is developing an Advanced Heavy Water Reactor (AHWR) with enhanced safety features. AHWR is a vertical pressure tube type reactor with heavy water as moderator and boiling light water as coolant to generate 920MWt power (Sinha and Kakodkar, 2006). The reactor is designed with $(Th–Pu)O_2$ and $(Th–^{233}U)O_2$ based 54 fuel pins clusters in 452 coolant channels. The average inlet and outlet temperature of the coolant are about 261 and 285^{o}C respectively with steam quality of 18.2% at 7MPa during full-power operation. The reactor has been designed with several advanced safety features such as negative reactivity coefficients of fuel temperature, coolant void and power; core heat removal by natural circulation of boiling light water and passive emergency core cooling in case of LOCA etc. (Vijayan et al., 2017). The core-life cycle of the reactor is designed with self-sustenance in ^{233}U fissile loaded with the fuel (Sinha and Kakodkar, 2006; Kannan and Krishnani, 2013). The reactor has also been assessed for the $LEUO_2$ with ThO_2 fuel as an alternate core design and named as AHWR300-LEU (Sinha, 2011). However, as an attractive option of thorium fuelled breeder reactor, the conceptual design of Indian Molten Salt Breeder Reactor (IMSBR) has also been initiated for the third stage (Vijayan et al., 2015).

1.4. Generation-IV reactor concepts

Nuclear reactor designs are categorized by "generation" such as Generation I, II, III, III+, and IV according to their development and deployment characteristics like thermal-efficiency, operational-safety, non-proliferation security, economical-feasibility as well as high fuel utilization and low nuclear waste generation capacity (Goldberg and Rosner, 2011). The early prototypes reactors developed during 1950-65, are considered as Generation-I, and most of these are permanently shut down and decommissioned now. The commercial power reactors, which are designed to be economical and reliable, are known as Generation-II. These class of reactors comprise of conventional PWRs/VVERs, BWRs, PHWRs and AGRs in operation around the globe and their design consists of traditional active safety features. The Generation-III nuclear reactors are essentially APWRs, ABWRs and modern PHWRs with evolutionary improvements in the fuel technology and thermal efficiency. These reactor designs consist of passive safety systems, modularized construction and longer operational life. Whereas the reactors like AP-1000 and ESBWR are called as Gen-III+ reactors after significant improvements in their safety over Generation-III (Goldberg and Rosner, 2011).

Generation-IV reactor concepts are the future reactor designs expected for the deployment by 2020-30 (WNA, 2020). This class of reactors are designed to make use of nuclear fuel more efficiently with low nuclear-wastes generation and proliferation resistance (Pioro and Duffey, 2019). The aim of Generation-IV reactor designs is to the efficient, safe, economical, reliable and sustainable production of nuclear energy for the long term. With these aims in mind, the

Generation IV International Forum (GIF) has selected the six reactor technologies for further R&D (GIF, 2020; Todreas and Kazimi, 2012), which are as follows:

i. ***Gas-cooled fast reactor (GFR)*****:** The GFRs are high-temperature helium-cooled fast reactors with a closed fuel cycle. The cores consist of hexagonal fuel assemblies of mixed-carbide-fuelled pins with ceramic-clad structure for outlet temperature of helium about 850^{o}C. These reactors have high efficiency for electricity generation and capable of carbon-free hydrogen production (Stainsby et al., 2011).

ii. ***Lead-cooled fast reactor (LFR)*****:** The LFR concept features a lead or lead-bismuth eutectic (LBE) cooled fast-spectrum reactor (Alemberti et al., 2020). The thermo-physical properties of these coolants support for high-temperature operation at low pressure and are relatively inert to water and air. The lead or LBE cooled reactors have several applications such as efficient production of electricity and green hydrogen through thermo-chemical processes (Sinha et al., 2016).

iii. ***Molten-salt reactor (MSR)*****:** The MSR is distinguished by its core with the fuel dissolved in the molten fluoride salt. The fuel salt also acts as the primary coolant in MSR. The first such reactor built and demonstrated during 1965-69, was the MSRE (Haubenreich and Engel, 1970). These designs have several inherent safety features and can be a potential breeder (Merle-Lucotte et al., 2008). India has also initiated a programme for IMSBR designs for the better utilisation of the large thorium reserve in the third stage (Kannan and Krishnani, 2013; Vijayan et al., 2015 and Srivastava et al., 2021).

iv. ***Supercritical water-cooled reactor (SCWR)*****:** SCWRs are light-water-cooled reactors that operate at high temperature and high-pressure, i.e. above the thermodynamic critical point of water (374°C, 22.1 MPa). Unlike current generation water-cooled reactors, the coolant will have significantly higher enthalpy rise in the core of SCWR, which facilitate in the reduction of mass flow rate for a given thermal power with outlet enthalpy to superheated conditions. This reactor will have higher conversion efficiency for electricity production than the current generation of water-cooled reactors in addition of many other significant advantages (GIF, 2020).

v. ***Sodium-cooled fast reactor (SFR)*****:** SFR designs are sodium-cooled fast-spectrum breeder reactors of compact size with outlet temperature ranging between 500-550°C. The thermo-physical properties of sodium make it a better choice of fast reactor coolant for high temperature and low-pressure operation. However, chemical activity of sodium with water and air requires a sealed coolant system (GIF, 2020). Indian design of PFBR is one of the examples of such a reactor system (Devan et al., 2011; Sinha et al., 2016).

vi. ***Very-high-temperature reactor (VHTR)*****:** In the conceptual design of VHTRs, these are graphite-moderated helium-cooled TRISO-coated particles fuelled reactors for core outlet temperatures between 900-1000^{o}C (GIF, 2020). These reactor concepts enable several high-temperature process heat applications of nuclear energy such as carbon-free hydrogen production and are also highly efficient if used for electricity production. The reactor core can be built of either prismatic block type or pebble-bed type (WNA, 2020). The Japanese HTTR, HTGR and Indian design of CHTR are the prismatic block type core concepts where TRISO fuel-compacts are filled in the bores of hexagonal assemblies. The reactor cores such as PBMR, HTR-10 and Indian design of IHTR-600 are pebble-bed type fuelled with fuel pebbles of tennis ball size made of TRISO particles dispersed in graphite. The VHTRs are designed with many inherent safety features, including the highly negative reactivity coefficients, use of ceramic-based core materials of large heat capacity and chemically inert single-phase coolant. The IHTR and CHTR designs are described in the section-1.6 and 1.7.

1.5. Hydrogen production and other advantageous applications of HTRs

The hydrogen is flexible, clean fuel and can be stored, transported and produced by a variety of the methods. It integrates well with the current and future energy conversion methods. Most of the hydrogen (~95%) currently produced worldwide is from the fossil fuels through steam reforming of natural gas, partial oxidation of methane, and coal gasification, which release CO, CO_2 and other greenhouse gases as major by-products. The VHTR technologies have potential for sustainably supplying energy for the carbon-free/green hydrogen production through the thermo-chemical splitting of water into H_2 and O_2 molecules (Revankar, 2019). The efficient thermo-chemical process to generate hydrogen from water is the sulfur-iodine (S-I) cycle, which is a three-step process as follows:

a) $I_2 + SO_2 + 2\,H_2O \rightarrow 2\,HI + H_2SO_4$ (at temperature ~120°C)

b) $2\,H_2SO_4 \xrightarrow{heat} 2\,SO_2 + 2\,H_2O + O_2$ (at temperature ≥ 830°C)

c) $2\,HI \xrightarrow{heat} I_2 + H_2$ (at temperature ~ 450°C)

In step a), the reaction is exothermic where HI is separated by distillation. The reaction in step b) is an endothermic and also requires high temperature (>830°C) where water, SO_2 and residual H_2SO_4 are separated from the oxygen by-product through condensation. In step c), it is also an endothermic reaction, where iodine and any accompanying water or SO_2 are separated. Finally the hydrogen product remains as a gas. The net process can be as follow:

$$2\,H_2O \rightarrow 2\,H_2 + O_2$$

In the S-I cycle, the sulfur and iodine are recyclable and not consumed in the process. Moreover, the materials used are in the fluid state (gas or liquid), which is suitable for the continuous operation in close-cycle. This method is very much fitting for industrial-scale efficient production of carbon-free hydrogen. But the process requires heat at very high temperatures, approximately 950°C and advanced materials for process apparatus as the acids are more corrosive at high temperature. The S-I cycle has the highest reported efficiency

(~56%) for thermal to hydrogen conversion and even higher at higher temperatures (Banerjee et al., 2007). The Japan Atomic Energy Agency has successfully demonstrated nuclear hydrogen production using the S-I cycle in the helium-cooled HTTR (Kubo et al., 2004).

There are other hybrid cycles which use both high temperatures and some electricity, such as copper–chlorine (Cu–Cl) cycle. The Cu-Cl cycle is classified as a hybrid thermo-chemical cycle because it uses an electrochemical reaction in one of the reaction steps. This cycle operates at 530°C but has a conversion efficiency of about 43% (Naterer et al., 2008). This cycle also involves the handling of acids. However, it is found to be less corrosive for the structural materials. The Cu used in this cycle is in solid-state, thus may require mechanical handling in the cyclic process. The VHTRs are also more suitable for high-temperature electrolysis of water for hydrogen production (Badwal et al., 2013).

The VHTRs have great potential to be utilised for other industrial high-temperature process heat applications of nuclear energy (Yan, 2016). The VHTR designs have inherent safety features and it utilises the fuel better to result in high discharge burnup. These reactors, if used for electricity generation, would have higher efficiencies (40-50%) over the conventional nuclear power reactors (~30-40%) (Pioro and Duffey, 2019). The higher conversion efficiencies of VHTRs would result in a low thermal discharge to the surroundings resulting in balanced eco-system. Even the waste heat from such power plants has high potential to be used in the processes such as thermal water desalination. Keeping these advantages in mind, India is also pursuing its high-temperature reactor programme, which is discussed in the next section.

1.6. Indian high temperature reactor programme

A comprehensive high temperature reactor programme has been initiated in India to fulfil the country need for process heat applications of nuclear energy utilising thorium fuel cycle

(Gupta et al., 2008; Dwivedi et al., 2010; Sinha, 2011; Kannan and Krishnani, 2013; Sinha et al., 2016 and Dulera et al., 2017). As the future need of the environmentally benign fuel, hydrogen production through the thermo-chemical splitting of water is the primary aim of the programme. The efficient S-I cycle requires heat at more than 850°C for hydrogen production. Therefore, a challenging goal for the high temperature reactors technology development in India is to achieve coolant temperature of 1000°C (Sinha et al., 2016). As a first step, a prototype Compact High Temperature Reactor (CHTR) is being developed as a technology demonstrator for Indian HTRs (Dwivedi et al., 2010). Also, an Indian core design of 600 MWt high temperature reactor is being conceptualised.

The design options of Innovative High-Temperature Reactor (IHTR) are being evaluated for commercial production of nuclear hydrogen (Dulera and Sinha, 2007; Sinha, 2011; and Kannan and Krishnani, 2013). In the envisaged design of IHTR, the core is pebble-bed type annular cylinder of graphite reflector filled with ^{233}U-Th based TRISO fuel pebbles. The reactor consists of molten lead or fluoride salt as coolant and graphite pebbles as moderator to achieve 950°C core outlet at 600MWt nominal power. The design have several passive features for inherent safety such as negative reactivity coefficients, core heat removal under the natural circulation of coolant during normal operation and passive rejection of decay heat under the shut-down condition etc. (Singh et al., 2013). The reactor would be utilised for the hydrogen production by S-I cycle, desalination of sea-water and electricity generation. However, the option of prismatic design of the core is also evaluated for thermal-hydraulics and temperature distributions view-point (Dulera et al., 2017). The development and research for IHTR components such as structural materials, technologies related to the fuel, the coolant and reactor safety are in progress. Many of the technologies developed for CHTR would be utilised for IHTR (Sinha, 2011). In the following section, the design characteristics of CHTR core are discussed in detail.

1.7. The Compact High Temperature Reactor

In the envisaged design of Compact High Temperature Reactor (CHTR), it is a100 kWt core, consists of Th-^{233}U based TRi-structural ISOtropic (TRISO) fuel, beryllium oxide (BeO) as moderator and lead-bismuth eutectic (LBE) as coolant. CHTR is designed as prismatic block type vertical reactor for 15 effective full power years of core life-cycle without refuelling and reshuffling (Dwivedi et al., 2010). The proliferation-resistant thorium-based TRISO particles are used as the fuel, which have leak-tightness limit of about 1600^{o}C to ensure safe operation at high temperature with deep burn-up. The BeO as moderator and reflector, are used in CHTR for the high-temperature core design with compact size. The BeO moderator has better neutron-scattering properties over graphite. The only use of graphite as moderator in other thermal-spectrum HTRs, results in their bigger core sizes. The neutron transparent LBE is a better choice of liquid metal coolant for natural circulation cooled CHTR as it is inert to water. Also, the high boiling point (1670°C) of the LBE ensures that the core can be operated at a wider range of temperatures without risk of the coolant boiling. Use of LBE as the primary coolant eliminates the requirement of high pressure operation, unlike helium cooled HTRs. If the leakage of the primary coolant would occur in CHTR, it solidifies and prevents further leakage and retains well the iodine and other radioactive-products. The design of CHTR incorporates several passive safety features such as the negative reactivity coefficients of the fuel and moderator temperatures, core heat removal by natural circulation of LBE, passive rejection of decay heat to the atmosphere using a set of heat pipes etc.

At nominal power, the CHTR is designed to attain outlet temperature 1000^{o}C under the natural circulation of LBE coolant with inlet temperature and mass flow at 900^{o}C and 6.7 kg/s respectively. The 19 hexagonal fuel assemblies (FAs) in the core (Figure-1.1 and 1.2) are made of beryllium oxide moderator with centrally located graphite fuel tube. Each graphite tube (Figure -1.3) has twelve equally spaced longitudinal bores of 1.0 cm diameter for fuel. These bores are filled with fuel compacts of TRISO coated particles embedded in the graphite matrix. The TRISO particles (Figure -1.4) are tiny micro-spheres of (^{233}U + Th) carbide kernel coated with three types of layers of soft pyrolytic carbon, SiC and hard carbon. The soft carbon layer acts as a cushion to accommodate fission products and kernel swelling. The SiC layer in TRISO fuel acts like a micro pressure vessel and is the main barrier to prevent the release of fission products and gases. The outer and inner hard carbon coatings in the particles are acting as protective layers to SiC to avoid corrosion.

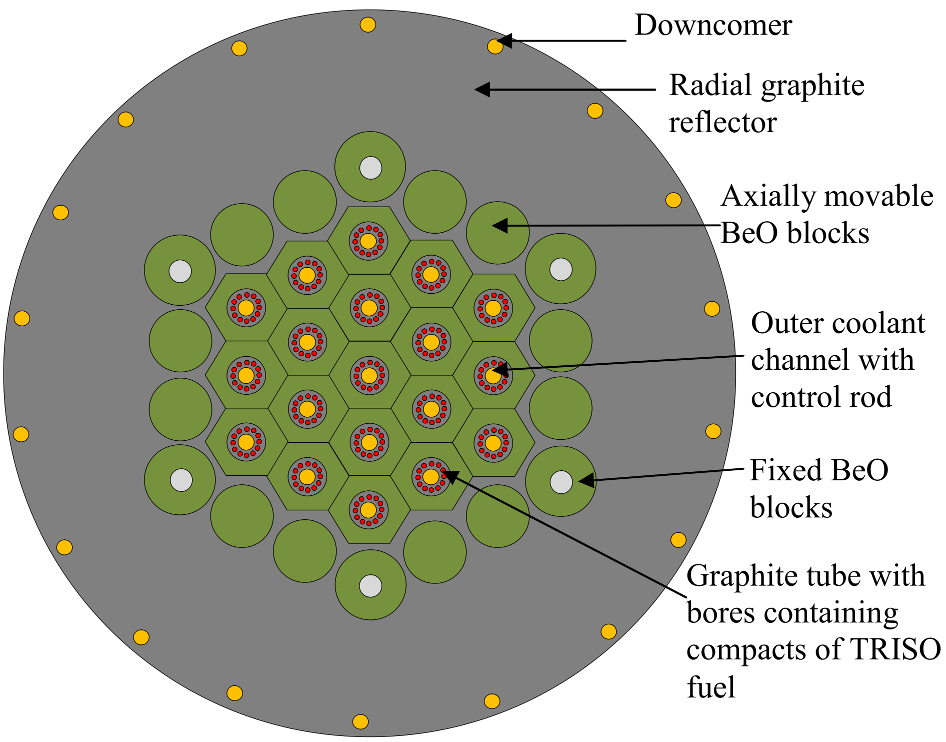

Figure-1.1: Cross-sectional schematic view of CHTR core

In the conceptual design of CHTR (Figure -1.2), the central bores of diameter 3.5 cm in each assembly are acting as coolant channel where LBE flows from the lower to the upper plenum under natural circulation. During normal operation, the coolant is returning from the upper to the lower plenum through eighteen downcomers. A set of sodium heat pipes inserted in these downcomers from the upper plenum passively transfer core heat to the secondary side.

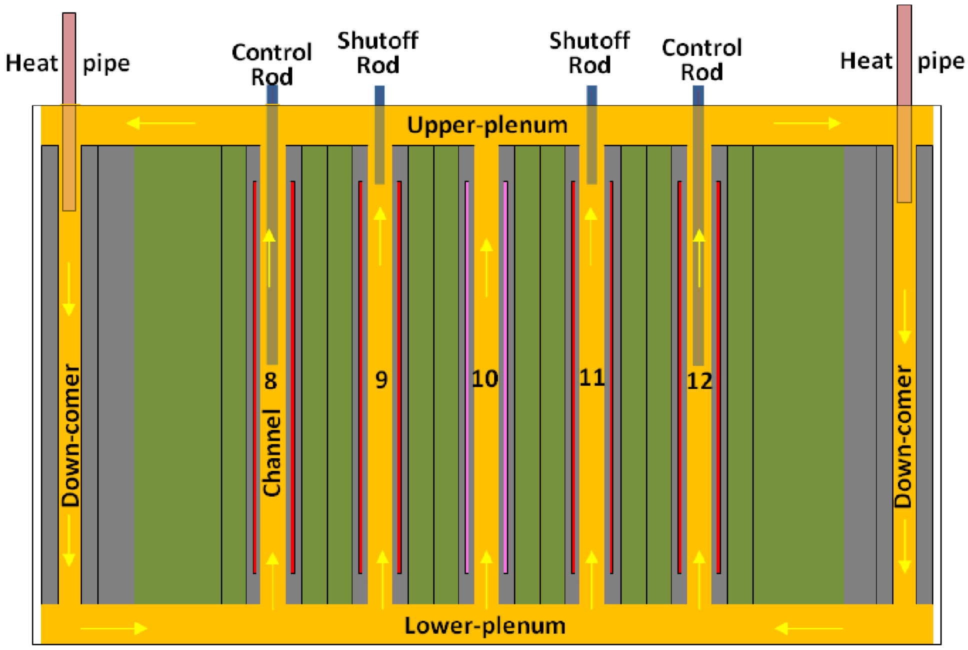

Figure-1.2: Axial schematic view with channels connected at lower and upper plenum

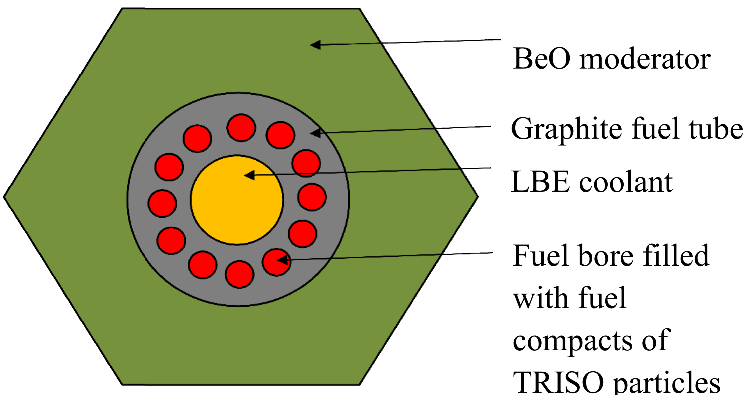

Figure -1.3: Cross-sectional schematic view of the fuel assembly/ channel

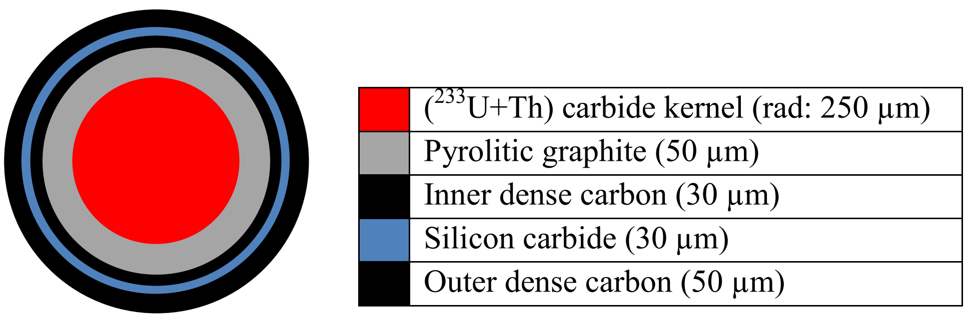

Figure -1.4: Radial schematic view of TRISO coated particle

Table-1.1: Main core design parameters of CHTR

Attributes	Values
Reactor power	100 kWt
Fuel	^{233}U-Th in TRISO particles
Fissile inventory	33.75 wt%
Core burnup	68000 MWd/t
Fuel channels/ pitch	19/13.5 cm
Core height/diameter	107.5 cm/ 127.0 cm
Axial reflector thickness	15 cm top and bottom
Moderator/ Reflector	BeO/ BeO and Graphite
Coolant	Pb-Bi Eutectic (LBE)
Coolant inlet/outlet temp.	900°C/ 1000°C
Core mass flow rate	6.7 kg/s
Number of downcomers	18
Power regulation	12 rods of Ta alloy
Primary SDS	6 shut-off rods
Secondary SDS	12 movable BeO blocks

The initial core reactivity in CHTR is high due to high fissile content loaded in the fuel for desired core life-cycle with the high temperature operation. In the design, about 30 g gadolinium is mixed in the fuel kernels of the central fuel assembly for passive control of initial excess reactivity (Dwivedi et al., 2010). The fuel assemblies/ channels of the core are surrounded by 15 cm thick top and bottom axial reflector blocks and radially with eighteen BeO blocks followed by graphite reflector (Figure -1.2). These core components are contained in a reactor shell made of Nb-1%Zr-0.1%C alloy, which is found to be suitable material for high temperature applications and also corrosion resistant against LBE coolant (Tewari et al., 2011).The main design parameters of the core are given in Table-1.1.

The CHTR core has been designed with twelve control rods (CRs) made of tantalum alloy, which are partially inserted in the outer coolant channels from the top reflector side for power control and regulation (Figure -1.2). The tantalum alloy has high capture cross-sections for thermal neutrons. The high density, melting point and mechanical properties of the alloy are suitable to be used as control and shutoff rods in CHTR as these are to be inserted in the channels where LBE coolant flowing at high temperature. The reactor has two independent shutdown systems for protection. The primary shutdown system (SDS) contains six shutoff rods similar to the CRs, which are parked in the top axial reflector zone and fall by gravity in six inner coolant channels after actuation. The secondary shutdown system is based on the twelve axially movable BeO reflector blocks, which are to be withdrawn out of the core to introduce high neutron leakage. In the case of unprotected transient studies, the shutdown systems are supposed to fail. The design has six burnup compensation rods inserted in fixed BeO blocks for coarse control of reactivity during the core-life-cycle (Dwivedi et al., 2010).

Design of a high-temperature core with desired long refuelling intervals imposes several challenges such as reactivity management, control and safety during operation in addition to the materials compatibility. For material related studies and natural circulation experiments, a high-temperature LBE based Kilo Temperature Loop (KTL) has been installed and operated at BARC (Borgohain et al., 2016). For the Indian HTR programme, the development of high-temperature materials such as TRISO fuel, reactor-grade graphite and BeO blocks, reactor vessel and tantalum-tungsten based alloy is also in progress (Mollick et al., 2015; Mirji et al., 2016; Dulera et al., 2017 and Majumdar et al., 2020). In the era of Generation-IV reactor design with intrinsic safety features (Jérôme et al., 2014 and Sinha et al., 2016), extensive safety analyses of the advance reactor concept like CHTR is an essential aspect of R&D studies. Therefore, the rationality and necessity for the development of high fidelity multi-physics tools for high-temperature reactors are discussed in subsequent section.

1.8. The rationality and necessity of multi-physics tools for safety assessments of HTRs

Nuclear fission reactors are archetypal multi-scale, multi-physics systems necessitating high-fidelity tools to study the science of nuclear fission power. In the case of HTRs, as very limited experiments could have been performed, the numerical simulation capability to realistically model the core for neutronics physics and safety transient studies is the State-of-the-art. The high-temperature reactor cores consist of ceramic-based moderator & reflector materials, single-phase coolant and multi-layered coated fuel particles. In the HTRs, the nuclear fissions in the tiny kernels of the TRISO fuel particles are the primary heat source. The design of high temperature cores that rely on natural circulation for passive safety features is also challenging as in these cases, the temperature distribution and the mass flow rate are tightly-coupled. The multi-physics modelling and simulation tools are required for improved understanding and more realistic predictions of coupled neutronics - thermal-hydraulics (N-TH) phenomena in such advance reactors. The present research aims to develop a 3D multi-physics capability for simulations of coupled neutronics - thermal-hydraulics during safety transients in HTRs. In the present thesis, CHTR is considered as a representative core for the investigations of safety transients in the high-temperature reactor.

The modelling of all physical process on all the scales is computationally challenging due to complexity and large size core designs of nuclear reactors (Demaziere, 2020). The multi-physics calculations with multi-scale are essential to ensure a realistic description of all these physical phenomena in the cores. Hence multi-physics tools are necessary to evaluate safety margins more accurately for the safe and economical operations of current as well as next-generation reactors (Avramova et al., 2015; Magedanz et al., 2015). The development and applications of multi-physics tools for the safety analyses of water-cooled reactors have been reported in the literature by several researchers (Mylonakis et al., 2014; Wang et al., 2020). The MOOSE (Multiphysics Object-Oriented Simulation Environment) framework is developed and used for full core multi-physics analysis of AP1000 linking neutron transport code Rattle$S_N$ake, fuel performance code BISON, and thermal-hydraulics code RELAP-7 (Gaston et al., 2015). The coupling of neutronics code PARCS (Joo et al., 1998) with the TH code TRACE (Spore et al., 1992) is discussed for the stability study of BWRs (Ellis et al. 2013, Downar, 2006). The development of code package IRTRAN (Aghaie et al., 2012) reported the coupling of lattice code WIMS and core code CITATION (Fowler, 1999) with TH code RELAP5 for the multi-physics study of reactivity initiated transients in PWRs. DYN3D-ATHLET (Kliem et al., 2007) is another attempt of coupling a neutronics code DYN3D (Grundmann et al., 2000) and a TH code ATHLET (ATHLET, 2003) in three different way, i.e. the external, the internal and the parallel, for transients in LWRs. The neutronics code DYN3D also has integrated module FLOCAL based on a fuel rod model and a two-phase TH to provide various feedbacks through the cross-section libraries generated by cell codes. Ravnik et al. (2008) discuss CORD-2 (Trkov and Ravnik, 1994), a core design system for PWRs with multi-physics capabilities with neutronics by WIMS (Askew et al., 1966) and 3D diffusion code GNOMER (Trkov, 2008) with an integrated TH module CTEMP. The coupling of Monte-Carlo neutronics code MCNP (MCNP) was attempted with a simplified TH feedback module THERMO (Shaposhnik et al., 2010) using serial coupling for steady-state calculations. For the multi-physics study of transients and safety in Indian design of AHWR, the full core neutronics code ARCH has been externally-coupled with TH code RELAP5 (Gupta et al., 2013; Gupta and Kannan, 2017). The finite-difference method based 3D space-time code ARCH is developed with advanced numerical methods and modern computational techniques for neutron diffusion analysis of steady-state and transient scenarios in Hexagon as well as Cartesian lattice geometry-based reactor cores (Gupta, 2012 and Gupta, 2017). The development and coupling of neutronics code IQS3D with TH code ATMIKA reported for transient and safety analyses of Indian PHWRs (Fernando, 2018).

The several multi-physics tools have also been developed and used for next-generation reactor designs. The code SIMMER-III (Maschek et al., 2005) is a 2D multi-phase, multi-component fluid dynamics code coupled with neutronics based on space-time multi-group neutron transport for sodium-cooled fast reactors. The DYN3D-MSR reported by Krepel et al. (2007), is a modified version of neutronics and TH in DYN3D code to account the drift of delayed neutron precursors in MSRs. Coupled neutronics / TH calculation is reported for High-Temperature Reactors with the DALTON-THERMIX code system (Boer et al., 2008). An extension of the Multi-Physics Modeling with an implicit approach for nuclear reactor analysis is presented for the European lead-cooled fast reactor system, ELSY (Aufiero et al. 2011). The MSR code reported obtaining the solution of the coupled neutronic/TH problem by implementing the general-purpose finite element software COMSOL Multiphysics (Gammi et al. 2011). A multi-physics simulation tool FRENETIC is developed for the quasi-3D analysis of a lead-cooled fast reactor core with the hexagonal fuel assemblies (Bonifetto et al., 2013). The open-source software code DRAGON and OpenFOAM have been coupled with integrated tight coupling approach for TH feedbacks in neutronics (Wu et al., 2016). The development and validation of multi-physics codes have also been recently reported for design and safety simulations of HTRs (Rohde et al., 2012; Dwivedi and Gupta, 2015; Lemaire et al., 2017; Dwivedi et al., 2017; Kasselmann et al., 2018; Balestra et al., 2020).

Indian HTR designs are envisaged with enhanced safety features such as passive core heat removal during normal operation by natural circulation of coolant, unlike other forced circulation helium-cooled HTRs. The BeO moderator used in CHTR is also a unique design feature in comparison to other internationally designed and operated HTRs. Indian HTR concepts also use thorium-based TRISO fuel particles. In high-temperature core design, these fuels with partly mixed burnable poison gadolinium affect the neutron energy spectrum as well as the worth of reactivity devices during core-life-cycle and safety coefficient of fuel temperature. In addition to these, the high packing fraction of thorium-based TRISO in the fuel-compacts makes an impact on its conductivity, heat capacity and consequently the peak value of fuel temperature in the core. During operational or accidental transients in the prototype high-temperature core, any misbalances between heat generation by fission and heat removal under the natural circulation of coolant could consequently lead to a further rise in temperatures of the core materials. In these scenarios, negative reactivity coefficients of thermal-hydraulics (TH) feedbacks could arrest the increase in the power/ temperatures and could be vital to ensure the safety of the core. Thus the TH feedbacks play a crucial role as the passive safety feature of the designed core and need to be investigated thoroughly. Hence, an effort has led to developing an in-house 3D space-time neutronics capability with integrated thermal-hydraulics for feedbacks. The aim of the TH development was to focus on the core design evaluations rather than the detailed analyses of system thermal-hydraulics. In this thesis, the indigenous development and validation of 3D multi-physics code ARCH-TH (code for Analysis of Reactor transients in Cartesian and Hexagonal geometries with Thermal-Hydraulics feedbacks), and its application to investigate the safety transients such as postulated loss of regulation accident (LORA), anticipated transient without scram (ATWS), loss of flow accident (LOFA) and unprotected loss of heat sink accident (ULOHSA) in the core are discussed. The developed code can simulate the integrated core N-TH phenomena under the operating condition and anticipated transients in high-temperature reactors.

The high fidelity multi-physics investigations could prove the inherent safety features of the core clearly at the design stage by accurately predicting the reactor behaviour in operating conditions and anticipated transients. These studies are essential for assessing the safety margins in the prototype design of high-temperature core like CHTR under design basis as well as postulated case of safety transients. The multi-physics are found to be better in the parametric study and sensitivity analyses of new core than stand-alone neutronics and thermal-hydraulics codes. If any predicted anomaly or shortcomings are observed in the design in the safety investigations, it would be helpful to improve the core design accordingly.

1.9. Outlines of the thesis

The outline of the present thesis is as follows. The theory, modelling and development of 3D space-time neutronics in code ARCH-TH is discussed including Improved Quasi-static (IQS) scheme of transient simulations in the next Chapter 2. The methodology and developments of TH models in code ARCH-TH are reported subsequently in Chapter 3. The TH model for natural circulation in coupled multi-channel and thermo-physical properties of ceramic-based CHTR core materials are also reported in this chapter. This chapter also includes a short overview of other coupled N-TH tools and studies reported for their HTR designs in the literature.

Chapter 4 presents the benchmark problems and validation results of the developed neutronics and thermal-hydraulics capabilities in code ARCH-TH. The chapter also discusses the requirement of validation and verification of newly developed multi-physics code for nuclear reactor safety analysis. Chapter 5 describes the analyses of reactivity initiated transients in CHTR during start-up and normal operating condition with different TH models used and feedbacks considered in the simulations. The chapter also presents accident analyses of CHTR initiated due to postulated coolant blockage and increased flow in the channels. The new observations and results from these investigations are also highlighted. In Chapter 6, a novel analysis of the unprotected loss of heat sink accident (ULOHSA) in CHTR core cooled under the natural circulation is discussed. The research led to the new finding such as prediction of reverse flow in low powered channels of natural circulation cooled CHTR during ULHOSA. The possible design modifications are also assessed with the developed multi-physics tool to suppress the predicted flow reversal and improve the safety features of CHTR core.

Chapter 7 briefly summarizes all the present research studies performed and reported in the thesis. This chapter also presents the main conclusions drawn and scope for future development in code ARCH-TH and the safety investigations of CHTR.

CHAPTER 2

3D SPACE-TIME NEUTRONICS

2.1. Introduction

The neutronics of a nuclear reactor is governed by the distribution of neutrons and their interaction with the nuclides of constituting materials. The reactor is said to be critical when just as many neutrons being lost as are produced inside it. The critical reactor operates under steady-state where the core neutron flux/ power distribution and its level are practically independent of time in the absence of an external source. In the cases of reactivity perturbations and occurrences of an imbalance of the heat production and removal, the neutron flux/ power changes with time and the state of the core are called 'under transient'. In the reactor transient analyses, the prompt and delayed generations of fission neutrons are considered explicitly due to their consequences on the time variation of reactor power. The behaviour of the reactor core can be predicted accurately by solving the neutron transport equation, which is the linear Boltzmann equation for neutral particles (Bell and Glasstone, 1970). Although there has been growing interest in the transport based core neutronics analyses for more accurate predictions, neutron-transport tools require more efforts in coding and are computationally expensive. Even with the significant advances in the high-performance computing, direct whole-core neutron transport calculations are still unfeasible for the industrial applications and take even more computational time in multi-physics simulations (Choi et al., 2018). Whereas, an approximate form of the neutron transport equation, which is known as the diffusion equation, is sufficiently accurate to predict the many physics features of the nuclear reactors. In fact, diffusion theory-based codes are the workhorse computational tools for reactor physics analyses (Stacy, 2007).

The diffusion theory-based tools can accurately predict the neutron flux/power and its distribution in the core when the approximations considered in diffusion theory are satisfied. These include approximations such as the absorption of neutrons in the medium is much less than the scattering, the spatial neutron distribution varies linearly, and neutrons scattering is isotropic in the system etc. (Stacy, 2007; Glasstone and Sesonske, 1994). The direct applications of diffusion theory-based simulations of highly absorbing fuel pins and absorber rods as well as the boundary cells with high neutron leakage; could introduce large errors in the predictions. For these reasons, the reactor core calculations are usually performed by the two-step procedure (Dwivedi et al., 2017). The procedure emphasized as- (1) homogenized and condensed group cross-sections of lattice cells generated by transport theory code and then, (2) whole-core calculation by diffusion codes using these sets of generated cross-sections. In the first step, neutron-absorbing fuel pins and absorber rods are often smeared with highly scattering moderator medium to generate few-group cell homogenised parameters of the lattices.

In the present thesis work, the safety transients of CHTR have been analysed with indigenously developed multi-physics code ARCH-TH. The 3D core neutronics capability in code ARCH is based on the diffusion theory. The spatially homogenised and neuron energy-wise condensed cross-section parameters of each lattice types in CHTR core have been generated by in-house code ITRAN. The code ITRAN, its application for CHTR lattice calculations and core diffusion theory are discussed in the subsequent sections.

2.2. Transport theory code ITRAN and lattice calculation of CHTR

In the first step of neutronic calculations, each type of lattice cells of CHTR is being simulated in detail with integral transport theory code ITRAN (Krishnani, 1982). The code ITRAN uses first flight collision probability and interface-current methods for the numerical solutions of transport equations in 2D. In the study of CHTR, ENDFB-VI.8, 172 group library has been used for nuclear data input in code ITRAN. The code is utilised to generate homogenized condensed 5-group cross-sections (Dwivedi et al., 2017) of various fuel and reflector cells in the core at different fuel burnup levels. The detailed geometry of cells (e.g. fuel assembly), i.e. isotopic composition and distribution of materials with their density and temperatures are considered for the lattice physics simulations (Figure-2.1). As the volume packing fraction (~ 42%) of TRISO particles in the fuel compacts is high (Kim et al., 2005), these are smeared along with graphite matrix in each bore of the FAs for homogenized condensed cross-section parameters generation (Dwivedi et al., 2017).

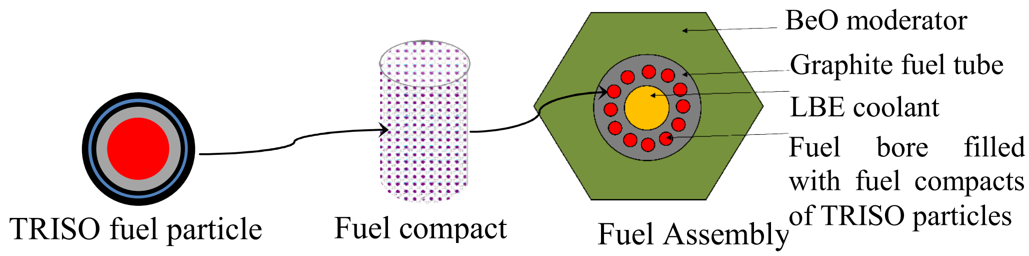

Figure-2.1: Cross-sectional schematic of CHTR fuel assembly where fuel bores are filled with compacts of TRISO particles

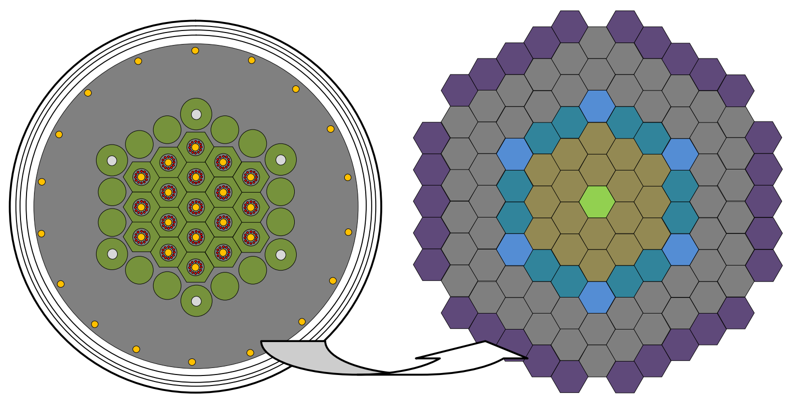

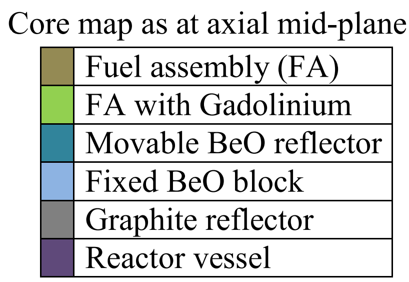

Finer details as downcomers and other under lying materials in hexagons are considered by filling the individual triangles. Each hexagon mesh is divided in 24 triangles (2^{nd} order division) in the simulation with code ARCH-TH

(a) The fuel and reflector cells in CHTR for lattice simulations

(b) The equivalent at axial mid plane for core calculation

Figure-2.2: Lattice simulations of the cells (a), Model for core calculation (b)

With the generated homogenised cross-sections of the cells, the whole core model of CHTR for further diffusion calculation is designed (Figure -2.2). The homogenised cross-sections are also tabulated as a function of temperatures of fuel, moderator and coolant for reactivity feedbacks for each type of the fuel cells. The multi-group delayed neutron parameters of CHTR are also generated by ITRAN and used as input in code ARCH (Gupta, 2012 and 2017). The code ARCH is integrated with TH modules and named as code ARCH-TH (Dwivedi et al., 2017). The full core of CHTR has been simulated with the code. The diffusion based neutronics capability in the code has been described in the following sections.

2.3. 3D space-time neutronics in code ARCH

For 3D space-time neutronics of nuclear reactors, the diffusion equation of the multi-group neutron flux as the function of space and time is described as follows (Stacy, 2007):

$$\frac{1}{v_g}.\frac{\partial}{\partial t}\phi_g(\boldsymbol{r},t) = \nabla D_g(\boldsymbol{r},t)\,\nabla\,\phi_g(\boldsymbol{r},t) - \Sigma_{r,g}(r,t)\phi_g(r,t) + \sum_{g'\neq g}^{G} \Sigma_{s,g'\to g}(\boldsymbol{r},t)\,\phi_{g'}(\boldsymbol{r},t)$$
$$+\frac{1}{k_0}(1-\beta)\chi_g^p \sum_{g'=1}^{G} \nu\Sigma_{fg'}(\boldsymbol{r},t)\,\phi_{g'}(\boldsymbol{r},t) + \sum_{d=1}^{D}\chi_g^d\,\lambda_d C_d(\boldsymbol{r},t) \quad \ldots\ldots\ldots(2.1)$$

Where, the index for neutron energy group varies as: g = 1.....G, here G is the total number of energy group (as G=5 for CHTR) in the analysis. The space and time dependence of delayed neutron precursors are described as follows:

$$\frac{\partial}{\partial t}C_d(\boldsymbol{r},t) = \frac{1}{k_0}\beta_d \sum_{g'=1}^{G} \nu\Sigma_{fg'}(\boldsymbol{r},t)\,\phi_{g'}(\boldsymbol{r},t) - \lambda_d C_d(\boldsymbol{r},t) \qquad \ldots\ldots\ldots(2.2)$$

Where the index d is varying as d =1.... D, for total D group of delayed neutron precursors (i.e. D=6 in CHTR studies reported in present thesis). In equation (2.1) and (2.2), r and t are representing the dependence of position and time of the functions, whereas the other symbols have the following meanings:

ϕ_g= neutron flux of g^{th} group,

C_d= precursor density of type$d$,

D_g= diffusion coefficient for g^{th} group of neutrons,

$\Sigma_{r,g}$= removal cross-section for g^{th} group of neutrons,

$\Sigma_{s,g'\to g}$= scattering cross-section from $g^{'} \to g$ group of neutrons,

$\nu\Sigma_{fg'}$= cross section for fission neutrons generated in g^{th} group,

v_g= speed of neutrons of g^{th} group,

$\chi^d, \beta_d, \lambda_d$= fission spectrum, delayed fraction and decay constant of type d precursor

χ^p = fission spectrum for prompt neutrons, and

k_0= eigenvalue adjusted to render the system critical at time $t\ = 0$.

Several numerical techniques exist for the spatial discretisation of the reactor core to determine the neutron flux and precursor density distributions with suitable boundary conditions such as finite difference method, nodal expansion methods etc. (Stacy, 2007). However, the nodal method is more accurate in the simulation with larger mesh sizes, i.e. to reduce the number of meshes in the computation, but such tools need more efforts for development. The finite difference method deals with the linear (first-order) variation of flux from one mesh to other adjacent meshes. In this case, a general rule of thumb is that the mesh sizes must be less than the neutron diffusion length in the medium (Stacy, 2007). However, the average diffusion length of the neutrons are longer in graphite or BeO moderated high-temperature reactor cores as compared to the light water reactors. Therefore finite difference method based codes are adequate to accurately predict the neutronics behaviour of HTRs even efficiently with larger mesh sizes. In case of CHTR simulations with the code, each hexagon mesh of the pitch 13.5 cm are divided into 24 triangles radially, i.e. sides of about 3.5 cm (2nd order division) (Figure- 2.1). The axial length (height) of these meshes are also of the same order (Dwivedi et al., 2017).

The code ARCH-TH reported in the present thesis is code ARCH with integrated TH modules for temperature feedbacks (Gupta and Kannan, 2017; Dwivedi et al., 2017 and 2020). The code ARCH (Analysis of Reactor Transients in Cartesian and Hexagonal Geometries) is developed with the finite difference method (FDM) for spatial discretization (Figure-2.3) and uses efficient Krylov sub-space based solvers such as BiCGStab with ILU preconditioner, Orthomin(1) (Van der Vorst, 2002) to solve the diffusion equations in sparse matrix format (Gupta, 2012 and 2017; Gupta and Kannan, 2017).

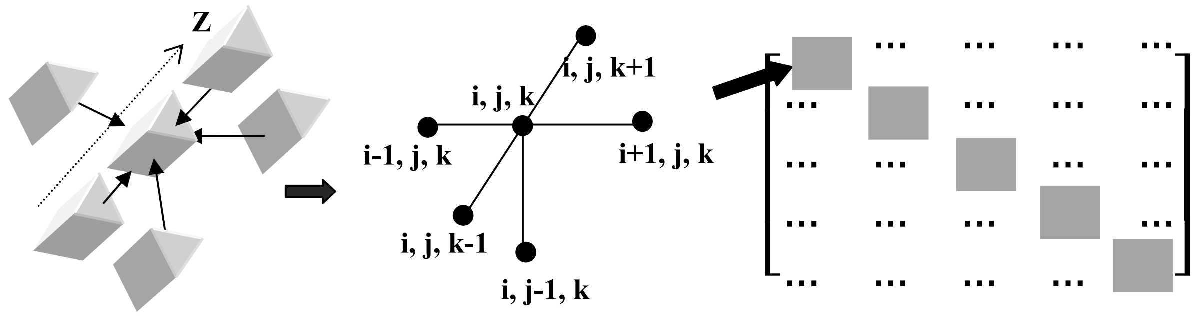

Figure-2.3: Generating a row of the coefficient matrix for triangular mesh (g, i, j, k) of hexagonal lattice based reactor core

The code ARCH has been developed in Fortran-90/95 with the modular structure for the ease of the code-user and further developments. The code can solve K-eigenvalue problem in the multiplying medium with and without an external source. In addition to reactor steady-state and transient calculations, the code has also options to perform core burn-up, refuelling/ reshuffling, and xenon spatial transient studies. It can compute multiple higher eigenmodes. The code is qualified well with benchmark validations (Gupta, 2012 and 2017).

The temporal integration of the left hand-side terms in equation (2.1) and (2.2), can be done using direct or indirect numerical methods. In the direct methods, the numerical solutions are being obtained at every time step by using scheme of forward differencing (explicit Euler), backward differencing (Implicit Euler) or θ-method (i.e. Crank-Nicolson method for $\theta =$

$1/_2$) for ($\frac{\partial}{\partial t}\phi_g$)term (Stacy, 2007). In the fully implicit module for reactor transient in code ARCH, the average group flux in the reference mesh with volume V_o is indicated by the subscript 'o', which is coupled to the five neighbouring meshes in 3D triangular-Z geometry (Figure-2.3) of the hexagonal lattice-based core. The group flux in the neighbouring meshes is denoted by subscript k, which varies from 1 to 5. The successive time steps are denoted by superscript 'n' at $(t - \Delta t)$ and 'n+1'at t. The discretised form of equation (2.1) is as follows:

$$\frac{\phi_{g,o}^{n+1} - \phi_{g,o}^{n}}{v_g . \Delta t}. V_o = \sum_{k=1}^{5} c_{k,g}\, \phi_{g,k}^{n+1} - c_{o,g}\phi_{g,o}^{n+1} - \Sigma_{r,g}\phi_{g,o}^{n+1}. V_o + \sum_{g' \neq g}^{G} \Sigma_{\,g' \to g}\, \phi_{g',o}^{n+1}. V_o$$
$$+ \frac{1}{k_0}(1-\beta)\chi_g^p \sum_{g'=1}^{G} \nu\Sigma_{fg'}\,\phi_{g',o}^{n+1}. V_o + \sum_{d=1}^{D} \chi_g^d\, \lambda_d C_{d,o}^{n+1}. V_o \quad \dots\dots\dots (2.3)$$

In equation (2.3), all the terms of group flux at next time step (n+1) are taken the LHS and the known quantities corresponding to the present time step 'n' can be put on the RHS of the difference equation. The similar equations of each group flux for each of the meshes are being solved. These large number of coupled linear difference equations can be expressed in matrix notation as follows:

$$A\,\phi = S \qquad \dots\dots\dots (2.4)$$

The matrix A has the order of N×G, where N and G are representing the total number of spatial meshes and the energy groups respectively for the given problem. The solution of A ϕ = S gives flux ϕ and precursor density C_d at time step $n+1$ if their values are known at step n for each of the meshes. This matrix equation has to be solved at every time step. The approach is very much CPU intensive. As the size of matrix A in equation (2.4) could be prohibitively large, in the conventional method used in the codes specially developed in earlier decades, the matrix A is not explicitly-constructed. For the group-by-group solution of the equations as given in equation (2.3) are obtained, starting from first (highest energy) group using Gauss-Seidel iterations with over relaxation. The overall conventional procedure for the solution is referred to as successive line over-relaxation (SLOR) method (Duderstadt and Hamilton,1976). In code ARCH, the solution is based on the explicit generation of the coefficient matrix, which is stored in the standard sparse formats (Saad, 1996) as shown in equation (2.4) as per the modern approach for space-time analysis. A more efficient solution can be obtained with Krylov subspace methods used in the code (Gupta, 2017).

For steady-state calculation, there is no distinction between prompt and delayed generations of neutrons. Therefore, the only-one fission source term (i.e. assuming $\beta = 0$) is considered in equation (2.1). The time derivative term will also be zero. Although the reactor is exactly steady (i.e. in critical-state with k_0=1) but due to error in modelling, the production may not be exactly equal to the loss terms in the equation. To accommodate this fact, the fission source term is divided by k_0, which is initially unknown. This k_0 is basically adjusted to get the exact balance for the steady-state. k_0 will be very close to 1.0, since we are modelling reactor to start the transient from initial steady-state condition. The initial values of precursors C_d at $t = 0$ can be obtained by equating the time derivative term to zero in equation (2.2) under steady-state, which comes out to be:

$$C_d(\boldsymbol{r}) = \frac{1}{\lambda_d k_0} \beta_d \sum_{g'=1}^{G} \nu \Sigma_{fg'}(r)\, \phi_{g'}(\boldsymbol{r}) \quad \dots\dots\dots (2.5)$$

To obtain the criticality equation for initial steady-state of the reactor, $\beta = 0$ is substituted in equation (2.1), which finally appears in the following form:

$$M.\phi = \frac{1}{k_0} F.\phi \qquad \dots\dots\dots (2.6)$$

The above equation is an eigenvalue problem, where matrices occur on both sides. The largest value of k_0 called k_{eff}. The corresponding eigenvector ϕ contains the flux distribution in all the meshes for each energy group. This is the steady-state flux required to initialize the kinetics calculation. For solving the eigenvalue in equation (2.6), it also requires to solve source equation similar to equation. (2.4). This can be done as follows. In general, a guess vector ϕ^1 and guess eigenvalue k_0^1 are considered to start with. Then, $S^1 = \frac{F.\phi^1}{k_0^1}$ is estimated to find out ϕ^2 after solving $M.\phi^2 = S^1$. Then a better guess for eigenvalue $k_0^2 = \frac{k_0^1.\phi^2}{\phi^1}$ is estimated. Now $S^2 = \frac{F.\phi^2}{k_0^2}$ is estimated to find out ϕ^3 by solving $M.\phi^3 = S^2$. These iterations are continued until given convergence criterion are satisfied for both k_0^i and ϕ^i. Thus, the equation $M.\phi^{i+1} = S^i$ is being solved repeatedly. This procedure is known as power iterations, which though converge monotonously, but quite slow. For the efficient solution of the K-eigenvalue problem, a Krylov subspace method, ORTHOMIN (Suetomi and Sekimoto1991) is implemented in the code. The method is implemented directly as well as via a matrix-free approach using fixed source calculations similar to equation (2.4).

The direct methods for temporal integration of equations (2.1) and (2.2) have simple algorithms to implement. But these methods require much smaller time steps (~ $10^{-4}s$) according to the neutron generation time and the core reactivity for accuracy resulting in more computational time, and particularly the explicit Euler method also suffers from a problem of numerical stability (Stacy, 2007). In the indirect methods of time integration, the neutron group flux in equation (2.1) and (2.2) is factorised into the product of amplitude and shape functions as:

$$\phi_g(\boldsymbol{r},t) = \psi_g(\boldsymbol{r},t).A(t) \qquad \text{………(2.7)}$$

Where, $A(t)$ is the amplitude function, which has only time dependence with $A = 1$ at time $t = 0$. Whereas, $\psi_g(\boldsymbol{r},t)$ is the shape of neutron group flux, which is space and weakly time dependent function and is same as the neutron group flux at $t = 0$. Here $t = 0$ is considered as the starting point of the reactor transients. In the next section, it is explained that by weighting equations (2.1) and (2.2) with the static adjoint flux and integrating over volume and energy, the point kinetics equations for the amplitude function can be obtained in addition to the shape and precursor equations.

If an assumption is made that the shape of neutron flux (ψ_g) does not change in the core during the transients and remain as at $t = 0$, then we need not solve the shape function, which is time consuming 3D calculations. In that case, the reactor can be assumed as point reactor, where the amplitude of total core flux/power is varying but shape or profile just as the initial during the transients. Thus to estimate the variation of core power, the only point kinetics equations of amplitude function are being solved, which do not account the change in the power profile during transients (Stacy, 2007).

However, during the transients, power/ flux profile may change, particularly in large reactor cores during asymmetric fast transients. Therefore, the contemplation of shape change of the flux/ power profile during the transient is essential for accurately predicting the core behaviour and safety margins. In the so-called adiabatic scheme, the 3D calculations for the shape function are performed at various time intervals with the instantaneous core configuration without explicitly considering the precursors, i.e. β=0 in equation (2.1) (Stacy, 2007). Thus the group fluxes are predicted with multiplying the shape function with instantaneous amplitude value computed by point kinetics solution. This result in an improvement in the analysis as compared to point kinetics method only used for predictions.

The other indirect methods are quasi-static (QS) and improved quasi-static method (IQS), which are computationally efficient as compared to direct methods and are also sufficiently accurate for the transient simulations. The IQS based module has also been incorporated in code ARCH for reactor transient, which discussed in detail in the subsequent sections.

2.4. Improved Quasi-Static (IQS) method

The improved quasi-static (IQS) method (Ott and Meneley, 1969), is one of the factorisation methods that attain fast computation in spatial neutron kinetics analyses. It involves factorization of the neutron flux as the given equation (2.7). These functions can be obtained by solving the amplitude and shape equations, respectively, which are decomposed from the original neutron diffusion equation. Although the 3D numerical calculation for the shape equation is time-consuming, due to their weak time dependence, relatively larger time meshes (i.e. the macro time steps) can be considered as compared to the direct methods. The rapidly varying amplitude function can be easily solved, with smaller time intervals (the micro time steps) as point kinetics solutions take negligible time as compare to 3D calculations of the shape functions. The IQS method results in more efficient computations of those reactivity initiated transients where the temporal variation of the shape function is relatively slower than that of the amplitude function, i.e. transients involving high variations in total flux/power but lesser in the profile.

The factorisation of neutron flux in equation (2.7) is defined at $t = 0$ with $A(0) = 1.0$ and $\phi_g(\boldsymbol{r}, 0) = \psi_g(\boldsymbol{r}, 0)$. For unique definition of the factorisation at $t > 0$, the following normalization condition for shape function is imposed (Ott and Meneley, 1969):

$$\int_{core} d\boldsymbol{r} \sum_{\boldsymbol{g=1}}^{\boldsymbol{G}} \phi_g^*(\boldsymbol{r}) \frac{1}{v_g(\boldsymbol{r})} \psi_g(\boldsymbol{r}, t) = \gamma \qquad \dots\dots\dots \quad (2.8)$$

Here, $\phi_g^*(\boldsymbol{r})$ is the static adjoint neutron flux at position r, and γ is considered as a constant parameter during the transients. At each macro time step, the computed shape function is iterated and checked to satisfy the condition given in equation (2.8). After substituting equation (2.7) in (2.1) and few subsequent arrangements give the following shape equation (Ikeda and Takeda, 2001):

Shape Equation:

$$\frac{1}{v_g}\left(\frac{\partial}{\partial t}\psi_g(\boldsymbol{r},t)+\frac{\boldsymbol{\psi_g}}{\boldsymbol{A(t)}}\frac{\boldsymbol{dA}}{\boldsymbol{dt}}\right)$$
$$=\nabla D_g(\boldsymbol{r},t)\,\nabla\,\psi_g(\boldsymbol{r},t)-\,\Sigma_{r,g}(\boldsymbol{r},t)\psi_g(r,t)+\sum_{g'\neq g}^{G}\Sigma_{s,g'\to g}(\boldsymbol{r},t)\,\psi_{g'}(\boldsymbol{r},t)$$
$$+\frac{1}{k_0}(1-\beta)\chi_g^p\sum_{g'=1}^{G}\nu\Sigma_{fg'}(\boldsymbol{r},t)\,\psi_{g'}(\boldsymbol{r},t)+\frac{\boldsymbol{1}}{\boldsymbol{A(t)}}\sum_{d=1}^{D}\chi_g^d\,\lambda_d C_d(\boldsymbol{r},t)\ \dots\dots\dots(2.9)$$

The shape function in equation (2.9) appears to be similar to equation (2.1) except in terms with amplitude function $A(t)$ (highlighted in bold letters). Therefore, the approach to solving the shape function could be the same as in the direct method discussed in the previous section. Whereas, the weakly-time dependence of shape function facilitates to consider longer time steps in 3D simulations resulting in faster computation. If the explicit time dependence of shape function is not considered (i.e. term $\frac{\partial}{\partial t}\psi_g(\boldsymbol{r},t)=0$), then the method is called as Quasi-static (QS). For improved accuracy, if shape function is considered to be varying linearly with time, then it is known as improved quasi-static (IQS). These methods, additionally require point kinetics solver for amplitude equations. The point kinetics equations for the amplitude are obtained by multiplying both sides by static adjoint neutron flux in the given equation (2.9) & (2.2), and integrating over energy and space, then imposing condition in equation (2.8); as follows (Ikeda and Takeda, 2001):

Amplitude Equations:

$$\frac{dA(t)}{dt}=\frac{\rho(t)-\beta(t)}{\Lambda(t)}\,A(t)+\sum_{d=1}^{D}\lambda_d\,P_d(t)\qquad\dots\dots\dots\ (2.10)$$

$$\frac{dP_d(t)}{dt}=\frac{\beta_d(t)}{\Lambda(t)}\,A(t)-\lambda_d P_d(t)\qquad\dots\dots\dots\ (2.11)$$

Here, the point kinetics parameters, e.g. dynamic reactivity $\rho(t)$, neutron generation time $\Lambda(t)$, integrated effective delayed neutron fraction $\beta(t)$ and integrated precursor in the delayed group $P_d(t)$, are defined as follows (Stacy, 2007):

$$\frac{\rho(t)}{\Lambda(t)} = \int_{core} d\boldsymbol{r} \sum_{\boldsymbol{g=1}}^{\boldsymbol{G}} (\frac{\phi_g^*}{\gamma}) \Bigg[-\Delta\left(-\nabla D_g(\boldsymbol{r},t)\,\nabla + \Sigma_{r,g}(\boldsymbol{r},t)\right)\psi_g(r,t)$$
$$+ \sum_{g' \neq g}^{G} \Delta\Sigma_{s,g'\to g}(\boldsymbol{r},t)\,\psi_{g'}(\boldsymbol{r},t) + (\chi_g^p - \beta\chi_g^p$$
$$+ \beta\chi_g^d) \sum_{g'=1}^{G} \Delta\nu\Sigma_{fg'}(\boldsymbol{r},t)\,\psi_{g'}(\boldsymbol{r},t) \Bigg] \quad \ldots\ldots\ldots (2.12)$$

$$\frac{\beta_d(t)}{\Lambda(t)} = \int_{core} d\boldsymbol{r} \sum_{\boldsymbol{g=1}}^{\boldsymbol{G}} \left(\frac{\phi_g^*}{\gamma}\right) \left[\beta_d \chi_g^d \sum_{g'=1}^{G} \nu\Sigma_{fg'}(\boldsymbol{r},t)\,\psi_{g'}(\boldsymbol{r},t)\right] \ldots\ldots\ldots (2.13)$$

with $\frac{\beta(t)}{\Lambda(t)} = \sum_{d=1}^{D} \frac{\beta_d(t)}{\Lambda(t)}$

and where;

$$\frac{1}{\Lambda(t)} = \int_{core} d\boldsymbol{r} \sum_{\boldsymbol{g=1}}^{\boldsymbol{G}} (\frac{\phi_g^*}{\gamma}) \left[\chi_g^p \sum_{g'=1}^{G} \nu\Sigma_{fg'}(\boldsymbol{r},t)\,\psi_{g'}(\boldsymbol{r},t)\right] \quad \ldots\ldots\ldots (2.14)$$

and

$$P_d(t) = \int_{core} d\boldsymbol{r} \sum_{\boldsymbol{g=1}}^{\boldsymbol{G}} (\frac{\phi_g^*}{\gamma}) \left[\chi_g^d C_d(\boldsymbol{r},t)\right] \quad \ldots\ldots\ldots (2.15)$$

These parameters in equation (2.12) to (2.15) are computed with the latest form of shape function and are assumed to be varying linearly within each macro time steps. However, point kinetics equations in (2.10) and (2.11) can be solved at smaller time intervals (i.e. micro time steps) for the fast varying amplitude function. The IQS module in code ARCH-TH has also been incorporated for transient simulations with longer time steps (Dwivedi et al., 2013).

2.5. 3D core neutronics in code ARCH-TH with IQS module

The IQS based core transient module has been incorporated in addition to fully implicit (FI) module in code ARCH-TH. The FI module in the code is unconditionally stable but requires smaller time steps (~$10^{-3}s$), thus consume considerable computational time for longer duration of transient especially when coupled with thermal-hydraulics. Therefore, the IQS based module has been incorporated in the code for efficient simulations of multi-physics phenomena in reactor cores (Dwivedi et al., 2013; Gupta and Kannan, 2017). In the temporal integration of equation (2.9) and (2.10) in the IQS module, two-tiered time scale has been adapted (i.e. the macro and the micro steps for the shape and amplitude function respectively) as illustrated in Figure-2.4.

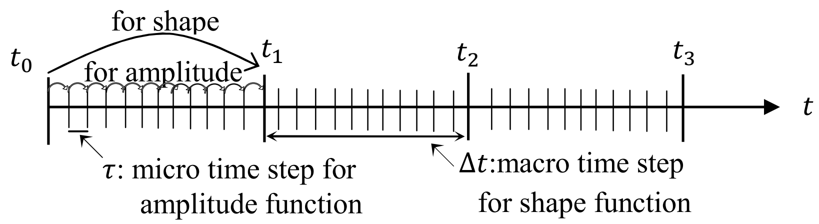

Figure-2.4: Two-tiered scheme for time marching in the IQS method

For solving the shape function in equation (2.9), time derivative of shape function (the first term in L.H.S.) can be replaced by a backward differencing (i.e. implicit Euler) as:

$$\frac{\partial}{\partial t}\psi_g(\boldsymbol{r},t) = \frac{\psi_g(\boldsymbol{r},t) - \psi_g(\boldsymbol{r},t-\Delta t)}{\Delta t} \qquad \dots\dots\dots(2.16)$$

where Δt is the macro time step size. In this approach, delayed source term of precursors in equation (2.9) is calculated directly from the flux history and then treated as inhomogeneous source. Thus, the shape function of the core flux is computed at the macro time steps of the order of $10^{-2} - 10^{-1}s$. The size of the macro steps depends upon the change in the flux/ power profile in the transients. In the method, the explicit temporal variation of the shape function is considered as linear in the given equation (2.16). Therefore, if the excessively long time step is taken in the simulation, then the approximate value of computed shape function may not satisfy the condition in the equation (2.8), which will result in multiple iterations (i.e. time-consuming 3D calculations) for γ-convergence at that step. Whereas fast varying amplitude function is computed at several micro-steps within each macro interval (Figure-2.4). The order of micro time steps (τ) are about $10^{-4} - 10^{-3}s$. For point kinetics solution of amplitude function in equation (2.10) and (2.11), the options of implicit Euler (IE) and RK-4 methods are available (Dwivedi et al., 2013 and 2017).

The value of amplitude function and its derivatives are obtained by solution of equation (2.10) and (2.11) and updated in equation (2.9) after each macro intervals Δt, (i.e. $\Delta t = m.\tau$). The point kinetic parameters defined in equation (2.12) to (2.15), are recomputed at each macro steps after modifications in the cell parameters according to change in material properties due to control rod movements and TH feedbacks with latest shape function. In the IQS module, the shape function is computed as follows:

$$\left[-\nabla D_g(\boldsymbol{r},t)\,\nabla + \Sigma_{r,g}(\boldsymbol{r},t) + \frac{1}{v_g}\left(\frac{1}{\Delta t} + \frac{\psi_g}{A(t)}\frac{dA}{dt}\right)\right]\psi_g(\boldsymbol{r},t) - \sum_{g'\neq g}^{G} \Sigma_{s,g'\to g}(\boldsymbol{r},t)\,\psi_{g'}(\boldsymbol{r},t)$$
$$-\frac{1}{k_0}(1-\beta)\chi_g^p \sum_{g'=1}^{G} \nu\Sigma_{fg'}(\boldsymbol{r},t)\,\psi_{g'}(\boldsymbol{r},t)$$
$$= \frac{1}{v_g\Delta t}\psi_g(\boldsymbol{r},t-\Delta t) + \frac{1}{A(t)}\sum_{d=1}^{D}\chi_g^d\,\lambda_d C_d(\boldsymbol{r},t) \quad \ldots\ldots\ldots (2.17)$$

The precursors $C_d(\boldsymbol{r},t)$ is calculated with time-integrated method (Stacy, 2007) as follows and then substituted in the equation (2.17):

$$C_d(\boldsymbol{r},t) = C_d(\boldsymbol{r},t-\Delta t)\exp(-\lambda_d\Delta t)$$
$$+\frac{\beta_d}{\lambda_d}\left[\left(\frac{1-\exp(-\lambda_d\Delta t)}{\lambda_d\Delta t} - \exp(-\lambda_d\Delta t)\right)A(t-\Delta t)\sum_{g'=1}^{G}\nu\Sigma_{fg'}(\boldsymbol{r},t-\Delta t)\,\psi_{g'}(\boldsymbol{r},t\right.$$
$$\left.-\Delta t)\right] - \frac{\beta_d}{\lambda_d}\left[\left(\frac{1-\exp(-\lambda_d\Delta t)}{\lambda_d\Delta t} - 1\right)A(t)\sum_{g'=1}^{G}\nu\Sigma_{fg'}(\boldsymbol{r},t)\,\psi_g^l(\boldsymbol{r},t)\right] \ldots\ldots\ldots (2.18)$$

In equation (2.18), $\psi_g^l\,(\boldsymbol{r},t)$ is the latest available form of the shape function. The shape function is required to compute the values of point kinetics parameters in equations (2.12) to (2.15) for every macro interval before solving the equation (2.17).

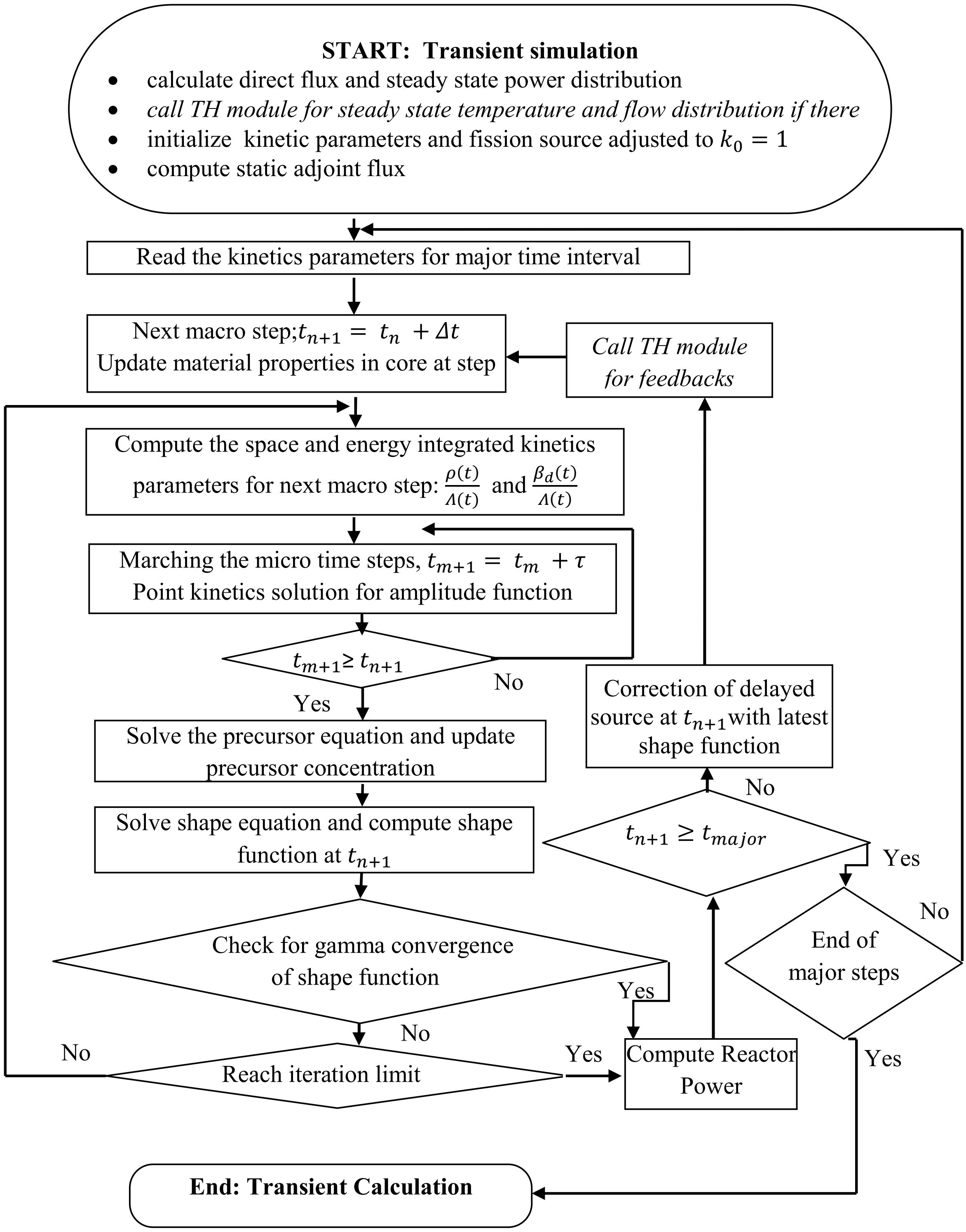

Figure 2.5: Flow chart of the IQS module in code ARCH-TH

In the IQS module of code ARCH-TH, for the first guess of shape function at the next macro step, its form at the previous step is considered as the best-known value. However, during the iterations, to satisfy gamma convergence as given in equation (2.8), the latest value of shape function is considered for the successive guess at the step. At each macro time steps, $\frac{1}{A(t)}\frac{dA(t)}{dt}$ and $C_d(\boldsymbol{r},t)$ are computed with equations (2.10), (2.11) & (2.18) and substituted in equation (2.17) to compute the shape function. The new shape function is checked to satisfy the gamma (γ) convergence till the given iteration limit is reached, then marching to the next macro time step for the shape function. The flow chart of the IQS module of code ARCH-TH is given in Figure-2.5. In the code, major time intervals (t_{major}) are considered according to different actions of control rod withdrawals, shutoff rod insertions or no device movements (i.e. time delay in the actions). During transient simulations, scenarios may arise that many spatial meshes in the core appear in partially rodded conditions during the course of control rod movements. In this condition, the equivalent homogenised condensed group cross-section parameters of these meshes are calculated with volume and flux weighting schemes for the remedial of well-known CUSP effect (Srivastava et al., 2013). The computational efficiency of the IQS module in code ARCH-TH over the FI module has also been compared particularly in case of CHTR transients (Dwivedi et al., 2013).

The temperature and density feedbacks are considered in the multi-physics analyses of the transients. The TH module in the code is called to compute the changes in the core TH parameters and cross-sections, which are being updated at each macro time-steps for feedbacks (Figure-2.5). The various models for thermal-hydraulics have been developed as integral modules in code ARCH-TH for feedbacks, which are discussed in detail in the next chapter. The code-to-code validation of neutronics capability in code ARCH-TH has also been carried out for well-known AER benchmarks of reactor dynamics of the hexagonal lattice-based core. The benchmark validation results of the code are compared and reported in Chapter 4 of the present thesis.

2.6. Conclusion

The performance of safety analyses of core transients is the essential aspects of the design and operation of advance nuclear reactors in the era of generation-IV reactor designs. Accurate core simulations are vital to these analyses, but require capabilities and tools for the multi-physics phenomena in nuclear systems. In this perspective, the in-house code system (ARCH-TH + ITRAN) has been developed for Indian design of natural circulation cooled high-temperature reactors (HTRs) like CHTR. The lattice physics of CHTR cells are being computed by neutron transport theory-based code ITRAN. The whole core neutronics of CHTR is being simulated with diffusion code ARCH-TH using cell homogenised few group cross-section parameters. The finite difference method based code ARCH-TH solves the neutron diffusion equations in sparse matrix format using Krylov subspace method based advance solvers and techniques for core neutronics. The code has been developed with IQS module to consider larger time steps for faster transient simulations, which has been the central point of discussion in this chapter. The neutronics validation of code ARCH-TH has been presented in Chapter 4 of the thesis. For reactivity feedbacks due to change in thermal-hydraulics conditions in CHTR during transients, the various developed TH models in the code are reported in the subsequent Chapter 3.

CHAPTER 3

MODELING OF THERMAL-HYDRAULICS OF HIGH TEMPERATURE REACTOR CORE

3.1. Introduction

The development of an accurate and efficient multi-physics analysis tool for neutronics and thermal-hydraulics (TH) simulations and its benchmark validation is a crucial step for the design and safety evaluation of high-temperature reactors (HTRs). The international group of developers of the next-generation reactors (Ortensi et al., 2011) has estimated that the multi-physics tools and methods currently available for the design and safety analyses of HTRs have lagged behind the state-of-the-art as compared to water-cooled reactor technologies (Rohde et al., 2012 and Lemaire et al., 2017). The codes are also inadequately verified for realistic safety transients due to the lack of experimental data for such reactor systems. The fuel in HTRs consists of millions of tiny TRISO-coated particles with kernels of uranium, which is proven to have the improved fuel integrity at high temperatures with burnup compare to the conventional fuel rods/pins with clad. Especially prismatic HTR designs consist of inverted fuel assemblies (i.e. fuel outside coolant channel) in contrast to the traditional fuel designs in LWRs and PHWRs (Todreas and Kazimi, 2012). The inverted fuel designs allow better core cooling, which in turn allows greater power density and total core power (Chapin et al., 2004). Also, HTRs are designed to be cooled with single-phase coolant in the whole range of operations with ceramic-based core materials of high heat capacities. These design characteristics of HTRs require special attention and capability for TH analyses.

The Indian CHTR is a novel concept of the high-temperature reactor with peculiar design features for enhanced safety. The design includes the features such as core heat removal by natural circulation of molten metal coolant during normal operation, use of beryllium oxide as high-temperature moderator, loaded with thorium-based TRISO fuel with high packing fraction and passive heat transfer to secondary side using a set of heat pipes etc. (Gupta et al., 2008, Sinha 2011; Kannan and Krishnani, 2013; Dulera et al., 2017 and Dwivedi et al., 2020). These features entail coupled neutronics (N)- TH capability and tools to precisely assess the design and safety of the core. During intentional or unintentional transients in CHTR, the larger heat generation by fission compared to the removal by natural circulation result in the further rise in core temperatures. However, negative temperature reactivity feedbacks of fuel and moderator could arrest this increase in the fission power and could be vital to ensure the safe and stable core operations. The feedbacks of TH with the natural circulation of coolant in CHTR core neutronics are crucial to the inherent safety features of designed core and need to be investigated thoroughly. Therefore, integrated TH modules in code ARCH have been developed for multi-physics simulations of safety transients in Indian designs of HTR and named as ARCH-TH (Dwivedi et al., 2015, 2017, 2018, 2019 and 2020). The developed TH modules in the code are of the following three types:

(i) Adiabatic heating of fuel during transients,

(ii) 1D-radial heat conduction in multi-channel with given coolant mass flow, and

(iii) TH model for natural circulation in the coupled multi-channel of close loop system

The detailed modelling and descriptions of these TH capabilities in code ARCH-TH have been discussed in the following sections.

3.2. TH model for adiabatic heating of fuel

In model of adiabatic heating of fuel, it is considered that excess heat generated in the fuel during transients is deposited in it. This assumption is valid mostly for the fast power excursion of short duration in the core. The model considers the change in temperature of all the fuel meshes for fuel temperature (Doppler) feedback during large reactivity transients as follows:

$$m_f c_f \frac{dT_f}{dt} = p_t - p_0 \qquad \dots\dots\dots \quad (3.1)$$

where m_f and c_f are the mass and isobaric heat capacity of the fuel in the mesh with average temperature at T_f. The instantaneous and initial thermal powers of the fuel mesh are denoted by p_t and p_0 respectively. The left-hand side term for temperature change in equation (3.1), is numerically integrated with implicit Euler method for each of the fuel meshes, which also require initial temperatures as input (Grundmann and Rossendorf, 2000). The model is simple and requires only thermo-physical parameters of the fuel. Therefore, initially, TH module in code ARCH has been incorporated to consider fuel temperature feedback during reactor transients based on adiabatic heating of the fuel (Dwivedi et al., 2015). The module provides a better insight into peak fuel temperature changes over the point kinetics analysis with lumped TH, as in this case, 3D power profile variation is being considered to estimate fuel temperature in each of the meshes. It has been observed that the model is mostly applicable in case of large reactivity transients which could die out in short time, such as unprotected LORA during the approach to criticality while core temperature is mostly at the coolant inlet temperature. The change in cell homogenised group parameters due to change in fuel temperatures is described in section-3.5 of this chapter. The adiabatic fuel heating based TH module in the code is validated with AER-Dyn002 benchmark problem, and results are discussed in detail in the next chapter. The postulated case of inadvertent withdrawal of control rod in CHTR during the first approach to criticality has been studied using this module as given in the Chapter 5.

The heat transfer from the fuel to the outer regions in reactor core increases at higher fuel temperatures resulting in the slower rise of fuel temperature during the transients and lesser fuel temperature feedback effect to the varying core power. The heat conduction from fuel to the adjacent moderator and then to coolant, alters the temperatures of these materials, which could also introduce reactivity feedbacks, which in turn modify the variation of core power and temperatures during transients. These reasons, in addition to the limited application of adiabatic fuel heating based model, motivated us to develop and integrate the TH module based on heat conduction. Therefore, a TH module has been developed based on 1D-radial heat conduction in each axial meshes of the fuel assemblies/ channels of CHTR with given inlet mass flow rate. The heat conduction based TH module in code ARCH-TH is described in the subsequent section.

3.3. TH model for 1D-radial heat conduction in multi-channel core

For temperature feedbacks in the steady-state as well as during the transients; 1D-radial heat conduction in the multi-channel model-based TH module has also been developed in code ARCH-TH (Dwivedi et al., 2017). The nuclear heat generated in the fuel present in twelve bores of each of the fuel channels is conducting to the adjacent regions of graphite fuel tube and BeO moderator and ultimately transferred to lead-bismuth eutectic (LBE) coolant flowing through the centre of each fuel tube (Figure-3.1). For solving 1D-radial heat equation in hexagonal axial meshes of the channels (Figure-3.2), the outer surface of each hexagonal axial mesh is assumed to be circular and twelve fuel bores are an annular shape conserving their cross-sectional area (Figure-3.1). In the present model, heat transfer in the axial direction is being ignored due to the large ratio of height to diameter of the fuel assembly. Additionally, it is assumed that single-phase coolant is flowing in each cylindrical coolant channel with a given inlet temperature and mass flow rate (Figure-3.2). The heat flux at the outer surface of the BeO moderator is also neglected by imposing adiabatic boundary condition due to relatively small temperature gradient at these boundaries during normal-operation. In the model, time-dependent radial heat conduction equations are solved for the heat transfer from fuel to adjacent region and finally to coolant in each axial mesh of every fuel assembly (FA)/channel. These axial meshes in each FA are simulated through the lumped coolant flow model as outlet coolant temperature of every mesh is taken as the inlet for the next elevated axial mesh in the channel.

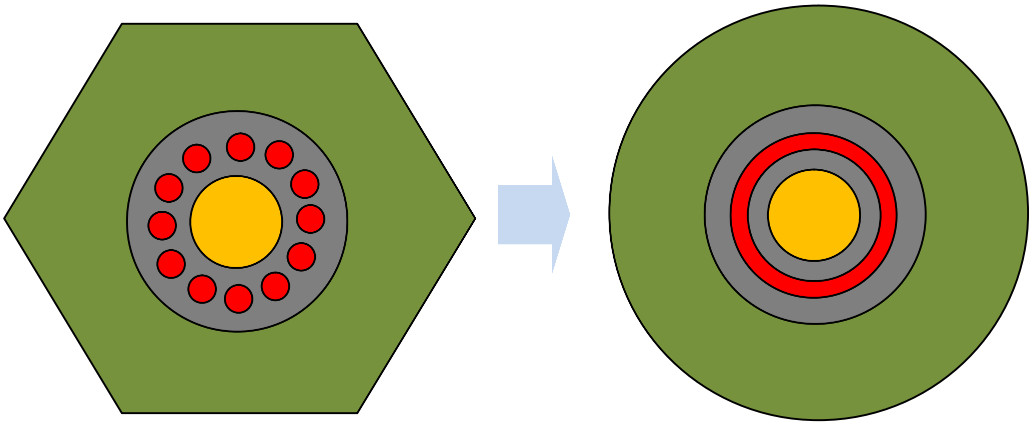

Figure-3.1: Cross-sectional schematic view of fuel channel in CHTR and its equivalent 1D radial model in cylindrical geometry

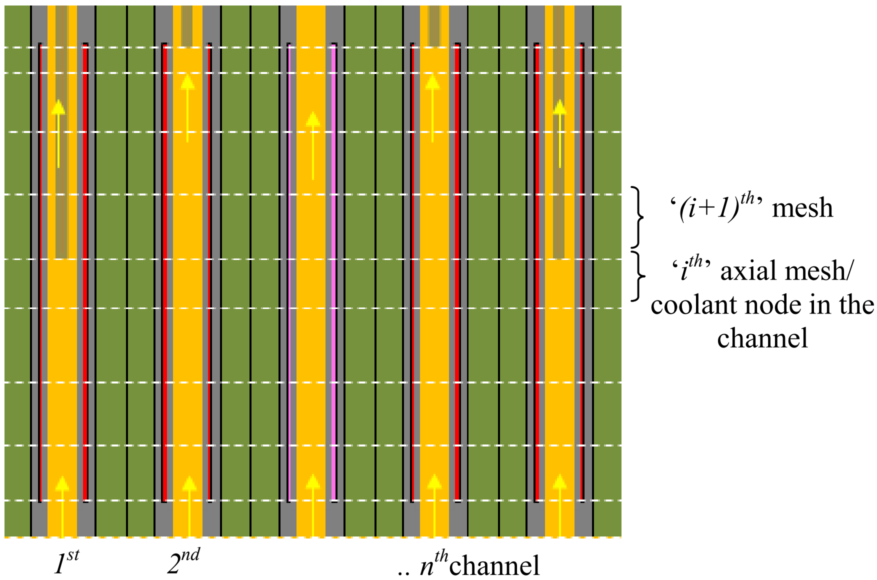

Figure-3.2: Axial schematic of channels with meshes/ nodes with coolant flow

In the model, the time-dependent radial heat equation has been numerically solved by the corner-mesh finite difference scheme. The corner mesh scheme has been preferred as it gives better information about nodal temperatures (Jain, 1989). The time-dependent heat conduction equation in 1D-cylindrical geometry (Todreas and Kazimi, 2012) is as follows:

$$\rho_m\, c_p\, \frac{\partial T(r,t)}{\partial t} \;=\; q'''(r,t) + \frac{1}{r}\frac{\partial}{\partial r}\left[rk\, \frac{\partial T(r,t)}{\partial r}\right] \quad \ldots\ldots\ldots (3.2)$$

where ρ_m, c_p and k are material density, isobaric heat capacity and thermal conductivity at position r respectively. $q'''(r,t)$ is the power density at position r and time t. $T(r,t)$ represents the temperature at position r and time t. At the interface of two conducting material as A and B, the following boundary condition is applied to temperature $T(r,t)$:

$$k_A \left[\frac{\partial T}{\partial r}\right]_A \quad = \quad k_B \left[\frac{\partial T}{\partial r}\right]_B \qquad \ldots\ldots\ldots (3.3)$$

The derivatives are taken at the two sides of the interface. At the interface of conducting material and convective (coolant) material (i.e. at the inner wall of fuel tubes in CHTR core), the boundary condition is as follows:

$$k_A \left[\frac{\partial T}{\partial r}\right]_{r_w} \quad = \quad h\,(\,T_w - T_b) \qquad \ldots\ldots\ldots (3.4)$$

where derivative is taken at the boundary of the conductive and convective materials. The variable h is the heat transfer coefficient; T_w and T_b are the temperatures of the surface of the coolant channel wall and average bulk temperature of the coolant in the mesh respectively.

The heat transfer coefficients h is determined as follows:

$$h \;=\; \frac{k_c\, N_u}{D_h} \qquad \ldots\ldots\ldots (3.5)$$

where k_c and D_h are the thermal conductivity of coolant and hydraulic diameter of the coolant channel. Here N_u is the Nusselt number. Nusselt number has been computed by Cheng & Tak correlation for low Prandtl number fluid flow of LBE coolant in CHTR. This correlation is proposed in Cheng and Tak (2006) and given as follows:

$$N_u = A + 0.018 \times \, {P_e}^{0.8} \qquad \text{… … … (3.6)}$$

where A is defined as follows,

$$A = \begin{cases} 4.5 & if \qquad P_e \leq 1000 \\ 5.4 - 9 \times 10^{-4} \times Pe & if \; 1000 < P_e \leq 2000 \\ 3.6 & if \qquad P_e > 2000 \end{cases} \qquad \text{… … … (3.7)}$$

where P_e is the Peclet number and defined as: $P_e = R_e \times P_r$ … … … (3.8)

The CHTR transient analyses reported in the present thesis, Cheng & Tak correlation has been considered over the other correlations option available in the TH module. Cheng and Tak reviewed various empirical heat transfer correlations for liquid metal LBE cooled systems. They have carefully assessed many correlations applicable for different Peclet number ranges and CFD analyses. Then a new correlation is developed, which is applicable for a wide range of Peclet numbers in molten LBE (Chen and Tak, 2006). The correlation also confirms well to experimental results (Borgohain et al., 2011 and 2016). Therefore, among the other correlation options in the code, Cheng and Tak's correlation has been used. The other correlations available in the module for computation of heat transfer in case of low Prandtl fluid flow are Lubarski & Kaufman, Ibragimov, Notter & Sleicher and Kirrilov & Ushako correlations (Borgohain et al., 2011; Dwivedi et al., 2017). As temperature predicted in the fuel is dependent on the heat transfer coefficient computed through these correlations, the correlation obtained from TH experiments with TRISO fuel heating condition is desired for CHTR transient analyses, which could also be incorporated in the code if found in future.

In equation (3.8), Reynolds number R_e and Prandtl number P_r are defined as:

$$R_e = \frac{G_c \, D_h}{\mu} \qquad \text{… … … (3.9)}$$

$$P_r = \frac{c_p \, \mu}{k_c} \qquad \text{… … … (3.10)}$$

where G_c is the mass flux, μ is the dynamic viscosity of the coolant. In case of CHTR, G_c and D_h are taken as follows:

$$G_c = \frac{C_w}{\pi\,(r_c^2 - r_r^2)} \qquad \ldots\ldots\ldots (3.11)$$

for annulus channel: $D_h = 2\,(r_c - r_r) \qquad \ldots\ldots\ldots\ (3.12)$

where C_w is the average coolant mass flow rate in each channel. The change in given inlet temperature and mass flow rate of coolant in each of the channels is assumed to be negligible during reactor transient in CHTR. Here, r_c is the radius of the coolant channels in the fuel tubes and r_r is the radius of the absorber rods inserted in the channels for reactor control.

The change in properties of LBE coolant such as isobaric specific heat c_p, mass density ρ_c, viscosity η, and thermal conductivity k_c with temperature (T_c) are being considered as follows (OECD-NEA, 2007):

$$c_p = 159 - 2.72 \times 10^{-2}.T_c + 7.12 \times 10^{-6}.T_c^2 \qquad \ldots\ldots\ldots (3.13)$$

where isobaric specific heat c_p is in $J.kg^{-1}.K^{-1}$.

$$\rho_c = 11096 - 1.3236.T_c \qquad \ldots\ldots (3.14)$$

where unit of LBE density ρ_c is in $kg.m^{-3}$.

$$\eta = 4.94 \times 10^{-4}.exp(754.1/T_c) \qquad \ldots\ldots\ldots (3.15)$$

The unit of viscosity η is in $Pa.s$.

$$k_c = 3.61 + 1.517 \times 10^{-2}.T_c - 1.741 \times 10^{-6}.T_c^2 \qquad \ldots\ldots\ldots (3.16)$$

where unit of LBE thermal conductivity k_c is in $W.m^{-1}.K^{-1}$.

The 1D-radial heat conduction equations are being solved by discretizing the conducting regions in several fine radial divisions/meshes in each axial mesh of the channels. For feedbacks, volume-weighted average temperatures of each type of material (fuel/moderator) are being computed in every axial mesh of each fuel assemblies in the core. The heat conduction equations have been solved with the fully-implicit method. The Bi-conjugate Gradient Stabilized technique has been used for the solution of matrices of heat conduction in each axial meshes (Gupta, 2017). The TH in the code is also optionally coupled with point kinetics model. The TH module is validated for steady-state and transient cases of LBE cooled XADS and MYRRHA benchmark problems (Dwivedi et al., 2017). The predictions of developed TH module have been compared with the reference results and discussed in detail in the subsequent Chapter 4. The TH model in code ARCH-TH has been utilised for multi-physics analyses of anticipated transient without scram (ATWS) in operating core condition of CHTR and studies are presented in Chapter 5.

The TH model described in this section requires inlet mass flow rate and temperature of the coolant in the channels as input, which are conservatively being considered as invariable during the transients. The invariable mass flow rate and inlet temperature of coolant during the transients is more applicable for the forced circulation system with ideal heat sink. Whereas, the core heat removal in CHTR is based on the natural circulation of LBE coolant in coupled vertical multi-channel under normal operating condition. The natural circulation mass flow rates depend upon the heating condition and overall thermal-hydraulics design of the core. In that case, the channels may have different mass flow rates and could be varying during transients. Therefore, as the next step, the conduction based TH model has been augmented for natural circulation of single-phase coolant in coupled multi-channel system and optionally available in code ARCH-TH.

3.4. TH model for natural circulation of coolant in coupled multi-channel

For natural circulation in the closed-loop model of CHTR, the 1D-radial heat conduction based TH model has been further developed in code ARCH-TH (Dwivedi et al., 2018 and 2020). The mass, energy and momentum conservation equations of coolant in CHTR are solved for 1D flow in every segment of the primary circuit with N number of channels connected at upper and lower plenums only where N =19 in the core (Figure-3.2). The outlet coolant after transferring heat to the secondary side with use of the heat pipes at the upper plenum is returning to the lower-plenum through nDC number of downcomers (DCs) where nDC is 18 in the present case of CHTR (Figure.- 1.1 & 1.2 of Chapter 1). The DCs located in radial graphite reflector are thermally isolated by gas-gap between DC tubes and graphite reflector. The coolant in DCs after passing through the portions with heat pipes (primary heat exchanger) has been considered with temperature as per given inlet core temperature during steady-state.

The closed-loop model for coolant dynamics simulation in the core is given in Figure-3.3. All coupled 19 channels of CHTR are found to be asymmetrically heated due to the non-flattened radial power profile and gadolinium mixing in the central FA. The channels also have different hydraulic conditions from lower to the upper plenum. There are partially inserted control rods in twelve outer coolant channels and six primary shutoff rods parked in the top reflector zone in six inner coolant channels in the operating condition. Whereas, there is no absorber rod inserted in the central FA. The 19 channels/ FAs are acting as hotter segments/ risers with a radial arrangement from the central FA as shown in Figure-3.3. The ex-core segments, i.e. upper and lower plenums and the downcomers except the portions with heat pipes are considered as adiabatic sections. Therefore, the outlet coolant only loses heat in the primary heat exchanger (HX)/ segment with heat pipes. In Figure-3.3, the upper plenum of the core is represented horizontally by segments S#20, S#21, S#22 and S#23. The vertical section of the downcomers with and without heat pipe is shown as S#24 and S#25 respectively. The lower plenum is represented horizontally by segments S#26, S#27, S#28 and S#29. For the simulations, all the inlets and outlets of each segment in the primary are provided as input. Divisions of upper and lower plenum portions have been carried out by keeping segment lengths as per the radial gaps between each ring of FAs and average diameters to keep their volumes conserved.

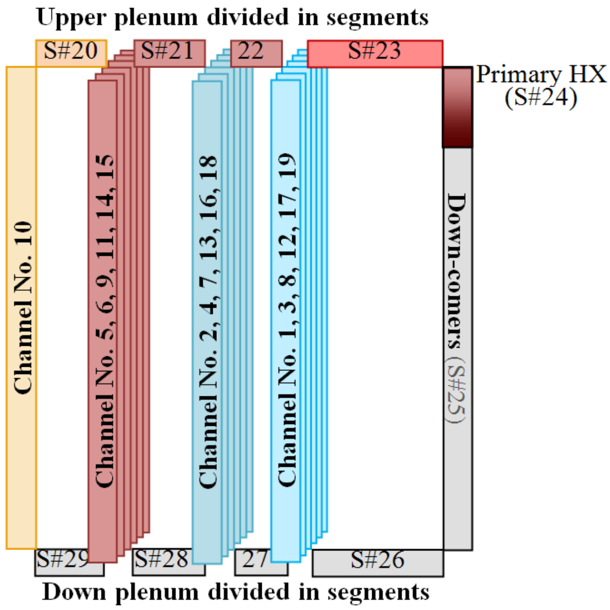

Figure-3.3: The closed-loop model of CHTR for coolant dynamics simulation

For incompressible fluid flow, the mass flow rates in each ex-core segments in the primary loop is computed by summing the inlet(s) and outlet(s) to zero for mass conservation. The segment mass flow rates are found to be independent of the locations inside it and are only the function of time (i.e. there is no cross-flow). In the 1D model of single-phase coolant flow, the fundamental equation of momentum conservation is as follows (Todreas and Kazimi, 2012):

$$\frac{\partial}{\partial t}(\rho u) + \frac{\partial}{\partial x}(\rho u u) = -\frac{\partial p}{\partial x} - \rho g \sin\theta - \frac{f \rho u^2}{2D} - K \frac{\partial}{\partial x}\frac{\rho u^2}{2} \qquad \dots\dots\dots (3.17)$$

where ρ and u are the density and flow speed of the fluid at position x and time t. And after integrating over the Δx mesh length in one-dimensional flow, we get,

$$\Delta x \frac{\partial}{\partial t}(\rho u) + (\rho u u) = -\Delta p_{\Delta x} - \Delta x \rho g \sin\theta - \frac{f \Delta x \rho u^2}{2D} - K \frac{\rho u^2}{2} \qquad \dots\dots\dots \ (3.18)$$

where θ is the inclination angle of mesh in the segment with θ = 90° for vertical upward flow, θ = −90° for downward flow and either 0° or 180° for horizontal flow.

For single-phase coolant like LBE in CHTR, the pressure drop due to acceleration defined by the second term at the left-hand side of the equation (3.17) and (3.18) is found to be small and thus neglected (Borgohain et al., 2016; Dwivedi et al., 2020; and Todreas and Kazimi, 2012). The equation (3.18) in terms of mass flow rate can be written as:

$$\frac{\Delta x}{A}\frac{\partial W}{\partial t} = -\Delta p_{\Delta x} - \rho g.\Delta x \sin\theta - \left(f\frac{\Delta x}{D} + K\right)\frac{W^2}{2\rho A^2} \qquad \ldots\ldots\ldots (3.19)$$

where W $(= \rho u A)$ is the mass flow rate of coolant in the mesh of length Δx with hydraulic diameter D and area of mass flow A. The parameter f is the Darcy friction factor and K is the loss coefficient to account the pressure loss due to an abrupt change in flow direction and /or geometry. The correlations to compute Darcy friction factor and Form factor has been discussed later in this section. To compute the pressure drop in the nth channel after summing over all its axial meshes, the equation (3.19) will be:

$$\left(\sum_{i=1}^{iz}\frac{\Delta x_i}{A_i}\right)_n \frac{\partial W_n}{\partial t} = -\Delta p_n - \left(\sum_{i=1}^{iz}\rho_i \Delta x_i \sin\theta_i\right)_n g - \left(\sum_{i=1}^{iz}\left(f_i\frac{\Delta x_i}{D_i} + K_i\right)\frac{1}{2\rho_i A_i^2}\right)_n W_n^2 \quad \ldots\ldots (3.20)$$

where i is the index of the axial mesh in the n^{th}channel. Assuming all the downcomers have similar physical and thermal-hydraulic conditions, the above equation for downcomer will be:

$$\left(\sum_{i=1}^{iz}\frac{\Delta x_i}{A_i}\right)_{dc} \frac{\partial W_{dc}}{\partial t} = \Delta p_{dc} - \left(\sum_{i=1}^{iz}\rho_i \Delta x_i \sin\theta_i\right)_{dc} g - \left(\sum_{i=1}^{iz}\left(f_i\frac{\Delta x_i}{D_i} + K_i\right)\frac{1}{2\rho_i A_i^2}\right)_{dc} W_{dc}^2 \ \ldots (3.21)$$

where $W_{dc} = \frac{\sum_n W_n}{nDC}$ is the mass flow rate in the downcomer. After considering the value of $\sin\theta_i$ in the equation (3.20) and (3.21), these can be written in a simplified form as follows:

$$S_n \frac{\partial W_n}{\partial t} = -\Delta p_n - G_n - F_n W_n^2 \qquad \ldots\ldots\ldots (3.22)$$

and,

$$S_{dc} \frac{\partial W_{dc}}{\partial t} = \Delta p_{dc} + G_{dc} - F_{dc} W_{dc}^2 \qquad \ldots\ldots\ldots (3.23)$$

where the parameters,

$$S_n = \left(\sum_{i=1}^{iz} \frac{\Delta x_i}{A_i} \right)_n \qquad \ldots\ldots\ldots (3.24)$$

$$G_n = \left(\sum_{i=1}^{iz} \rho_i \Delta x_i \right)_n g \qquad \ldots\ldots\ldots (3.25)$$

and,

$$F_n = \left(\sum_{i=1}^{iz} \left(f_i \frac{\Delta x_i}{D_i} + K_i \right) \frac{1}{2 \rho_i A_i^2} \right)_n \qquad \ldots\ldots\ldots (3.26)$$

In natural circulation condition, as the lower and the upper plenums are the common for all the channels and the downcomers, there must be equal pressure drops in all these channels/ legs. The pressure drops along the horizontal segments of the upper and lower plenum are found to be very small and thus neglected.

(i) *Estimation of initial steady state in coupled multi-channel*

The initial steady-state mass flow rate and the outlet temperature distribution in the coupled channels are being estimated (at $t = 0$) in the code as follows. The temperature and density profiles in all the channels are estimated as per their power with given inlet coolant temperature and initial guess of mass flow rate. This step is being performed to find out the channel pressure drops with estimated coolant temperature and density distribution. In the steady-state condition, left-hand side term of equation (3.23) should be equal to zero and will result in, $-\Delta p_{dc}(= G_{dc} - F_{dc}W_{dc}^2)$ as a guess for the inertial pressure drop. In natural circulation condition, Δp_{dc} must be equal to Δp_n for the n^{th} channel, or represented as p_{t_s} for all coupled channels. If the guess mass flow rates in the channels are matching with their actual values for the given configuration of steady-state then inertial pressure drop i.e. the term at the left-hand side of equation (3.22) should be zero. Otherwise, channel mass flow rates will be changed as per equation (3.22) assuming that the channels are heated in for pseudo time interval (Δt_s) before starting the steady-state simulation at constant power as follows:

$$S_n \frac{W_n^{t_s+\Delta t_s} - W_n^{t_s}}{\Delta t_s} = -p_{t_s} - G_n - F_n(W_n^{t_s})^2 \qquad \dots\dots\dots (3.27)$$

or,

$$W_n^{t_s+\Delta t_s} = W_n^{t_s} + \frac{\Delta t_s}{S_n} \Delta P_n^{t_s} \qquad \dots\dots\dots (3.28)$$

where,

$$\Delta P_n^{t_s} = -p_{t_s} - G_n - F_n(W_n^{t_s})^2 \qquad \dots\dots\dots (3.29)$$

Thus, with this new set of mass flow rates in the channels, the steady-state density and temperature distribution of the coolant in the channels is computed to find out next $\Delta P_n^{t_s+\Delta t_s}$. This process is iterated for the given pseudo time interval (i.e. before starting transient) in the code or until the convergence of mass flow rates and outlet temperatures of the channels with inertial pressure drops (i.e. $\Delta P_n^{t_s+\Delta t_s}$) become negligibly small (i.e. $\leq 10^{-2}\ Pa$).

(ii) *Estimation of transient mass flow rate distribution in coupled multi-channel*

After estimating the mass flow rates and outlet temperatures of the channels in steady-state (at $t = 0$), the transient simulation is initiated. As all the heated channels of CHTR are connected at the lower and the upper plenum as common points along with downcomers, the coupling of the channels is considered with equal pressure drop criteria in equation (3.22) and (3.23) as follows:

$$\Delta p_1 = \Delta p_2 = \Delta p_3 = \cdots = \Delta p_n = \cdots = \Delta p_{19} = \Delta p_{dc} \qquad \dots\dots\dots (3.30)$$

As mass flow rate of n^{th} channel varies as per equation (3.22), subtracting this equation for 1^{st} channel to the n^{th} channel, the following equation can be obtained:

$$S_n \frac{\partial W_n}{\partial t} - S_1 \frac{\partial W_1}{\partial t} = -\big((G_n + F_n W_n^2) - (G_1 + F_1 W_1^2)\big) \qquad \dots\dots\dots (3.31)$$

it can be written as,

$$S_n \frac{\partial W_n}{\partial t} - S_1 \frac{\partial W_1}{\partial t} = -(P_n - P_1) \qquad \dots\dots\dots (3.32)$$

or,

$$\frac{\partial W_n}{\partial t} = \frac{S_1}{S_n}\left[\frac{\partial W_1}{\partial t}\right] - \frac{1}{S_n}(P_n - P_1) \qquad \dots\dots\dots (3.33)$$

where,

$$P_n = (G_n + F_n W_n^2) \qquad \dots\dots\dots (3.34)$$

Equation (3.33) represents a set of $(N-1)$ equations for N number of coupled channels in the system. Therefore, if the change in mass flow rate is known for any one of the channels, we can estimate the mass flow rates in the rest of the coupled channels at the next time step using equation (3.33). Similarly, adding equation (3.22) for the first channel to the equation (3.23) for the downcomer, we can get the following for the coupling of first channel to DC:

$$S_{dc} \frac{\partial W_{dc}}{\partial t} + S_1 \frac{\partial W_1}{\partial t} = (G_{dc} - F_{dc} W_{dc}^2) - (G_1 + F_1 W_1^2) \qquad \dots\dots\dots (3.35)$$

or,

$$S_{dc}\frac{\partial W_{dc}}{\partial t} + S_1\frac{\partial W_1}{\partial t} = P_{dc} - P_1 \qquad \text{... ... ... (3.36)}$$

Since, $W_{dc} = \frac{\sum W_n}{nDC}$ therefore equation (3.36) is written as:

$$\frac{S_{dc}}{nDC}\sum\left[\frac{\partial W_n}{\partial t}\right] + S_1\frac{\partial W_1}{\partial t} = P_{dc} - P_1 \qquad \text{... ... ... (3.37)}$$

Substituting equation (3.33) in equation (3.37), we can get the following:

$$\frac{S_{dc}}{nDC}\left[\sum\left\{\frac{S_1}{S_n}\left[\frac{\partial W_1}{\partial t}\right] - \frac{1}{S_n}(P_n - P_1)\right\}\right] + S_1\frac{\partial W_1}{\partial t} = P_{dc} - P_1 \qquad \text{... ... ... (3.38)}$$

After rearranging the terms in equation (3.38), the following can be obtained:

$$S_1\frac{\partial W_1}{\partial t} = \frac{(P_{dc} - P_1) + \frac{S_{dc}}{nDC}\sum\frac{1}{S_n}(P_n - P_1)}{\left(1 + \frac{S_{dc}}{nDC}\sum\frac{1}{S_n}\right)} = R^t \qquad \text{... ... ... (3.39)}$$

The mass flow rate in the first channel at the next time step can be estimated with parameter R^t in equation (3.39) at time t. The superscript of R^t is denoting its value at time step t. Therefore, the mass flow rate in the first channel at the next time step $(t+1)$ can be obtained from equation (3.39) as follows:

$$S_1\frac{W_1^{t+1} - W_1^t}{\Delta t} = R^t \qquad \text{... ... ... (3.40)}$$

or,

$$W_1^{t+1} = W_1^t + \frac{\Delta t. R^t}{S_1} \qquad \text{... ... ... (3.41)}$$

For all other coupled heated channels, the mass flow rate at the next step can be estimated from the equation (3.33) as follows:

$$W_n^{t+1} = W_n^t + \frac{\Delta t}{S_n}.\left(R^t - (P_n - P_1)^t\right) \qquad \text{... ... ... (3.42)}$$

For the downcomers, the mass flow rate will be;

$$W_{dc}^{t+1} = \frac{\sum W_n^{t+1}}{nDC} \quad \ldots\ldots\ldots (3.43)$$

Thus the momentum conservation in parallel multi-channel of CHTR for the natural circulation of coolant is solved with the help of equations (3.28), (3.41), (3.42), and (3.43).

Assuming inviscid and incompressible fluid flow (Todreas and Kazimi, 2012), the coolant energy conservation equation in the axial meshes of the channels can be written as:

$$[(\rho_c c_p V_c)^i]\frac{dT_c^i}{dt} = [h^i A_s^i(T_w^i - T_c^i) - W_n {c_p}^i\,(T_c^i - T_c^{i-1})] \quad \ldots\ldots\ldots (3.44)$$

Where, T_c^i and T_c^{i-1} are the coolant and inlet temperatures in i^{th} mesh of length Δx, volume V_c and wall surface area A_s^i. The channel wall temperature in the mesh is T_w^i. The coolant in the mesh has mass flow rate W_n, density ρ_c and isobaric specific heat c_p. The parameter h^i is the heat transfer coefficient in the mesh and is computed with the correlation suggested by Cheng and Tak (2006) at every time step. The axial conduction in coolant mesh is ignored at present. The heat transfer coefficients in the meshes of adiabatic segments are being considered as zero. The heat transfer coefficient has also been assumed as zero for the downcomer segment with heat pipe (primary HX) during the loss of heat sink. Equation (3.44) for the mesh with multi-inlet of different temperatures T_c^j and mass flow rates W_j is modified as follows:

$$[(\rho c_p V_c)^i]\frac{dT_c^i}{dt} = \left[h^i A_s^i(T_w^i - T_c^i) - W_n {c_p}^i\,(T_c^i - \frac{1}{W_n}\sum_j W_j T_c^j)\right] \ldots\ldots\ldots (3.45)$$

The correlations to compute Darcy friction factor f as well as form factors K are taken from OECD-NEA, (2015). The friction factor f depending upon the Reynolds number R_e and channel wall roughness (ϵ) are estimated with following recommended correlations:

$$f = \frac{64}{R_e} \qquad\qquad forR_e < 2000 \quad \text{(laminar flow)}$$

$$= \frac{64}{R_e}.\left[1 + \frac{\left(\frac{R_e}{8}\right)^{12}}{(A+B)^{1.5}}\right]^{\frac{1}{1\,2}} \qquad forR_e \geq 2000 \quad \text{(turbulent flow)} \qquad \dots\dots\dots (3.46)$$

where,

$$A = \left\{2.457.\ln\left[\left(\frac{7}{R_e}\right)^{0.9} + 0.27.\left(\frac{\epsilon}{D_h}\right)\right]\right\}^{16} \qquad \dots\dots\dots (3.47)$$

and,

$$B = \left(\frac{37530}{R_e}\right)^{16} \qquad \dots\dots\dots (3.48)$$

The correlation for friction factor given in equation (3.46) applies to all the ranges of Reynolds number of coolant flowing in the channel with equivalent hydraulic diameter D_h.

The form loss coefficient (or form factor) K_i in i^{th} mesh due to sudden geometry changes at the inlet and outlet of the channels, and also at the position of control/shut-off rod tips in the channels are computed by following correlations (OECD-NEA, 2015):

a. *Sudden flow area contraction:*

$$K_{sc} = 0.5 \times \left(1 - \frac{A_1}{A_0}\right)^{\frac{3}{4}} \text{for} R_e \geq 10^4 \ \text{ where } \ A_0 > A_1 \ \dots\dots\dots (3.49)$$

b. *Sudden flow area expansion*:

$$K_{se} = \left(1 - \frac{A_0}{A_1}\right)^2 \text{ for } R_e \geq 3.3 \times 10^3 \ \text{ where } \ A_0 < A_1 \ \dots\dots\dots (3.50)$$

The temperature-dependent thermo-physical properties of the LBE coolant at each time-step are considered as discussed in the previous section. Graphite is used as the fuel tube, axial reflector and fuel compact matrix material in the CHTR. The temperature-dependent thermo-physical properties of graphite such as thermal conductivity and specific heat capacity (for temperature: 300 ≤ T ≤ 3000 °K) are being considered in the code with following correlations in equations (2) and (3) (ASTM C781-08, 2014; McEligot et al. 2016; OCED-NEA, 2017);

$$k_g = 134.0 - 0.1074\,T + 3.719 \times 10^{-5} T^2 \qquad \dots\dots\dots (3.51)$$

$$c_{p_g} = \frac{1}{11.07\,T^{-1.644} + 0.0003688\,T^{0.02191}} \qquad \dots\dots\dots (3.52)$$

Here, temperature T in the equation (3.51) is considered in °C. The temperature dependent thermal conductivity of beryllium oxide (BeO) is considered as per the data published in TABLE 4.17 of the IAEA-THPH, 2008. The temperature dependent specific heat capacity of BeO as moderator and reflector in the CHTR are being computed as follows correlation in equation (4) (IAEA-THPH, 2008);

$$\begin{aligned} c_{p_{BeO}} &= 1.455 + 0.606 \times 10^{-3}\,T - 5.44 \times 10^{5} T^{-2} && \text{at } 298 \le \mathrm{T} < 1200\ ^{\circ}\mathrm{K} \\ &= 1.791 + 0.201 \times 10^{-3}\,T && \text{at } 1200 \le \mathrm{T} \le 2820\ ^{\circ}\mathrm{K} \end{aligned} \qquad \dots\dots (3.53)$$

The effective specific heat of fuel compacts in CHTR is computed with the scheme based on the balance of energy and the smeared density with balance of mass (Strydom, 2018). In CHTR, the volume packing fraction of TRISO in fuel compacts is high (~ 42%). Therefore, effective thermal conductivity (ETC) of TRISO fuel compacts is estimated by the Chiew and Glandt model, which predicts accurate ETC (Folsom et al. 2015), which is as follows:

$$k_e = k_m \left(\frac{1 + 2\,\beta\,\phi + (2\beta^3 - 0.1\,\beta)\phi^2 + \phi^3 0.05 \exp(4.5\,\beta)}{1 - \beta\,\phi} \right) \qquad \dots\dots\dots (3.54)$$

where k_m is the temperature-dependent thermal conductivity of the graphite matrix and ϕ is the volume packing fraction of TRISO particles in fuel compacts. The parameter β ($= \frac{\mathrm{K}-1}{\mathrm{K}+2}$) is the reduced polarizability as a function of parameter K. Here, K is the ratio ($\frac{k_p}{k_m}$) of the thermal conductivity of the dispersed phase (TRISO particles, k_p) to the continuous graphite matrix (k_m). The ETC of TRISO fuel compacts computed with equation (3.54) is applicable for K ranging from 10^{-3} to 10^4; ϕ from 15% to 85% very well and the model represents close to the actual case of randomly-distributed particles in compacts (Folsom et al., 2015).

The developed TH module in multi-physics code ARCH-TH is capable of simulating the ***natural circulation of single-phase coolant in a single loop as well as the coupled multi-channel system***. In the TH module, the energy balance equations are being solved in the primary circuit only with a given inlet temperature of the coolant, i.e. further development for consideration of secondary side heat balance equations is in progress. The TH model in the code for natural circulation is validated with the experimental data obtained from KTL operation (Borgohain et al., 2016). The benchmark qualifications of TH capabilities in the code are discussed in the subsequent Chapter 4. The TH capability has been used to study the unprotected loss of reactivity regulation as well as the loss of heat sink accidents in CHTR under the natural circulation of LBE coolant, which are discussed in detail in Chapter 5 and Chapter 6 (Dwivedi et al., 2018 and 2020).

3.5. Temperature dependence of cell homogenized group parameters for feedbacks

The homogenized few-group cross-section parameters of the fuel assemblies in CHTR are being varied as per the change in temperatures of the fuel, moderator and coolant during the transient for reactivity feedbacks. The set of these parameters are generated by code ITRAN at different temperature of the material in the intervals of 50 to 100°C in the whole-range of the transient. For example, for fuel temperature feedback, T_{fuel} ±400°C data-set is generated keeping the moderator and coolant temperatures unchanged where T_{fuel} is the average temperature of the fuel in operating configuration. Similarly, the data-sets are being generated separately for moderator and coolant temperature feedbacks keeping the other materials' temperature unchanged. These data-sets for the fuel, moderator and coolant are given as inputs to the code ARCH-TH for their reactivity feedbacks in simulations. Therefore, according to the average temperature of the material in the axial mesh of assembly/ channel, the cross-section parameters are linearly interpolated (and extrapolated when it is lying outside the range of input temperature data-set) with following worked out formula:

$$\Sigma_{k,g}^{n}(t+\Delta t) = \Sigma_{k,g}^{n}(t) + \sum_{m}\left[\frac{\Sigma_{k,g}^{m}(i+1) - \Sigma_{k,g}^{m}(i)}{T^{m}(i+1) - T^{m}(i)}\right] \times \left[T^{n,m}(t+\Delta t) - T^{n,m}(t)\right] \ldots\ldots\ldots (3.55)$$

where, $\Sigma_{k,g}^{n}(t)$ is the macroscopic cross-section parameter in n^{th} mesh at time t, for k-type interaction in g^{th} energy group of neutrons. $T^{n,m}(t)$ is the average temperature of the material of type m (i.e. fuel, moderator or coolant) in n^{th} mesh at time t where average temperature is $T^{m}(i) \leq T^{n,m}(t) < T^{m}(i+1)$. The parameters $\Sigma_{k,g}^{m}(i)$ is the cross-section parameter for k-type interaction for g^{th} energy group of neutrons at temperature $T^{m}(i)$ of material type m. These are the given input data-sets where i is the index for temperature of the generated data-set. The group diffusion coefficients are being also changed as per the equation (3.55) where $\Sigma_{k,g}^{n}(t)$ is being replaced by $1/D_{g}^{n}(t)$. It is suggested to prepare data-sets of cell homogenized cross-sections by transport-based lattice code for the whole range of temperatures of the materials during transients at small temperature intervals, for better prediction of feedbacks. The linear interpolation scheme with generated data-sets at small temperature intervals is found to be admissible and computationally efficient. However, the temperature change of the macroscopic cross-section parameters can be considered with the higher order interpolation scheme or fitted formula with these generated data-sets in future.

The code ARCH-TH has been developed to consider the fuel, moderator and coolant temperature feedbacks under steady-state as well as during core transients. The neutronics in the code predicts detailed power level and its profile in the core during steady and transient conditions, which is being passed to the TH module at each macro-time step by so-called marching scheme (Gupta and Kannan, 2017). As per the instantaneous power distribution in the core, the TH module predicts temperatures in the fuel, moderator and coolant in each of the fuel assemblies/ channels in core like CHTR and change in the value of average temperature passes to neutronics for temperature feedbacks.

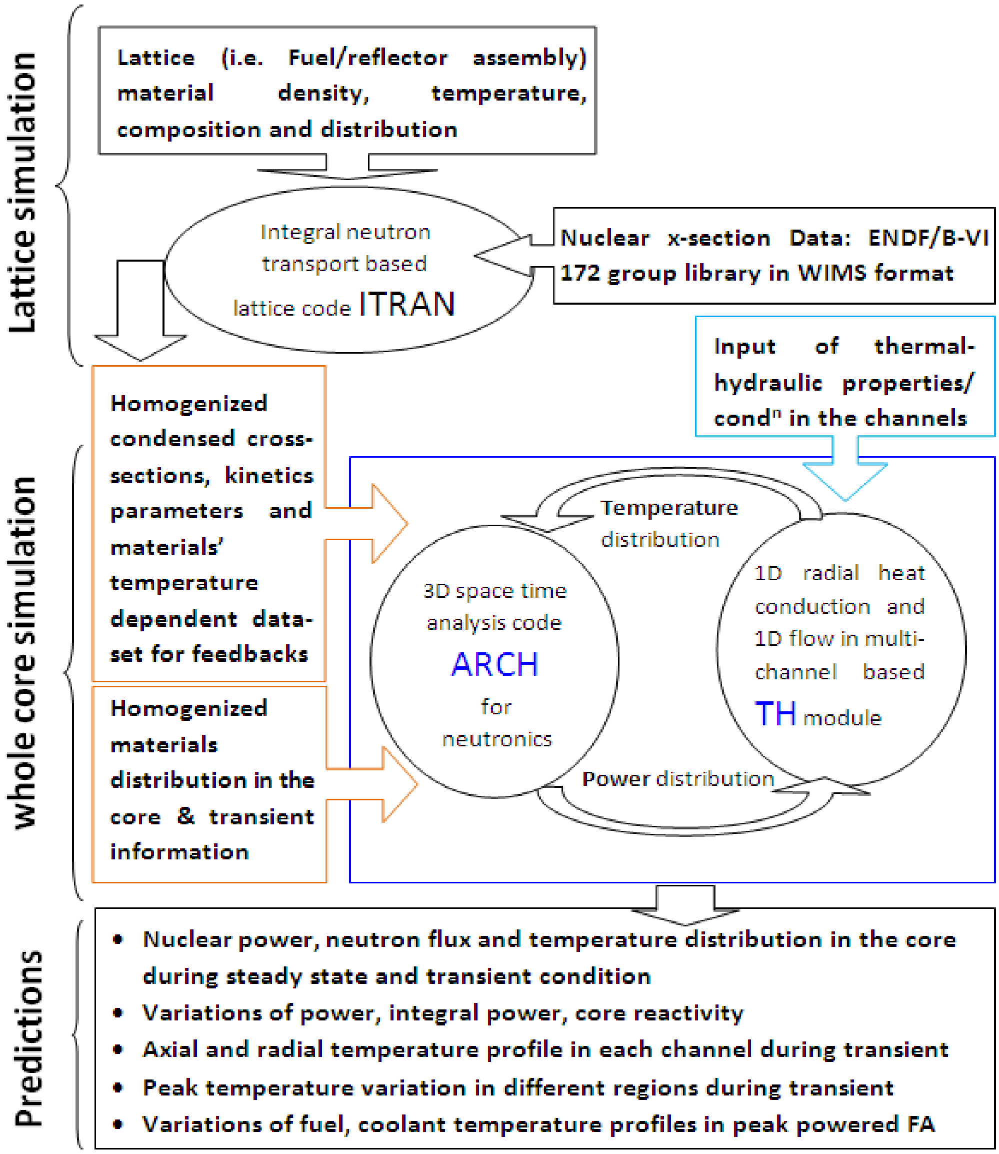

Figure-3.4: Model of calculations in deterministic 3D multi-physics code ARCH-TH

As the marching scheme of N-TH coupling requires smaller time steps, the nested scheme (i.e. Picard iteration) can be incorporated in future for higher accuracy in the transient predictions (Gupta and Kannan, 2017). The module also predicts pressure drops as well as mass flow rates, outlet temperatures of the channels under natural circulation. The computational model of multi-physics code ARCH-TH is illustrated by the flow-chart given in Figure -3.4. The user has the option to consider any of the material temperature feedback separately as well as together. The ATWS in CHTR has been studied and discussed with different feedbacks in Chapter 5.

3.6. The scheme of N-TH coupling in code ARCH-TH

The operator-split (OS) method is a traditional coupling approach and widely applied to couple the neutronics (N) and thermal-hydraulics (TH) codes (Wang et al. 2020). The integrated TH module is internally coupled through the OS method with the 3D neutronics code ARCH and extended code is named as ARCH-TH (Figure- 3.4). It means that the ARCH neutronics module is solving 3D space-time multi-group neutron diffusion equations with delayed neutron precursors' equations to predict the flux/ power profile in the core at the given steps of the transients. Then, it passes the information of core power generation rate to the TH module to consider the heat source effect on temperature, mass flow rate and pressure distributions in the core during the solution of respective governing equations. Then, the changes in macroscopic cross-sections due to variation occurred in the material temperatures are computed. This temperature effect on macroscopic cross-sections passes to code ARCH to estimate the reactivity feedbacks to subsequent time steps in the simulation.

In the data exchange in OS coupling, some memory can be released after the calculation by each physics code/ module. Therefore, the memory requirements are low. Moreover, the coupled system is developed by passing the coupling parameters. Hence, there is no much need to modify the sub-physics codes, resulting in coupling implementation easier. The OS coupling approach is advantageous because minor modifications are required to the existing code like ARCH, which is well developed, validated and long-used for single physics analysis, i.e. 3D space-time neutronics. Also, both the physics code/ modules, i.e. ARCH and

TH in code ARCH-TH, can be validated combined and separately with suitable benchmark problems and experiments in the particular physics domain.

In the OS coupling, physical parameters of one domain lag with other (i.e. TH parameters to consider feedbacks for instantaneous power prediction in ARCH-TH). Therefore, predictions of non-linear transients with the code would be lesser accurate than any tightly coupled code system, e.g. KARMA (Ragusa et al., 2010) and MOOSE (Gaston et al., 2015). The tightly coupled simulation tools are developed using Newton's methods like Jacobian Free Newton-Krylov (JFNK) (Mahadeven and Ragusa, 2007), where all the physical parameters are solved and updated synchronously. To higher accuracy in predictions, Picard iteration (i.e. Nested marching) could be applied in code ARCH-TH. It requires an outer iteration loop between the two physics fields (i.e. ARCH and TH) at each time step, where data exchange will be repeated until the achievements of desired convergence of physical parameters of both the fields. However, the iteration will be a CPU time-consuming calculation, which will affect the computational efficiency.

3.7. A short overview on multi-physics tools for the study of HTRs

The various physical phenomena occurring at different scales in prismatic and pebble-bed core designs of high-temperature reactor require multi-physics tools to accurately predict the core behaviours and the safety margins during operations as well as postulated accidental scenarios (Gerwin et al., 1989; OECD/NEA, 2005; Reitsma et al., 2006; Strydom et al., 2010; Ortensi et al., 2011; Avramova et al., 2015; OECD/NEA, 2019). The development of several such code packages/ multi-physics tools have been reported in the literature. The 3D thermal-hydraulics solver for pebble bed reactor was developed and coupled to the 3D kinetics code PARCS to perform coupled reactor simulations of reactors like PBMR-400 (Seker and Downar, 2007). The coupled neutronics-TH study is reported for pebble-bed HTR with DALTON-THERMIX code system (Boer et al., 2008). The development of the NEM/

THERMIX coupled code system is also attempted for simulations of pebble bed HTRs (Gougar, 2006; Mkhabela 2010). The nodal diffusion code DYN3D comprising a thermal-hydraulics model for flow in parallel coolant channels has been modified as DYN3D-HTR for 3D steady-state and transient analysis of helium-cooled prismatic block-type high-temperature reactors (Rohde et al., 2012). The multi-physics code system PHISICS/RELAP5-3D has been developed and validated for reactor benchmark on the prismatic core of MHTGR-350 (Strydom, 2016). The code MCS based on the Monte Carlo neutron transport was coupled with thermal-fluid code GAMMA+ to the multi-physics analysis of the prismatic core of high-temperature gas-cooled reactor (Lemaire et al., 2017). These multi-physics tools have been developed and are used for design and safety analyses of forced circulation gas-cooled pebble-bed and prismatic HTRs. The natural circulation design of Indian HTR cores such as CHTR requires the multi-physics tool to accommodate the peculiar design features. The beryllium oxide as a high-temperature moderator and thorium-based TRISO fuel with a high packing fraction in the core also need special attention in the simulation. Therefore, 3D multi-physics code ARCH-TH is developed and validated for design and safety studies of Indian HTRs, e.g. CHTR (Dwivedi et al., 2017 and 2020).

3.8. Conclusion

The designs of HTR require special attention and capability to simulated multi-physics phenomena in the core during the normal operations and transients. The Indian design of CHTR consists of additional safety features, e.g. core heat removal by natural circulation of LBE coolant during normal operations. A 3D multi-physics code ARCH-TH has been indigenously developed to analyse the design and safety transients in Indian HTR concepts such as CHTR. The code has been integrated with TH capabilities including models like simple adiabatic heating of the fuel as well as to simulate the natural circulation phenomena in the coupled multi-channel of CHTR core. The viability of the developed multi-physics code has been checked with benchmark validations as well as comparison with experimental data of natural circulation studies in LBE based high-temperature loop. The benchmarks and validation results of the code, have been discussed subsequently in Chapter 4. The safety transients of CHTR have been studied using the multi-physics code ARCH-TH and subsequently reported in the literature. The multi-physics studies of reactivity initiated transients, as well as perturbation caused by the change in TH conditions in CHTR core, are detailed discussed in Chapter 5 and Chapter 6 of the present thesis. The TH modules in the code can consider single-phase coolant flow in the channels at present. It is also planned to augment the TH modules for two-phase flow of coolant to enhance the in-house multi-physics capability for advanced designs of Indian water-cooled reactor. The plan for future development in the TH capability of ARCH-TH is discussed in detail in Chapter 7.

CHAPTER 4

BENCHMARK VALIDATIONS OF 3D MULTI-PHYSICS CODE ARCH-TH

4.1. Introduction

Verification and validation are the primary means to assess the accuracy and reliability of developed computational tools with its modelling and methods. These procedures are the basis to improve the credibility of simulations in several high-consequence fields, such as nuclear reactor safety (Oberkampf and Trucano, 2008). Designing a nuclear reactor and evaluating its safety levels have been tightly inter-linked for safe, reliable and economical operation of the related power plant. The modelling of multi-physics phenomena in complex systems (e.g. HTRs) may require approximations and simplifying assumptions, which brings up the importance of benchmark validations as a complementary activity to ensure the viability and correctness of the developed multi-physics code (D'Auria and Lanfredini, 2019). The indigenously developed reactor physics codes for design analysis and safety evaluation of Indian reactor concepts have also been validated against international benchmarks as well as with other codes for specific options (Gupta and Kannan, 2017).

The 3D multi-physics code ARCH-TH has been developed for design and safety analyses of Indian concepts of HTR. The integrated neutronics (N) and thermal-hydraulics (TH) capabilities in the code have also been qualified for accuracy and viability by simulations of benchmark problems as well as for the natural circulation of LBE in the experimental loop (KTL) operated at BARC (Dwivedi et al., 2017 and 2020; Borgohain et al., 2016).

An international benchmark activity on coupled N-TH analysis of prismatic helium-cooled MHTGR transients has been started in 2011 and has completed the initial phases with limited participation of experts from OECD member countries (Ortensi et al., 2011 and OECD, NEA

2017). The coupled neutronics- thermal-hydraulics benchmark on prismatic HTR transient is not yet available in the open literature, especially related to core design with natural circulation of coolant. The 3D multi-physics code ARCH-TH developed for Indian HTR concepts like CHTR have been validated with suitable benchmark problems on reactor transients and thermal-hydraulics as listed in Table-4.1.

Table-4.1: List of benchmark simulated for the validation of ARCH-TH

Sl. no.	Benchmark	Physics*	The compared parameters	References
1	AER-Dyn-001	N	Control rod worth, variation of power and reactivity in the transient, steady and transient power profile	Kereszturi et al., 1992 and 2000
2	AER-Dyn-002	N + T	Variation of power, reactivity, fuel temperature and power peaking in the transient, power distribution	Grundmann and Rossendorf, 2000
3	OECD/WPPT ADS benchmark Phase-I	TH + PK (no decay heat)	Temperatures of fuel, clad and coolant of average fuel pin/rod in XADS under steady state and beam interruptions	D'Angelo and Gabrielli, 2003
4	OECD/WPPT ADS benchmark Phase-II	TH + PK (with decay heat)	Temperatures of fuel, clad and coolant of average and hottest pins in XADS and MYRRHA under steady state and beam interruptions	D'Angelo and Gabrielli, 2004
5	*KTL experiments* for LBE natural circulation (NC)	TH	Temperatures and mass flow rate under steady and transient NC of LBE compared with experimental data	Borgohain et al., 2016

* N: Neutronics based on 3D space-time, T: Thermal, TH: Thermal-hydraulics, PK: point kinetics

The 3D space-time neutronics in ARCH-TH has been validated with benchmarks listed at serial number 1 and 2 (Table-4.1). The benchmark problems listed from serial number 1 to 4 are the designed reactor transient for code-to-code validation purposes. The heat conduction based TH in the code is validated with experimental data and ADS benchmarks (sl. no. 3 to 5). The benchmark results of the code are discussed in the following sections.

4.2. Neutronics validation of code ARCH-TH for reactor transients

The ARCH-TH code with IQS module for transient has been validated with the benchmark analysis of hexagonal lattice-based thermal reactor transient without any temperature feedback (AER-Dyn-001) as well as transient with adiabatic Doppler feedback (AER-Dyn-002). The results of the code have been compared with others in the following sub-sections.

(i) *AER benchmark of reactor transient without feedback (AER-Dyn-001)*

This benchmark problem deals with the case of asymmetric control rod ejection transient without any feedback in VVER-440 type geometry (Kereszturi et al., 1992). In the benchmark, initially, the core is critical at very low power (~zero) and power rise during transient is not very large (i.e. no change in core temperatures). The transient is initiated due to asymmetric control rod ejection followed by the activation of the shut-down system. The control rod is assumed to be ejected in the transient with a constant speed (Figure-4.1).

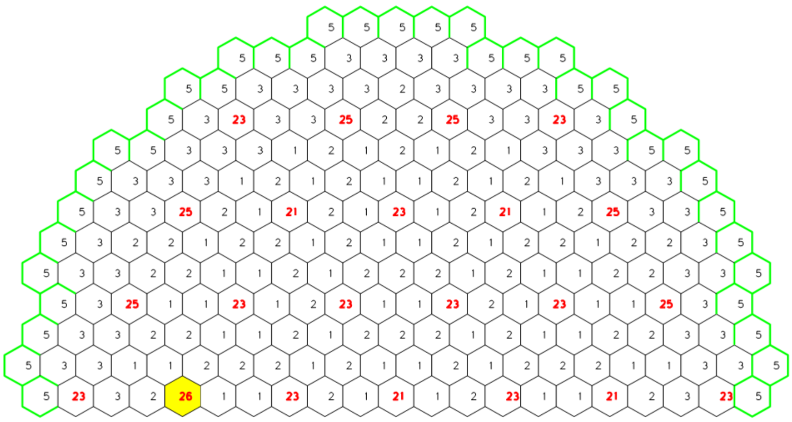

Figure-4.1: Half- core map in AER-Dyn-001 (the ejected rod marked as 26)

All the cross-sections and input parameters of the core are taken as given in the benchmark (Kereszturi et al., 1992). Steady-state simulation with ARCH-TH code shows that the reactivity worth of ejected control rod is 0.00484 as compared to 0.00482 (in k) with KIKO3D code (Dwivedi et al., 2017). The power variation during transient has been computed and compared with code KIKO3D and DYN3D (Kereszturi et al., 2000). The results obtained in neutronics simulations with IQS module are found to be matching well with reference results (Figure-4.2). It is observed that after 3.0 s of the transient (Figure-4.2), even with 1.0 s of macro-time steps in the simulation with IQS module in the code, the results are matching well, which indicates that the code could perform transient simulations efficiently with sufficient accuracy. The variations of core reactivity during transient have been predicted and are found to be in good agreement with KIKO3D (Figure-4.3). The axial power distribution in the given fuel assembly at various moments of the transient with ARCH-TH has also been predicted and compared (Figure-4.4).

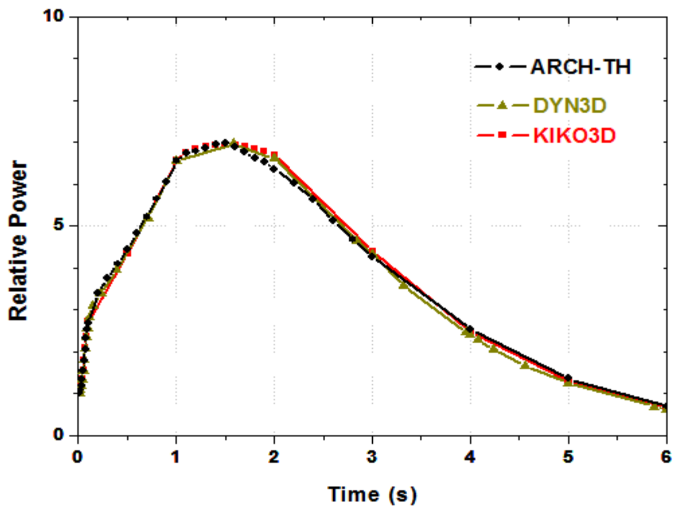

Figure-4.2: Variation of power with time in AER-Dyn-001

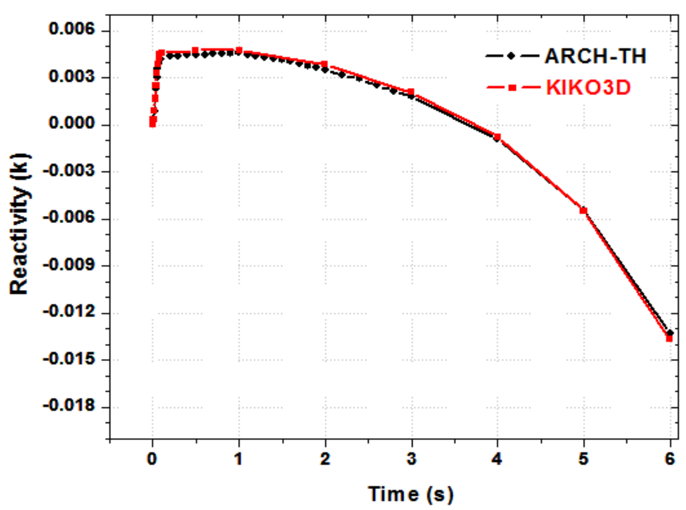

Figure-4.3: Variation of reactivity with time in AER-Dyn-001

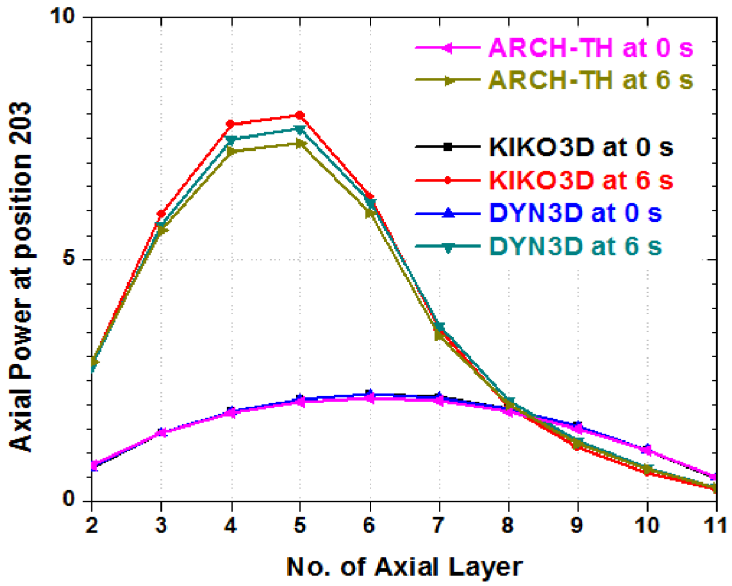

Figure-4.4: Axial power distribution in the 2^{nd} neighbour FA of the ejected rod at $t = 0$ and $t = 6\ s$

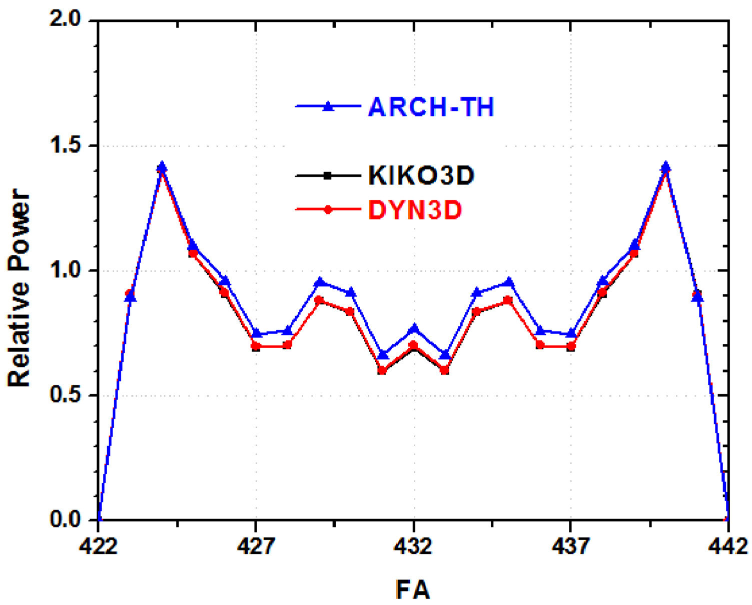

Figure-4.5: Normalized radial power distribution at $0\ s$ in 3^{rd} axial plane (ejected rod in 426)

The normalized radial power distributions have been estimated with ARCH-TH and compared for a given axial plane during the transient as shown in Figure-4.5 and 4.6. These results show that the core differential parameters like power/ flux distributions predicted by ARCH-TH are in good agreement with others (Dwivedi et al. 2017).

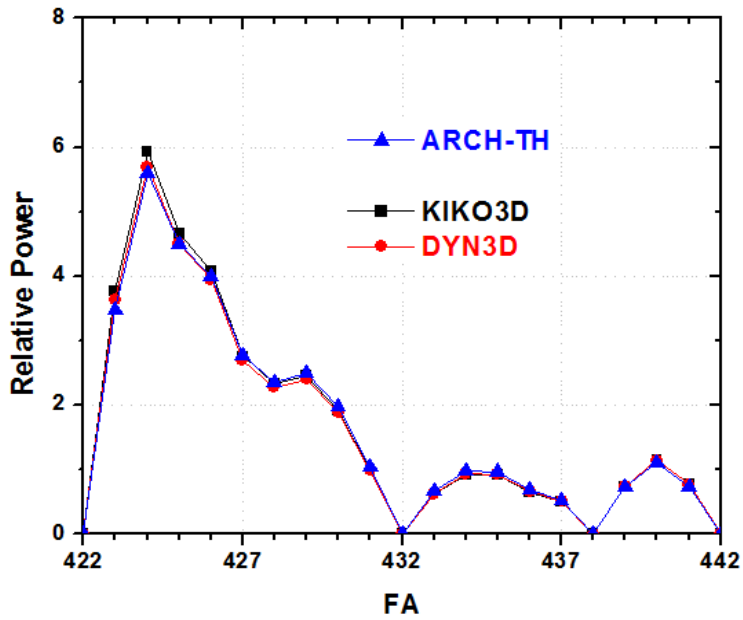

Figure-4.6: Normalized radial power distribution at $6\ s$ in 3^{rd}axial plane

(ii) *AER benchmark with adiabatic Doppler feedback (AER-Dyn-002)*

The Doppler feedback capability with adiabatic fuel heating model in ARCH-TH has been validated with VVER-440 based transient benchmark AER-Dyn-002 (Grundmann and Rossendorf, 2000). In the benchmark problem, the transient is initiated by the ejection of the eccentric rod (of reactivity worth \$ 2.0) in $0.16\ s$ at hot zero power during the end of core-life-cycle (Figure-4.7).

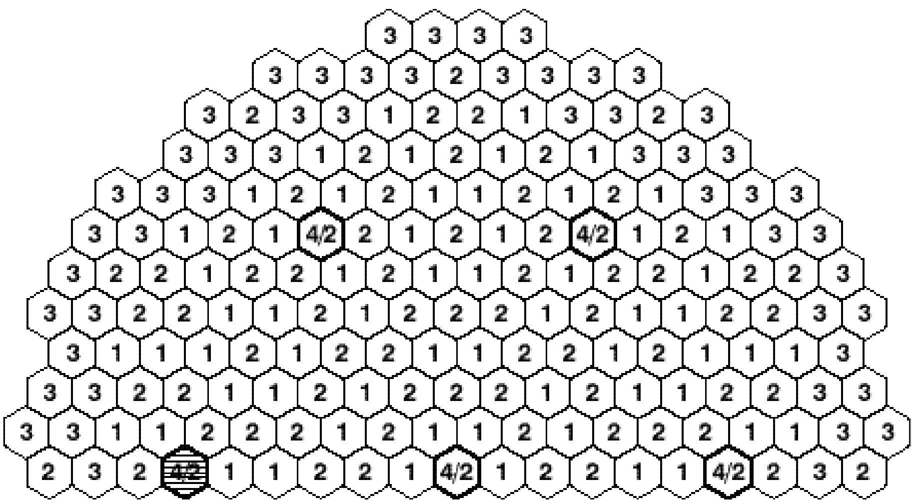

Figure-4.7: Core map with the fuel types (absorbers of bank K6 at positions of types 4/2)

The initial reactor power is taken as 1.375 kWt. The control rod removal speed is considered as 12.5 m/s. The feedback mechanism is based on the adiabatic increase of fuel temperature from the initial value of 260°C. The cross-section parameters and feedback formalism are also considered as per the given in the benchmark. The excess heat produced in the fuel is not to be removed during the transient. The fuel temperature feedback passively controlled rise in power during the transient. The transient is observed up to 2 s, and predictions of code ARCH-TH have been compared for this non-linear reactor transient case (Dwivedi et al., 2017). The results of ARCH-TH are found to be in good agreement with other codes (Grundmann and Rossendorf, 2000). The variation of nuclear power (Figure-4.8), peak fuel temperature (Figure-4.9), time integral power (Figure-4.10), core reactivity (Figure-4.11) have been predicted and found to be matching very well with code KIKO3D (Kereszturi et al., 2009). The variation of power peaking factor in the core is also computed and found to be matching well with DYN3D (Figure-4.12).

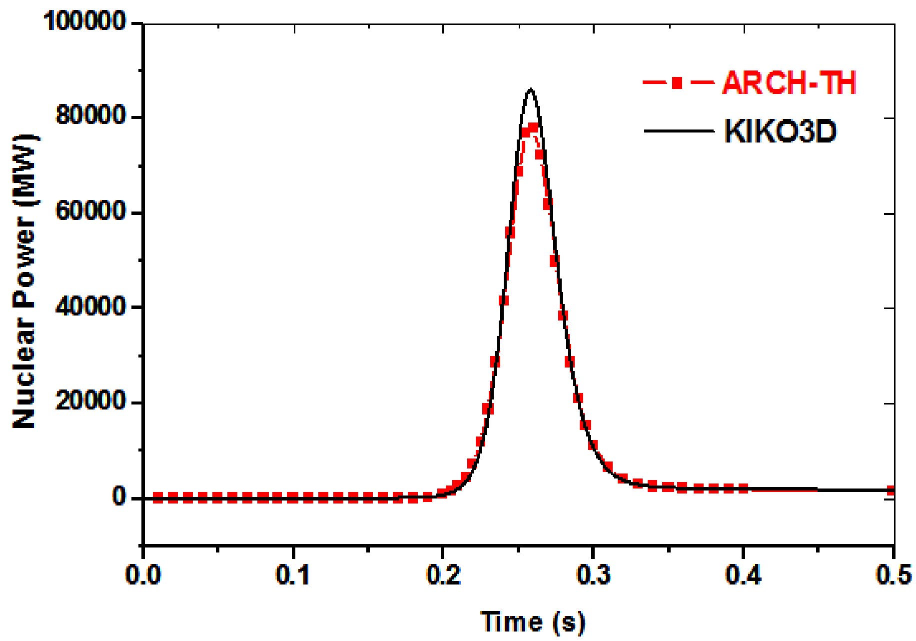

Figure-4.8: Nuclear Power variation with time in AER-Dyn002 benchmark

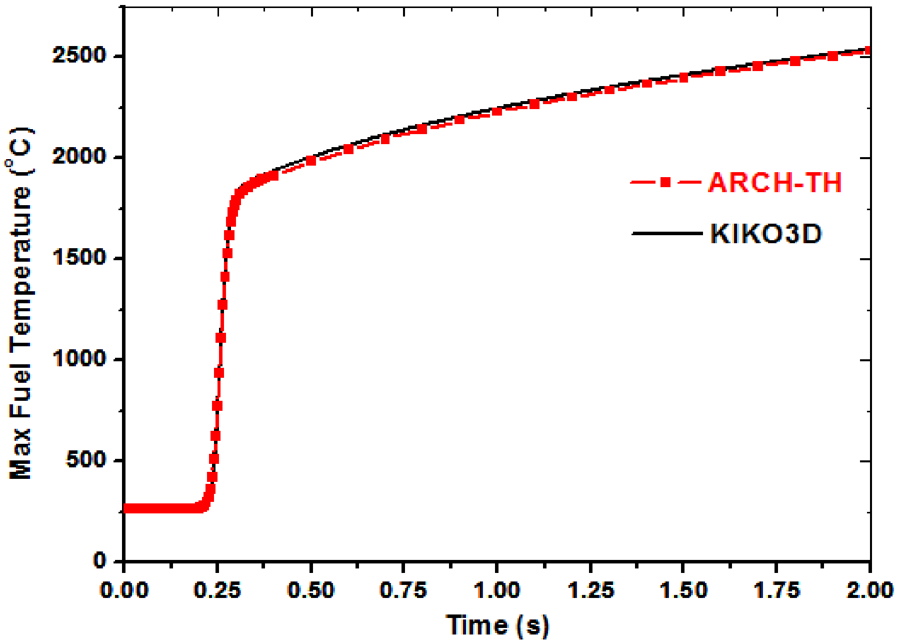

Figure-4.9: Variation of peak fuel temperature

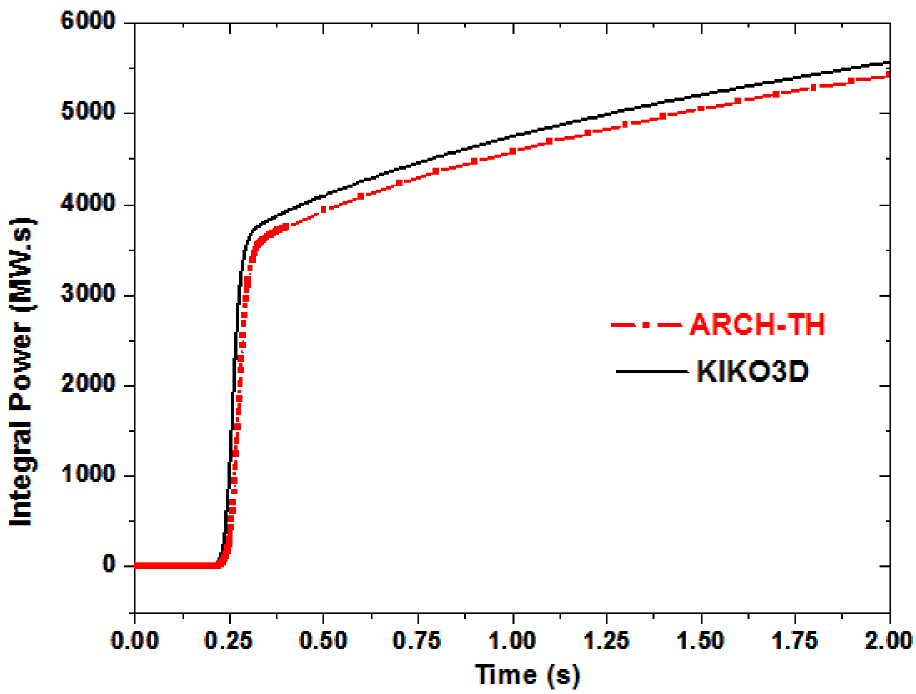

Figure-4.10: Variation of integral power with time

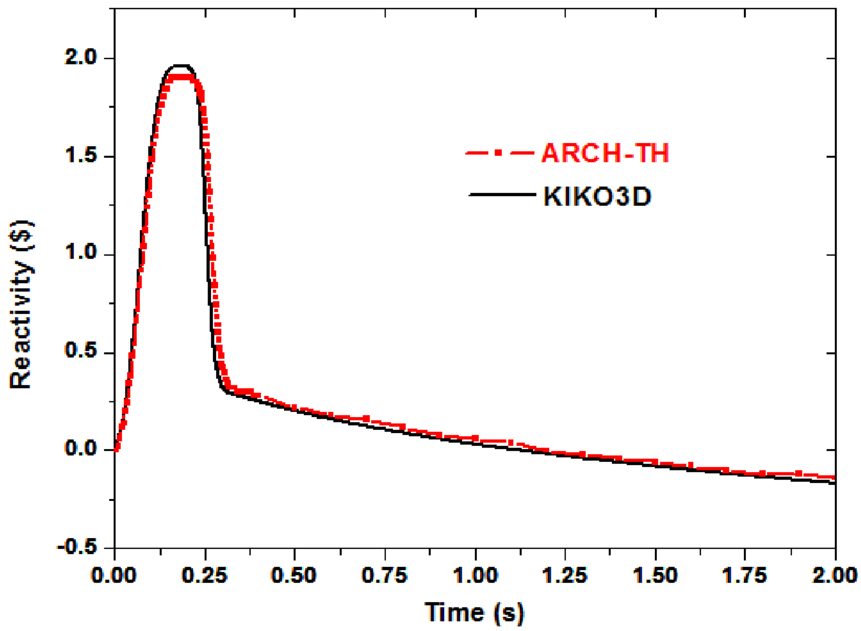

Figure-4.11: Variation of core dynamic reactivity

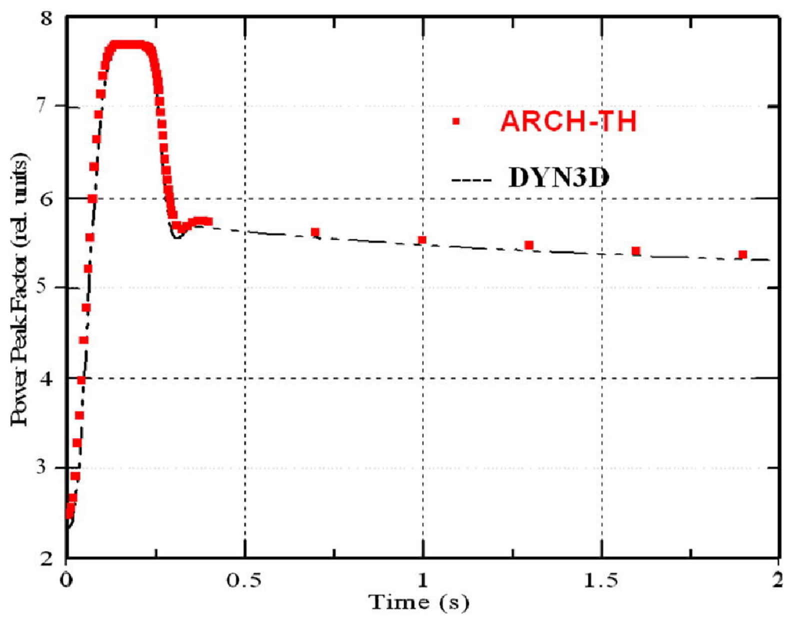

Figure-4.12: Variation of power peaking factor

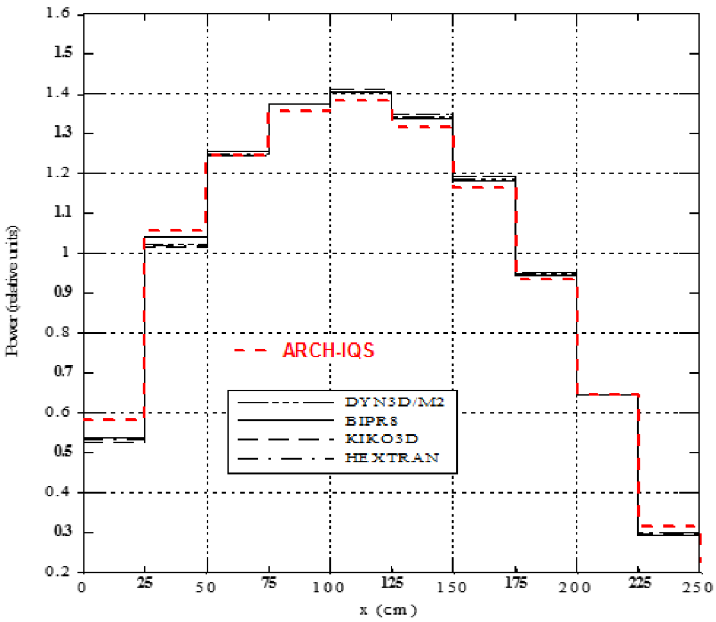

Figure-4.13: Normalized axial (radially averaged) power distribution at $t = 0\ s$

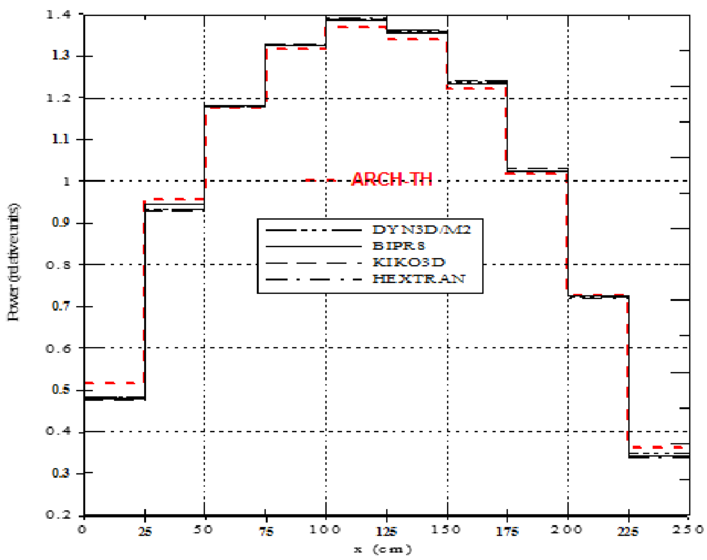

Figure-4.14: Normalized axial (radially averaged) power distribution at $t = 2.0\ s$

The normalised radially averaged axial power distribution during initial steady-state (t=0 s, Figure-4.13) as well as after 2 s of the transient (Figure-4.14), have been compared and observed to be in good agreement with other codes. In the literature, analysis of the AER-DYN-002 is reported for validation of the coupled codes RELAP5-3D/PHISICS for multi-physics studies of helium-cooled prismatic MHTGR-350 (Balestra et al., 2016 and 2020). It is observed that the results of code ARCH-TH are lying within the predicted uncertainty envelop for the benchmark by RELAP5-3D/PHISICS reported in Balestra et al., (2016).

The 1D-radial heat conduction based TH module in code ARCH-TH is developed for the study of multi-physics phenomena during steady and transients of single-phase LBE cooled system. The TH module has been also optionally coupled with point kinetics and then validated with benchmark problems of steady-state and beam-trip transients in LBE cooled XADS and MYRRHA (Dwivedi et al., 2017 and 2020). The predictions of the module have been compared with the reference results as discussed in the next section.

4.3. Benchmark qualifications of 1D- radial heat conduction based TH module

The 1D-radial heat conduction based TH module in ARCH-TH is primarily developed for the steady and transient analyses of single-phase molten metal (i.e. LBE) cooled reactor design, e.g. CHTR. The TH module integrated with point kinetics (PK) has been validated with benchmark analysis based on beam interruptions in LBE-cooled subcritical systems (D'Angelo and Gabrielli, 2003 and 2004). The same point kinetics solver is being utilized for solution of amplitude equations in IQS module of ARCH-TH code. The TH module in the code has been validated for the benchmark cases without and with decay heat considerations during transients, and results are compared and discussed in the following sub-sections.

(i) *The benchmark transients without consideration of decay heat*

The OECD/WPPT benchmark is designed for the steady-state operation as well as beam interruptions transients in LBE cooled, MOX fuelled eXperimental Accelerator Driven sub-critical design (XADS) (D'Angelo and Gabrielli, 2003). In the first exercise of the benchmark, the transients have been predicted without consideration of decay heat in simulations. The parameters and input data are taken for the TH module as provided in the benchmark report (D'Angelo and Gabrielli, 2003).

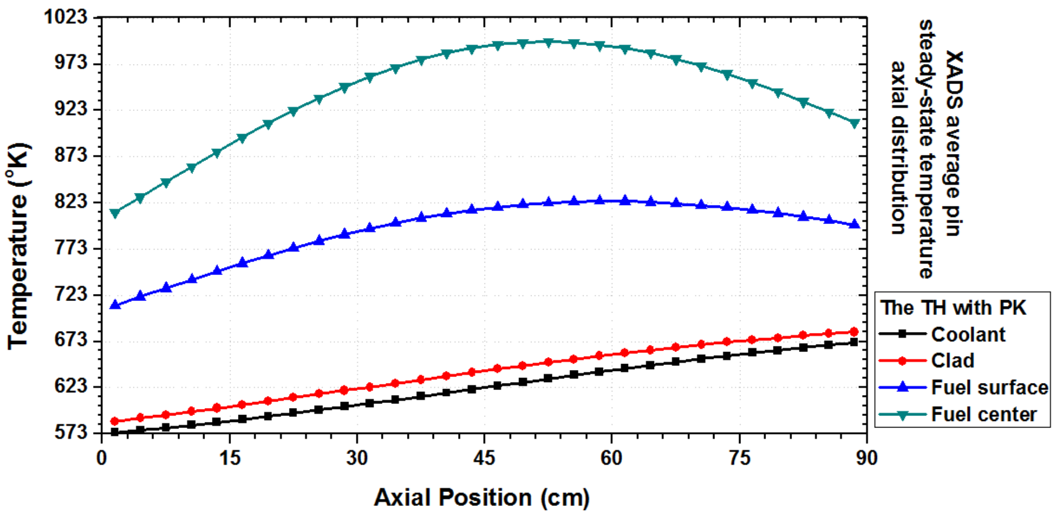

Figure-4.15: Steady axial temperature profile of the XADS benchmark with the TH module

The predictions of the TH module are compared for the steady-state axial temperature profile of fuel centreline, fuel-surface, clad-surface and LBE coolant of average powered pin in the design (Figure- 4.15). The beam interruptions transients have also been simulated with the TH module and temperature variations of fuel centreline at the mid-axial plane (Figure-4.16) and coolant outlet (Figure-4.17) have also been compared (D'Angelo and Gabrielli, 2003; Dwivedi et al., 2017). The beam as the source in XADS design is assumed to be interrupted for $1, 3, 6$ and $12\ s$ intervals and for an indefinite trip for the transients. The predictions of the TH module have been found in good agreement with the reference results (Dwivedi et al., 2017) reported for the benchmark (D'Angelo and Gabrielli, 2003). This benchmark exercise does not consider decay heat generation during beam interruptions, which will affect the change in temperatures and reactivity feedbacks. However, in the second exercise of the benchmark, consideration of decay heat during beam interruptions is reported in addition to computation of changes in temperature of peak powered pin of XADS and also in MYRRHA design (D'Angelo and Gabrielli, 2004), which are discussed in the next sub-section.

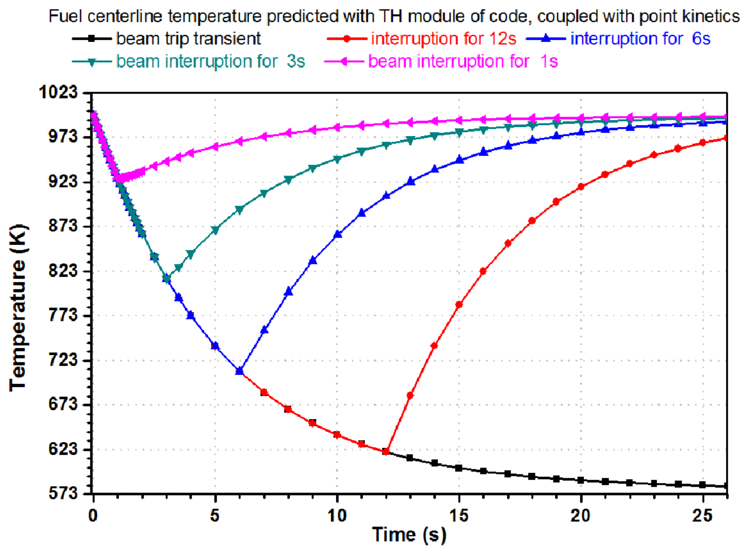

Figure-4.16: Fuel centreline temperature variations for beam interruptions in the benchmark

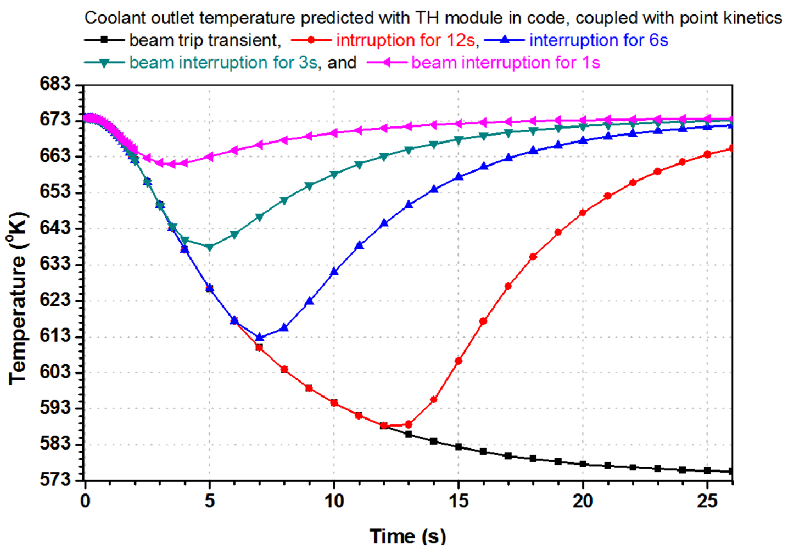

Figure-4.17: Coolant outlet temperature during beam interruption transients

(ii) *The benchmark transients with decay heat consideration*

The TH capability in ARCH-TH code has also been validated with the OECD/WPPT beam-interruption benchmark cases in ADS designs- XADS and MYRRHA (D'Angelo and Gabrielli, 2004) with consideration of decay heat during the transients. In the benchmark analysis, the variation of power due to decay heat is considered as per the correlations available in Todreas and Kazimi (2012). The input data and other TH correlations are taken as reported in the benchmark (D'Angelo and Gabrielli, 2004) for steady-state and transient simulations of LBE cooled, MOX fuelled assemblies of XADS and MYRRHA. The steady-state axial temperature profiles in the average, as well as the peak powered pins/rods in XADS and MYRRHA designs, are predicted for comparisons as shown in Figure-4.18 and Figure-4.19 respectively. The centreline temperature in the transients due to beam-interruption of 1 and 6 s in XADS and MYRRHA are compared in Table-4.2 and Figure-4.20. The predictions of the TH module (Dwivedi et al., 2020) are found to be matching well with other reference results reported in D'Angelo and Gabrielli (2004).

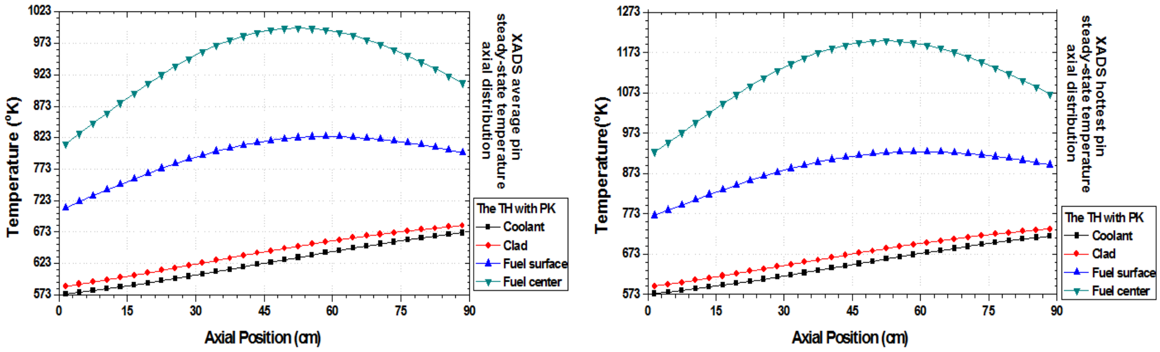

(a) average pin **(b)** hottest pin

Figure-4.18: Steady-state XADS axial temperature profiles predicted by the TH module in (a) average and (b) hottest pin

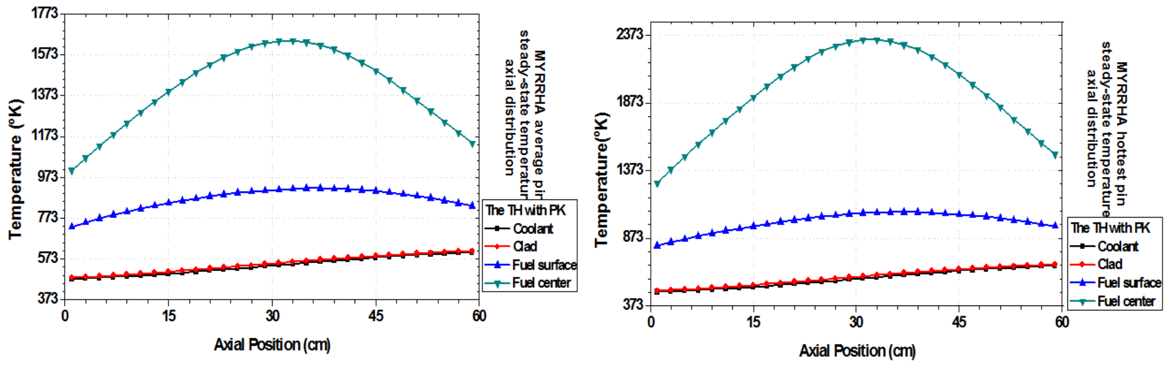

(a) average pin **(b)** hottest pin

Figure-4.19: Steady-state MYRRHA axial temperature profiles predicted by the TH module in (a) average and (b) hottest pin

In Table-4.2, the results of TH module are observed as well within the deviations reported in the benchmark reference values. These benchmark exercises are simulated with a given inlet temperature and mass flow rate (either outlet temperature) of LBE coolant in the system. The TH module for natural circulation in ARCH-TH code solves coolant momentum equations for the steady-state and transient mass flow rate of coolant in the natural circulation system. The natural circulation simulation capability in the code has also been validated by comparing its predictions with experimental data obtained from LBE based loop, which is presented in the following section.

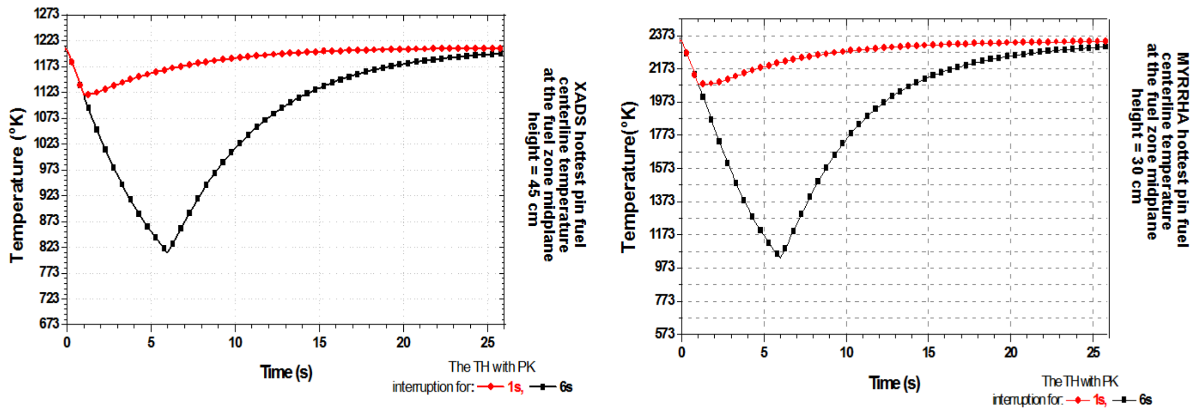

(a) XADS **(b)** MYRRHA

Figure-4.20: Peak fuel centre-line temperature variations predicted for 1 *s* and 6 *s* beam interruptions in the LBE-cooled ADS designs: (a) XADS and (b) MYRRHA

Table-4.2: Decrease in fuel peak temperature compared for the beam interruption transients

ADS design	Beam interruption	Decrease of peak fuel temperature (^oK)			
		Average pin		**Hottest pin**	
		The TH module	Benchmark reference value	The TH module	Benchmark reference value
XADS	1 s	62.3	~63 ± 2	88.7	~89 ± 4
	6 s	266.2	~270 ± 8	393.7	~390 ± 18
MYRRHA	1 s	193.7	~190±13	259.2	~260±21
	6 s	836.5	~825±58	1305	~1220±98

4.4. The TH validation with experimental data of LBE natural circulation loop

The TH module in code ARCH-TH has been validated for the steady and transient scenarios in Kilo Temperature Loop (KTL) operated at BARC for the natural circulation experiments of LBE (Borgohain et al., 2016). The design detail and operational conditions of the loop are considered as reported for the validation of LeBENC code by Borgohain et al. (2016). The modules of ARCH-TH for the analysis have been augmented as per the requirements such as consideration of power generated from heater, thermo-physical properties of niobium alloy used as the loop material, heat loss from outer surface of the loop segments etc.. The TH module is limited to solve the energy conservation at the primary side only. Hence the outlet temperature of the primary heat exchanger (PHX) in KTL is assumed as a given boundary condition in the simulation for natural circulation.

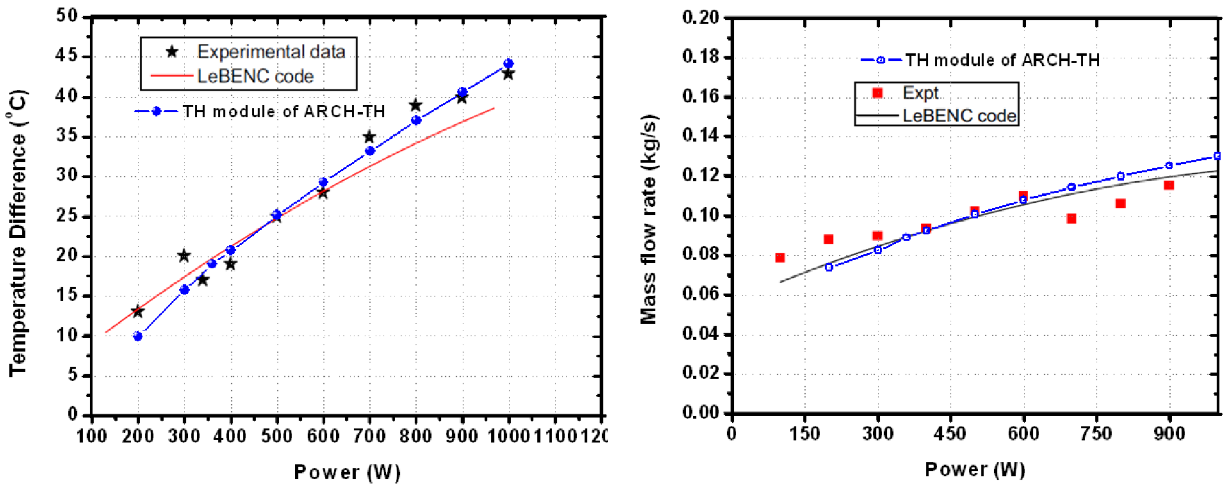

(a) Temperature rise across heated section **(b)** Mass flow rate

Figure-4.21: The prediction of TH module compared for steady state natural circulation in KTL at different power levels

The predictions of TH module are compared for the steady-state mass flow rate and temperature rise in the heated-section at different power levels of the heater as shown in Figure-4.21. The source start-up transients in the loop from the zero-power condition to 360 and 700W power, are also predicted. The temperatures at the inlet and outlet of the heated section (i.e. portion with external heater) and at the inlet of the PHX are compared in given Figure-4.22. The predictions of the TH module are found to be in good agreement with experimental data obtained from KTL operations under steady-state as well as source start-up transients (Dwivedi et al., 2020).

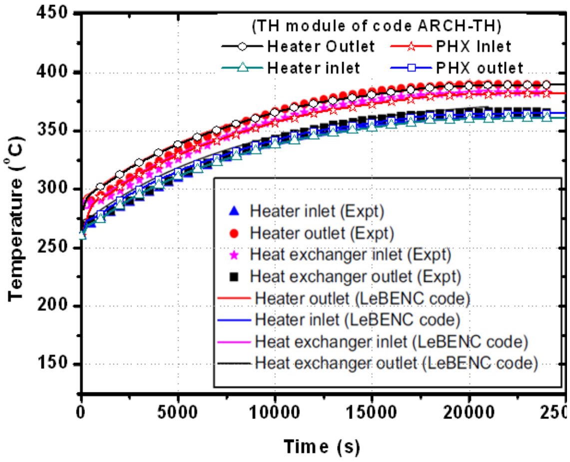

(a) Power level 360W

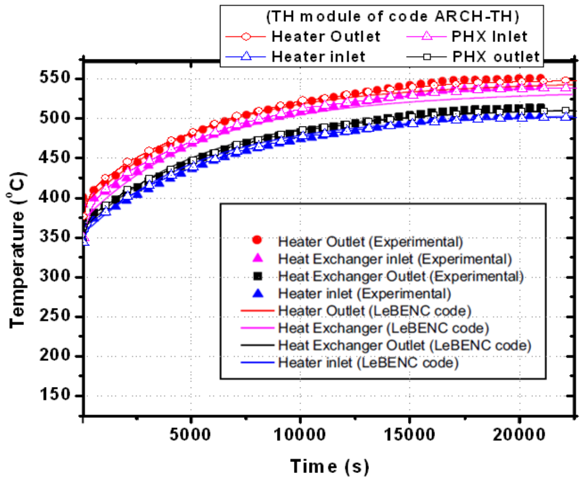

(b) Power level 700W

Figure-4.22: The prediction of TH module compared for heater start-up transients in KTL from zero power condition to different power levels

4.5. Conclusion

The developed neutronics and thermal-hydraulics capability in 3D multi-physics code ARCH-TH have been successfully validated with the appropriate benchmark problems in the literature. The neutronics validations of the code for VVER-440 reactor dynamics show that the predicted results, e.g. core power, reactivity, temperature and power distributions are in good agreement in the cases of without feedback as well as with fuel temperature feedback during transients. The results with the fuel temperature feedback in the transient (i.e. AER-Dyn-002) also qualify the adiabatic fuel heating based TH module in the code. The 1D-radial heat conduction based TH module in the code has been validated with OECD/WPPT beam-interruption benchmark problems for LBE cooled ADS designs- XADS and MYRRHA. The results of TH module are observed to be in good agreement with the benchmark reference values. The thermal-hydraulics in a high-temperature loop of LBE has also been simulated with natural-circulation capability in ARCH-TH code. The results of steady-state and transient natural circulation in the loop, are compared with experimental data obtained and found to be in good agreement. It is also planned to validate the code for coupled 3D full core neutronics - thermal-hydraulics with natural circulation HTR benchmark if and when available in future.

CHAPTER 5

ANALYSES OF REACTIVITY INITIATED TRANSIENTS IN COMPACT HIGH TEMPERATURE REACTOR

5.1. Introduction

The 100 kWt Compact High Temperature Reactor (CHTR) is a natural circulation cooled prismatic high-temperature core consists of ^{233}U-Th based TRISO particles in fuel compacts, BeO moderator and LBE coolant. The reactor core design is initially loaded with high fissile content in the fuel for the desired 15 effective full power years of refuelling interval during high-temperature operation (Table-1.1). The high fraction of ^{233}U content in the fuel is resulting in high initial excess core reactivity. It requires mixing of burnable neutron poison, i.e. gadolinium (Gd) in the fuel kernels of the central assembly in addition to the use of burnup compensation rods (BCRs) (Figure-5.1) to adequately control and shutdown reactor in all temperature conditions. The prompt reactivity feedback coefficient of fuel temperature becomes lesser negative at a higher temperature and with high fissile content (Stacy, 2007). The high fissile content, high-temperature operation and mixing of Gd consequently make the fuel temperature coefficient (FTC) less negative in CHTR (Dwivedi et al., 2010). Thus, it is important to assess the impact of FTC on the core safety during anticipated transients.

The CHTR is designed as an under-moderated core with an average-energy of neutron about 1.0 eV (Figure-5.2) (Dwivedi et al., 2017). The BeO moderator in CHTR is thermally-coupled with the fuel (Figure-1.3). The heating in the fuel-regions would lead to a delayed increase in the moderator temperature, which could also provide negative reactivity feedback in the core. Therefore, the consideration of moderator temperature feedback during transients and its consequences are also an essential aspect for the more realistic safety assessment of the reactor.

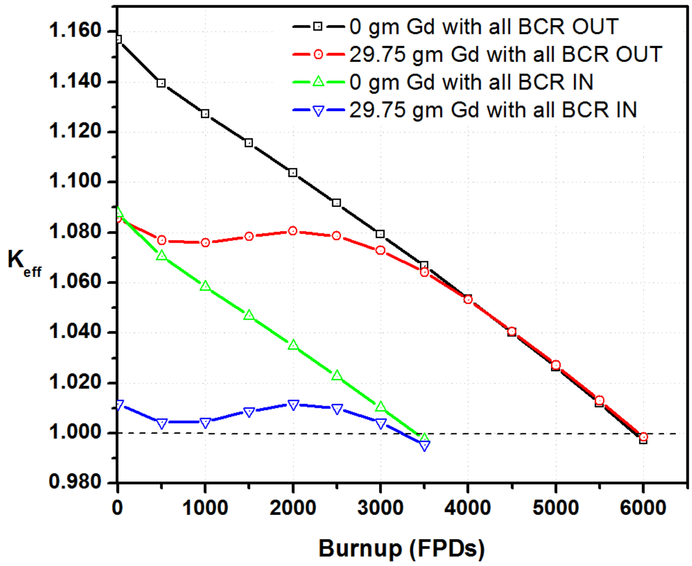

Figure-5.1: Variation of core reactivity in hot operating condition of CHTR with fuel burnup

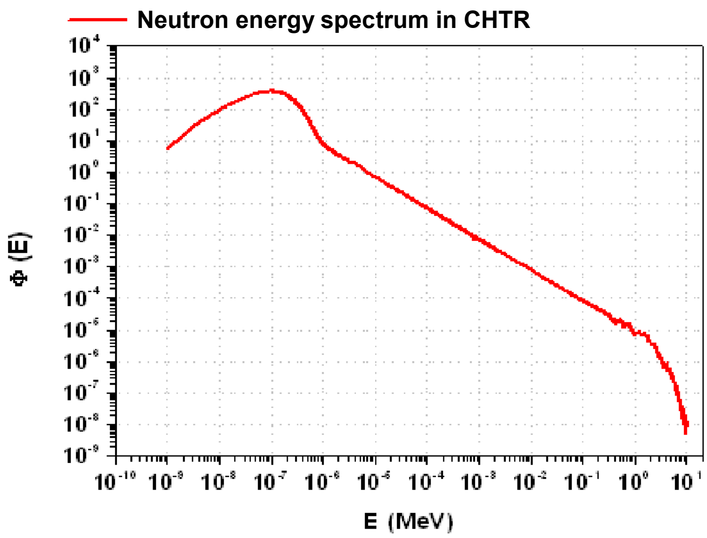

Figure-5.2: Normalized neutron energy spectrum in CHTR core

Reactor safety transients are defined as anticipated events to occur once or more during the operating lifetime of the reactor, e.g. malfunction of a control system. Whereas, reactor accidents are the events which are postulated but not supposed to occur during the operating lifetime. The design of the reactor must possess adequate safety and protection system to mitigate the adverse consequences of transients and accidents. In CHTR design, the reactivity worth of control and shut-down systems are given in Table-5.1 and Table-5.2 for initial core-life conditions. The design ensures that in any critical configurations of the core, the reactor will never be prompt-critical (with β_{eff} = 4.5mk) due to inadvertent withdrawal of a single control rod (Table-5.1). The primary and secondary shut-down systems in CHTR have adequate worth to shut down the reactor independently in all operating core conditions even if one rod fails to act (Table-5.2). The detail working mechanism and functions of these reactivity devices are already discussed in the section-1.6 of Chapter 1.

Table-5.1: The neutron multiplication factor ($\mathbf{k_{eff}}$) in various core configurations of CHTR

Reactor State (with SDS1&2 are deactivated and Gd in central assembly)	$\mathbf{k_{eff}}$ in Hot operation (1000°C)	$\mathbf{k_{eff}}$ in Reactor startup (200°C)	$\mathbf{k_{eff}}$ in Cold condition (27°C)
All burnup compensations rods (BCRs) IN/ OUT	1.0117 / 1.0822	1.0403 / 1.1142	1.0536 / 1.1285
All 12 CRs IN (partially in active core from the top)	0.99995 (11.3 cm)	0.99999 (24.6 cm)	0.9999 (26.4cm)
If CR of maximum worth OUT (reactivity)	1.00099 (1.04mk)	1.00338 (3.4mk)	1.00379 (3.8mk)

Table-5.2: Reactivity worth of shutdown systems (SDS) in CHTR in different conditions

Reactor State (All BCRs IN and CRs OUT)	$\mathbf{k_{eff}}$ in Hot operation (1000°C)	$\mathbf{k_{eff}}$ in Reactor startup (200°C)	$\mathbf{k_{eff}}$ in Cold condition (27°C)
The shut-down systems are not activated	1.0117	1.0403	1.0536
If all 6 primary shutoff rods (PSRs) IN (worth)	0.8494 (189mk)	0.8780 (178mk)	0.8907 (174mk)
If only 5 primary shutoff rods (PSRs) IN (reactivity worth)	0.8756 (154mk)	0.9044 (144mk)	0.9173 (141mk)
If all 12 BeO blocks of secondary SDS OUT (worth)	0.8759 (153mk)	0.9044 (144mk)	0.9163 (142mk)
If only11 BeO blocks of secondary SDS OUT (worth)	0.8860 (140mk)	0.9146 (132mk)	0.9267 (130mk)

The small power variations in CHTR is designed to be controlled and regulated by partially inserted 12 control rods. In the case of unintentional transients of over-power, the shutdown systems are designed for automatically activate and stop the nuclear chain reaction. The rapid actuation, i.e. insertion of shutoff rods and/or withdrawal of reflector blocks is called “scram” or “reactor trip”. However, in the high-temperature core under unseen accidental scenarios, the shutoff rods and reflector blocks may get stuck due to core deformation or related electronics malfunction and scrams could fail to act (HTRE, 1959). In these circumstances, the negative temperature feedbacks of reactivity could passively arrest the rise in power, and either safely stabilise the core power after the transient or automatically shut down the reactor. These concerns necessitate evaluating the consequences of anticipated transients without scram (ATWS) to assess and ensure the safety features of the core. The safety features must ensure that no transients or design-basis accidents, raise the temperature of TRISO fuel exceeding 1600°C in HTRs, which is the leak tightness safety limit of the SiC coated particles for retention of fission products and gases (Sawa et al., 2001). It is ultimately to prevent the fuel damage and consequent release of radioactivity to the environment exceeding the limits. Another safety limit considered in case of CHTR is the boiling point of primary coolant LBE (i.e. 1670°C) to avoid the sudden over pressurisation in primary heat transport system exceeding the boiling point (OECD-NEA, 2007).

Therefore, the envisaged core of CHTR has been evaluated with multi-physics code ARCH-TH for the safety transients of reactivity initiated under various temperature and feedback conditions and discussed in the following sections.

5.2. Inadvertent withdrawal of control rod accident during the core startup

The CHTR is designed to be cooled by natural circulation of LBE coolant in normal operating conditions. The melting point of LBE is 124°C at normal pressure (OECD-NEA, 2007). However, the control and primary shutoff rods are inserted for the drive in the coolant channels of CHTR. Therefore, for the smooth driving of these reactivity devices, it has been decided that during the approach to criticality, the core inlet temperature of LBE has to be maintained at least 200°C through external heating. Thus under subcritical (i.e. shutdown) conditions or critical core at very-low power, all the core materials will have the temperature almost the same as the coolant inlet.

The anticipated transient due to inadvertent withdrawal of a single control rod during start-up (i.e. at 200°C), has been investigated with code ARCH-TH (Dwivedi and Gupta, 2015). In the transient, about +3.5mk reactivity is added within 1.5 s in the critical core. The transient is followed up to 200 s in the simulation. The shutdown systems are assumed to fail to act in the analysis, and rising core power is being passively controlled and stabilise by negative fuel temperature feedback. In this case, the adiabatic heating of the fuel is considered with the initial temperature at 200°C. The core power and the peak fuel temperature have been predicted by code ARCH-TH. The results are compared with point kinetics analysis with lumped TH model (Figure-5.3 and Figure-5.4).

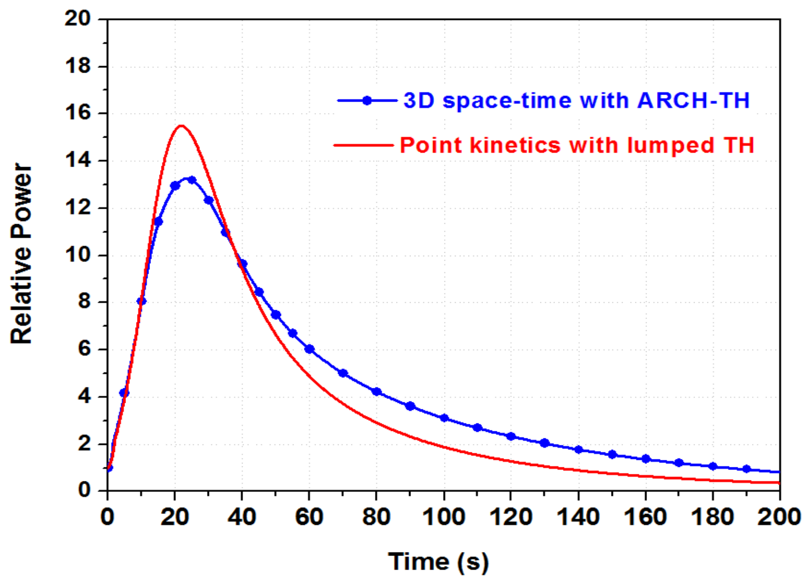

Figure-5.3: Variation of core power during the transient in start-up condition

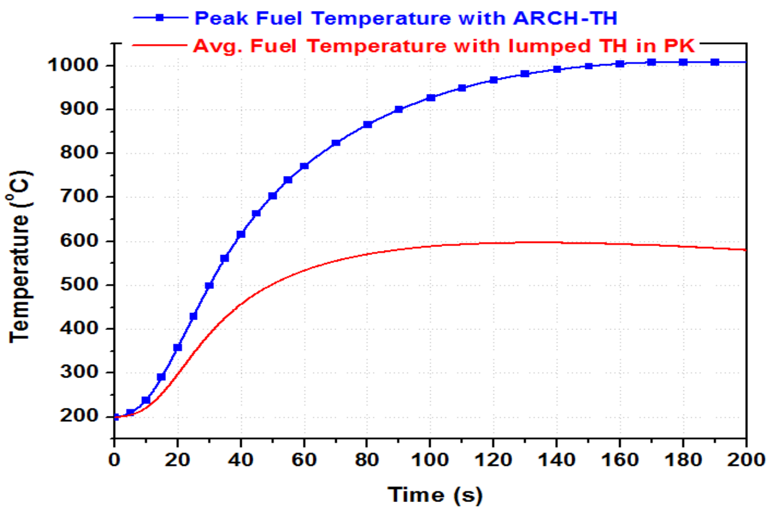

Figure-5.4: Variation of fuel temperature during the transient in start-up condition

The fuel temperature coefficient in the core start-up condition of CHTR is estimated as $-1.5 \times 10^{-5}/°C$, which is given as input in point kinetics analysis. However, for fuel temperature feedback, the few group cross-section parameters are being interpolated in 3D neutronics in ARCH-TH as discussed in the section-3.5 of Chapter 3. The peak fuel temperature is predicted by 3D space-time analysis in which heating is considered in each of the fuel meshes. Whereas, in point kinetics, only the average temperature is predicted with the assumption that fuel is lumped (Gupta et al., 2008). The prediction of 3D code ARCH-TH is considered to be more realistic over qualitative point kinetics analysis with lumped TH model for the fuel safety (Figure-5.4). The fuel temperature finally stabilises at higher value after the transient. It is found that the fuel temperature stays far below the safety limit of TRISO fuel during the transient even without scram.

The model of adiabatic heating of fuel, does not consider the transient heat transfer from the fuel and has limited application to fast power excursion during large reactivity transients, i.e. which involve too short time to heat to be conducted outside the fuel meshes. This TH model also requires initial temperature in the fuel and could not predict for steady-state. Therefore, all further analyses of CHTR transients have been carried out with 1D-radial heat conduction based TH module in ARCH-TH code and are presented in detail in the following sections.

5.3. Inadvertent withdrawal of control rod followed by scram at full power

The case of inadvertent withdrawal of a single control rod accident in the hot operating condition of CHTR at full power has been investigated with multi-physics code ARCH-TH. The transient has been simulated using 1D-radial heat conduction in multi-channel based TH module with an average mass flow rate 0.352 kg/s in the channels. This postulated scenario of loss of regulation accident (LORA) due to inadvertent withdrawal of a control rod, is resulting in the addition of +1.04mk reactivity in 2.3 s in the hot critical core. The transient is followed by the actuation of the trip at two different power levels, i.e. first at 110% of initial power and second at 200% of initial power (Dwivedi et al., 2016). The primary shutdown system (i.e. scram or reactor trip) has been assumed to activate with 0.5 s of time delay. The steady-state, as well as transient temperature profile in each of the fuel channels have been predicted to consider the reactivity feedbacks of the fuel, moderator and coolant temperatures. The transient has been studied with and without feedback. The core power (Figure-5.5), core reactivity (Figure-5.6) and peak fuel temperature (Figure-5.7) have been predicted and compared for different trip condition and feedback in the simulations.

Table-5.3: The main kinetics and safety parameters in hot operating condition of the core

Parameters	Value
Fuel Temperature Coefficient (FTC)	$-5.6 \times 10^{-6} / {}^{o}C$
Moderator Temperature Coefficient (MTC)	$-1.8 \times 10^{-5} / {}^{o}C$
Coolant Temperature Coefficient	$-3.8 \times 10^{-7} / {}^{o}C$
Neutron generation time (Λ)	1.524×10^{-4} s
Delayed Neutron Fraction (β)	0.0045

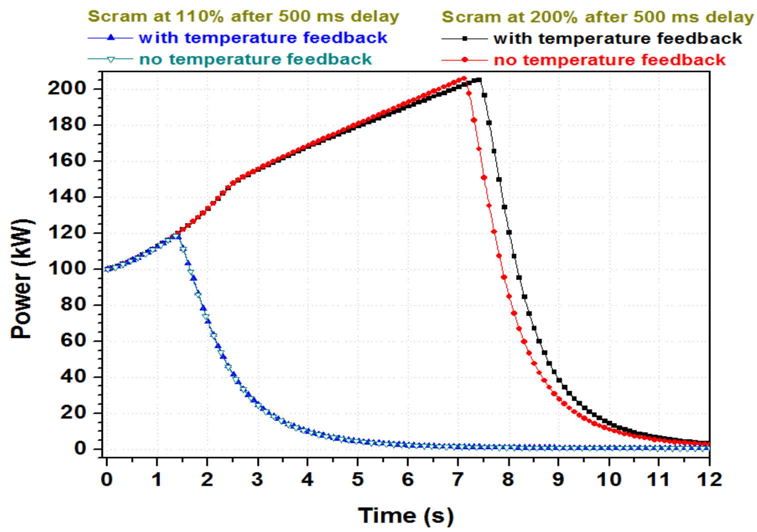

Figure-5.5: Power during LORA followed by scram in various trip and feedback conditions

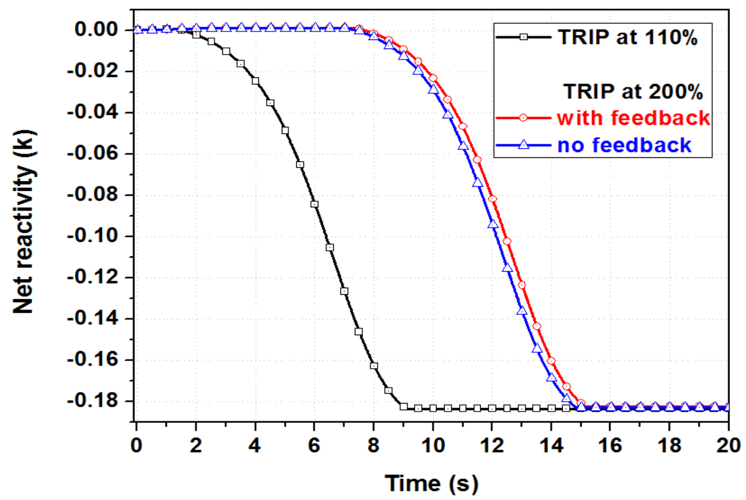

Figure-5.6: The net core reactivity during LORA followed by scram

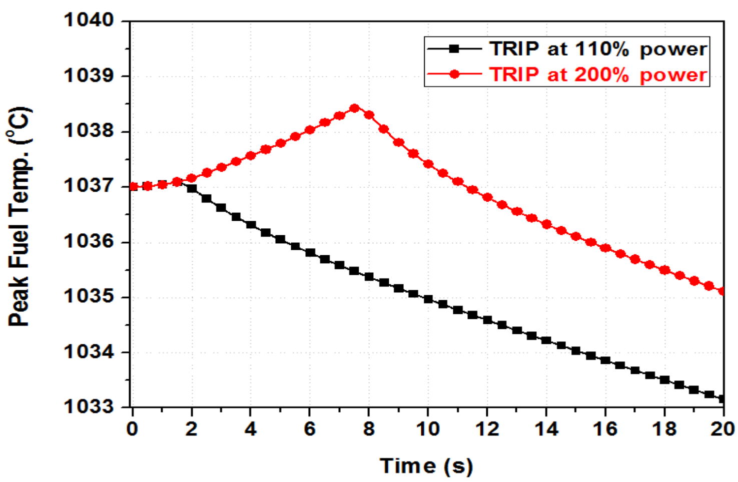

Figure-5.7: Peak fuel temperature during LORA followed by scram

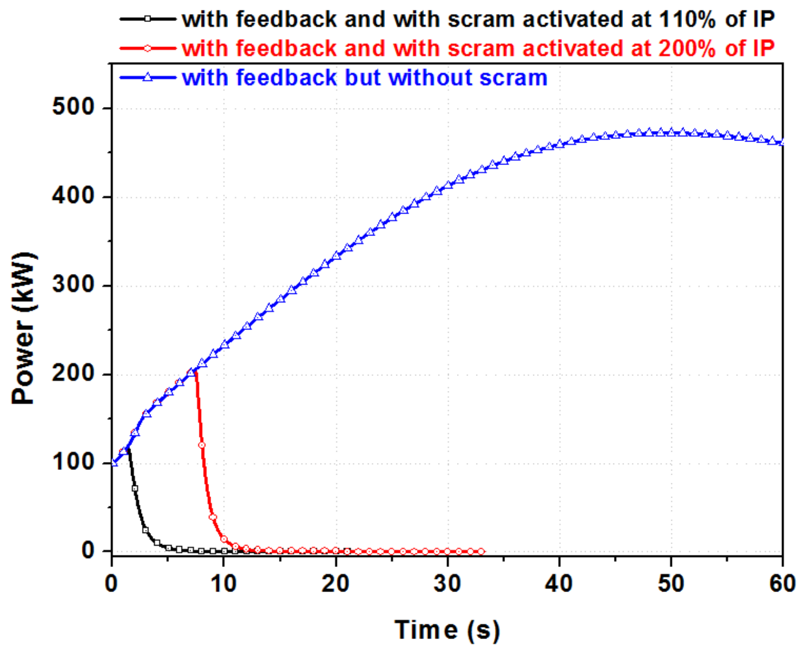

Figure-5.8: Power during LORA compared for the cases with scram and without scram

It is found that in the case of scram activated at 110% of the initial, the temperature feedback effect is negligible. Whereas, in the case of scram activated at 200% of initial power, the power rise is slightly controlled with temperature feedbacks compare to no feedback in simulation (Figure-5.5). The core kinetics parameters are given in Table-5.3 for the reference core condition. In the transient with scram, the small effect of temperature feedbacks is due to the low rise in core temperature during such transient (Figure-5.6 and Figure-5.7). The scram activations at different power levels (protected cases) are also compared to the transient without scram, i.e. anticipated transient without scram (ATWS) where power rise is passively controlled and stabilised by the fuel, moderator and coolant temperature feedbacks in CHTR (Figure 5.8). The results indicate that CHTR being a low power reactor, the transients have not much effect of temperature feedbacks when scram is activated. Therefore, all transients reported after this section have been studied assuming the case of without scram to investigate the inherent safety features of the designed core.

5.4. Inadvertent withdrawal of control rod without scram at full power

The analysis of anticipated transient without scram (ATWS) due to the inadvertent withdrawal of control rod in the hot operating condition of CHTR at full power has been carried out (Dwivedi et al., 2017). The study has been performed with the 1D- radial heat conduction based TH module of ARCH-TH. The transient core power has been predicted for different feedback considerations viz. with only fuel temperature feedback, with fuel and moderator temperature feedbacks as well as with fuel, moderator and coolant temperature feedbacks together. The transient is assumed to be initiated due to inadvertent withdrawal of a control rod, consequently about 1.0mk positive reactivity in 2.3 s has been added in the hot critical core of CHTR at full power during beginning of the core life-cycle. The various reactivity coefficients are given in the Table-5.3. The lower mass number, higher mass density, more inventory and higher macroscopic thermal scattering cross-section of BeO moderator are resulting in the higher contribution in the neutron energy moderation as compare to graphite in the fuel tube of the assembly/ lattice. In under-moderated core at operating temperature, if the temperatures of BeO and graphite are being varied together then the temperature coefficient (MTC) is found to be -1.8×10^{-5} /°C compare to -1.49×10^{-5} /°C where only BeO temperature is changed. The MTC is found to be more negative than the fuel temperature coefficient (Table-5.3). The coolant temperature and density feedback coefficient of reactivity in the hot operating condition of CHTR is negative but too small to show any significant effect during transients. The temperature coefficients have been estimated by ITRAN+ARCH code system.

The inlet temperature and mass flow rate in channels of CHTR at full power are 900°C and 0.353 kg/s respectively and are assumed to be invariable during the transient. For the ATWS scenario, it is assumed that no shutdown system is activated. The transient has been followed up to 600 s in the simulation. The nuclear power is rising to about 4.7 times of the initial power during the transient considering the feedbacks from fuel, moderator and coolant temperatures (Figure-5.9). The rise in power is being controlled passively by the temperature feedbacks. The study indicates that the coolant feedback is negligible, whereas the moderator temperature feedback effect is very significant (Dwivedi et al., 2015b). If only fuel temperature feedback is being considered then the rise in the transient power would be much higher (Dwivedi et al., 2019).

The core reactivity and temperatures are also estimated during the transient and presented only for the case of feedbacks from the fuel, moderator and coolant temperatures together. The variations of peak temperatures and reactivity in the core are shown in Figure-5.10 and Figure-5.11 respectively. The variations of axial temperature profiles in the fuel and coolant of the peak powered/hottest channel are presented in Figure-5.12 and Figure-5.13. The radially averaged normalized axial power distribution in steady core condition is shown in Figure-5.14.

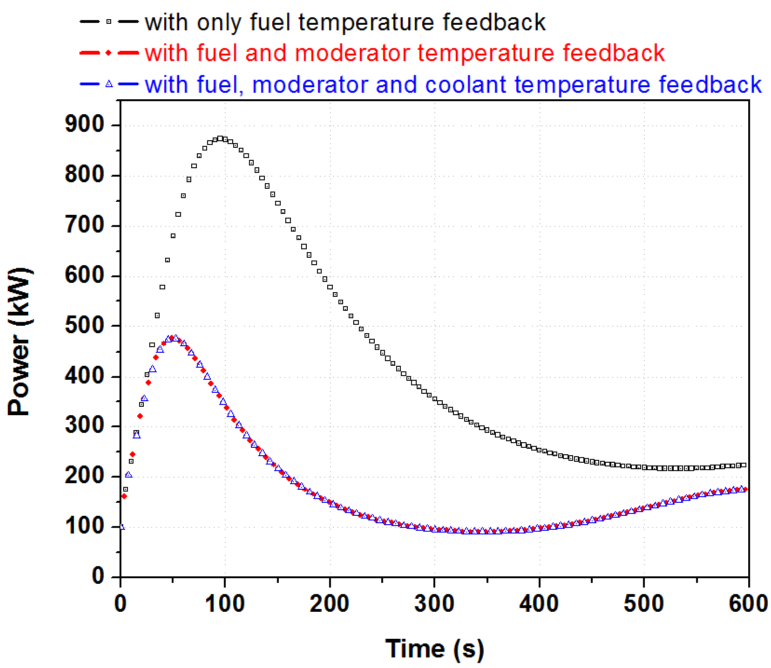

Figure-5.9: Power during ATWS in CHTR at full power with different feedback conditions

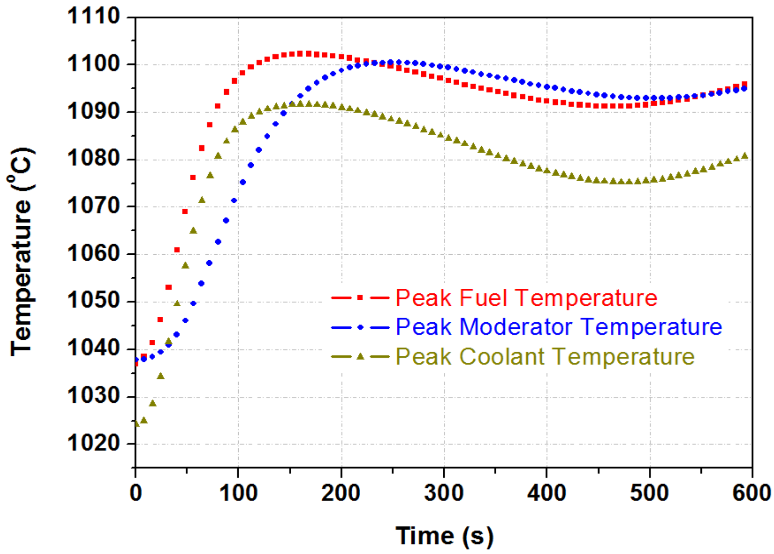

Figure-5.10: Peak temperatures of fuel, moderator and coolant during the transient

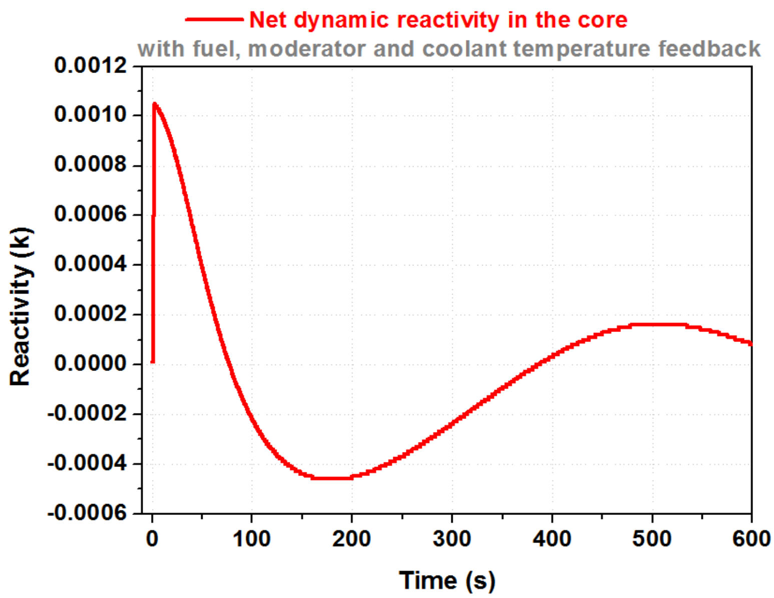

Figure-5.11: The dynamic reactivity in the core during the transient

The radial and axial peaking factor in the core are found to be 1.21 and 1.32. The radial temperature profiles have been predicted in all the axial meshes of the channels with the code during the transient. The temperatures in these plots at t=0 s, are representing for steady-state, i.e. before initiating the transient. The radial temperature profile in the peak powered axial mesh of the hottest assembly is shown in Figure-5.15.

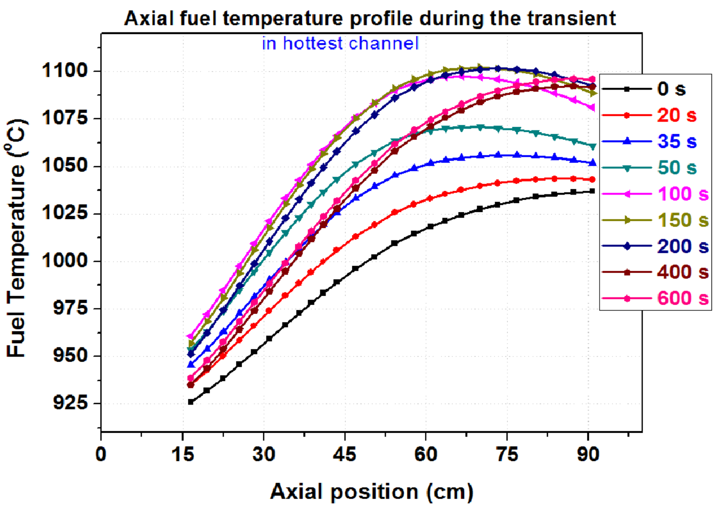

Figure-5.12: Fuel temperature in the hottest fuel assembly during the transient

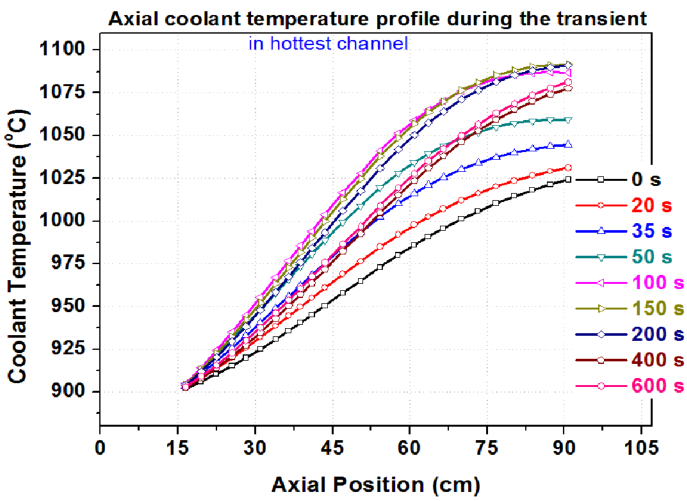

Figure-5.13: Coolant temperature in the hottest channel during the transient

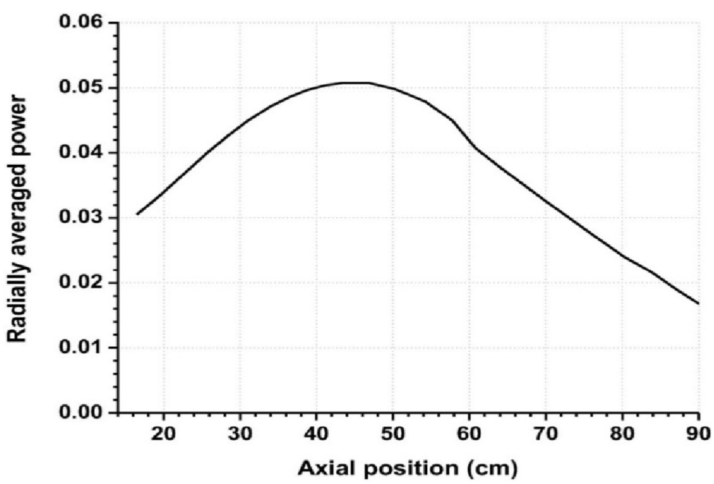

Figure-5.14: Axial profile of normalised power in CHTR

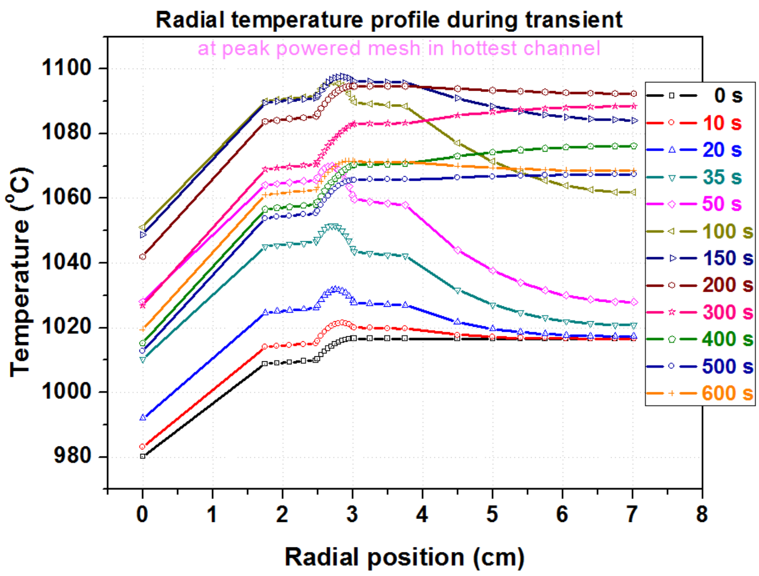

Figure-5.15: Radial temperature profile in peak powered mesh of the hottest channel

The Figure-5.12 show that peak fuel temperature point is shifting towards the centre of the assembly from 0 to 150 s of the transient due to the axially centre peaked power generation in the channel. Whereas, after about 150 s of the transient initiation, the peak fuel temperature point is again towards the top side and almost stabilizing after 600 s. The peak fuel temperature in the top-side mesh is appearing due to low-temperature gradient from fuel to coolant in the small power generating core and good heat transfer property of liquid metal coolant (i.e. LBE). The coolant temperature profile in Figure-5.13 shows that the heating of the coolant more appears in the central portion initially mainly due to axially centre peaked power generation and small flow rate of the coolant in the channel.

The radial temperature profile (Figure-5.15) in peak powered axial mesh (i.e. near the middle axial plane) shows that, during initial steady state, the maximum temperature point is at the outer surface of the fuel. The fuel is considered as an annular region for the simulation. Whereas, the adjacent BeO moderator is also predicted at the peak temperature of the fuel. It is because of the assumption of the adiabatic outer boundary of the channels. When the transient initiated and power starts to rise, the peak temperature point is lying in the annular fuel region like asymmetric parabolic profile (i.e. heat source) during initial 150 s. It is found that the core heat is eventually being transferred to the coolant flowing in each channel and peak temperature appears at the outer surface of the annular fuel region and so as the BeO moderator after the transient. The study shows that the peak temperatures of the fuel and the coolant stay well within safety margins during the unprotected case of reactivity transient (i.e. ATWS) in the core. The BeO moderator temperature feedback in CHTR plays a very significant role to passively control and stabilise the power during such a case of over-power transient without scram. *This property of BeO in the high-temperature core of CHTR has been investigated first time, which could be a major safety feature of BeO moderated thermal spectrum high-temperature core*.

The transient discussed in this section has been simulated with the limitation that the inlet mass flow rates and temperature of the coolant in the channels are invariable. Therefore, the designed safety characteristic of CHTR core has also been assessed for the postulated transients of coolant blockage (i.e. loss of flow) and overflow in the hot operating core at full power. In these cases, the core inlet temperature is assumed to be constant, but the mass flow can be changing with the given rate and time interval in the code. These postulated transients of coolant blockage and increase (i.e. overflow) have been discussed in the next section.

5.5. Postulated coolant blockage and overflow accidents at full power

The core heat removal in CHTR is based on the natural circulation of coolant, where mass flow rate in the channels will depend upon their nuclear heating and overall thermal-hydraulics design of the core. However, the designed neutronics safety in CHTR can be assessed by postulated accidents of coolant blockage and overflow in the channels, i.e. in the scenarios of imbalance in heat generation and removal in the core (Dwivedi et al., 2017[b]). These transients are investigated to check the impact of reactivity coefficients of temperatures on the safety of the core during thermal-hydraulics perturbations.

In the postulated transients are assumed to be started with the change in the coolant mass flow rate in the channels and no reactivity control and safety devices operated/activated. In the first case, the reactor is considered at full power operation initially, and transient started due to a reduction in mass flow rate from 100% of steady-state condition to 5% in 10 seconds. Whereas, in the second postulated case, a transient is started due to a rise in the coolant mass flow rate from 100% of steady-state condition to 500% at full power in 10 seconds. These transients have been simulated with code ARCH-TH, and the results are discussed in the following sub-sections.

a) *Postulated transient of coolant blockage without scram during full power operation*

It is the case of unprotected loss of flow accident (ULOFA), initiated due to postulated coolant blockage in the core (Dwivedi et al., 2017[b]). The transient is assumed to be initiated due to reduction in coolant mass flow rate from 100% (i.e. average 0.352 kg/s in each channel) in steady-state condition at full power to 5% of the initial (i.e. 0.0175 kg/s) in 10 seconds. The postulated variation of coolant mass flow rate in the channels for transient is given in Figure-5.16, which is taken as transient input in the code.

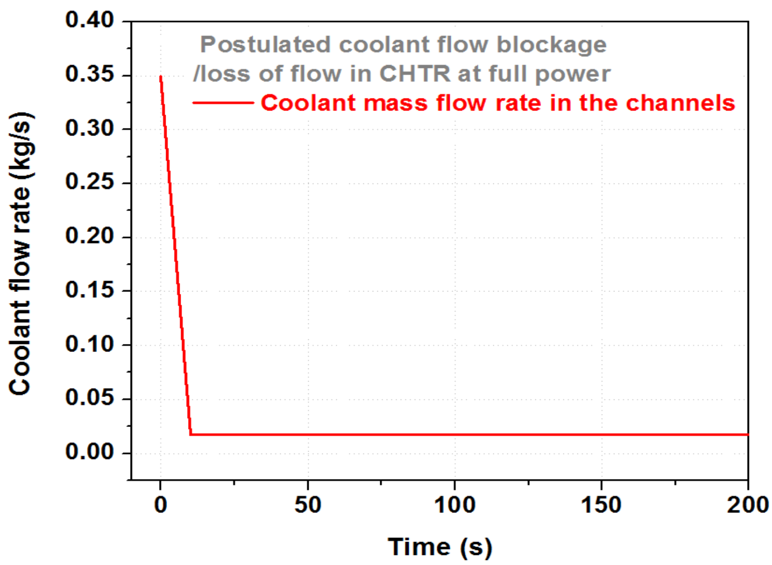

Figure-5.16: Coolant mass flow rate in the channels to initiate the transient

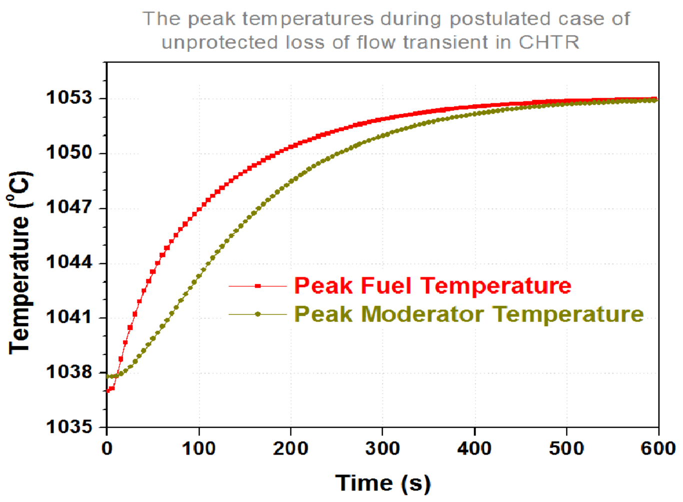

Figure-5.17: Peak temperatures of the fuel and moderator during the transient

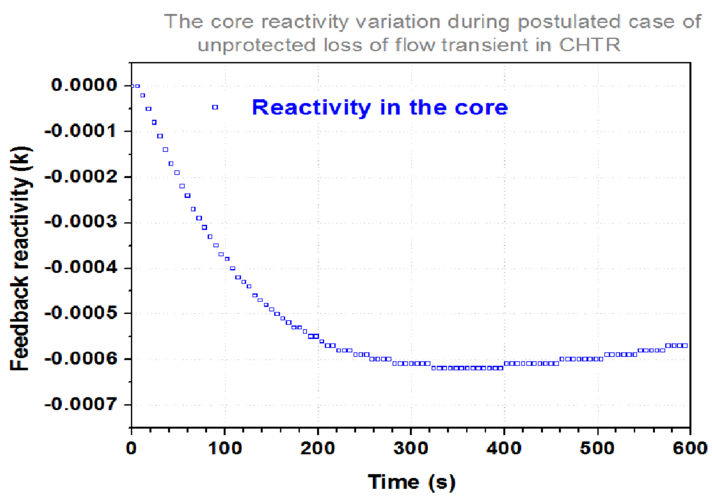

Figure-5.18: The core reactivity during the transient of coolant blockage

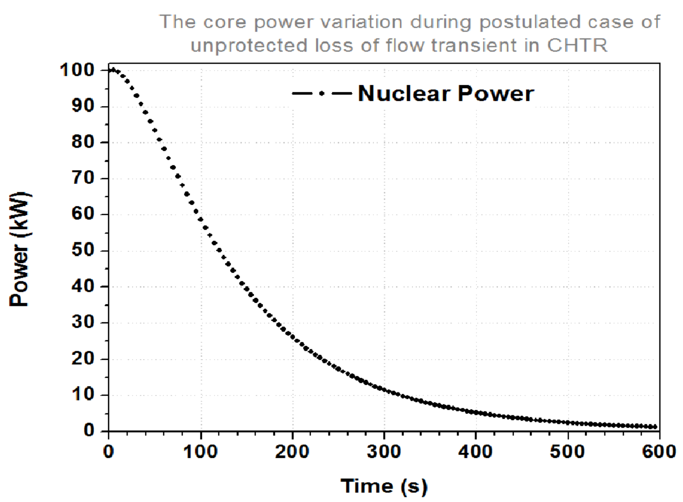

Figure-5.19: The power during the transient of coolant blockage

The transient has been followed up to 600 s. The variations of peak temperatures in the fuel and moderator are shown in Figure-5.17. The reduction in the coolant mass flow rate will result in a decrease in the core heat removal rate, and consequently, core temperature rises. The rise in temperatures of the fuel and moderator, introduce negative reactivity in the core and nuclear power started to decrease. The higher temperature of the fuel and coolant in the core introduces negative reactivity. Figure-5.18 shows core feedback reactivity variation during the postulated transient of coolant blockage. The variation of core power is predicted as shown in Figure-5.19.

As power density in CHTR core is low, the study shows that even in case of unprotected loss flow due to postulated coolant blockage, the rise in temperatures of the core materials are far below the safety limits and core shuts down passively during such circumstances (Dwivedi et al., 2017[b]). The case of coolant overflow in CHTR is studied and given in next sub-section.

b) *Postulated transient of overflow without scram during full power operation*

The postulated transient of coolant overflow is assumed to be started due to increasing in coolant mass flow rate from 100% (i.e. 0.352 kg/s in each channel in steady-state at full power) to 500% of the initial (i.e. 1.75 kg/s) in 10 s (Dwivedi et al., 2016[b]). The increase in the mass flow rate is taken as input in code for the transient (Figure-5.20).

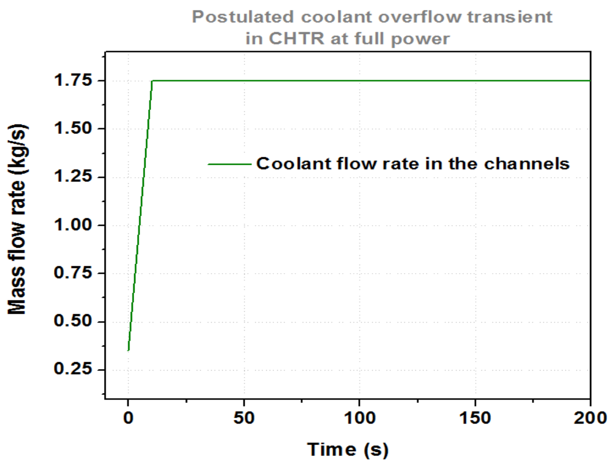

Figure-5.20: The mass flow in the channels for postulated overflow transient in CHTR

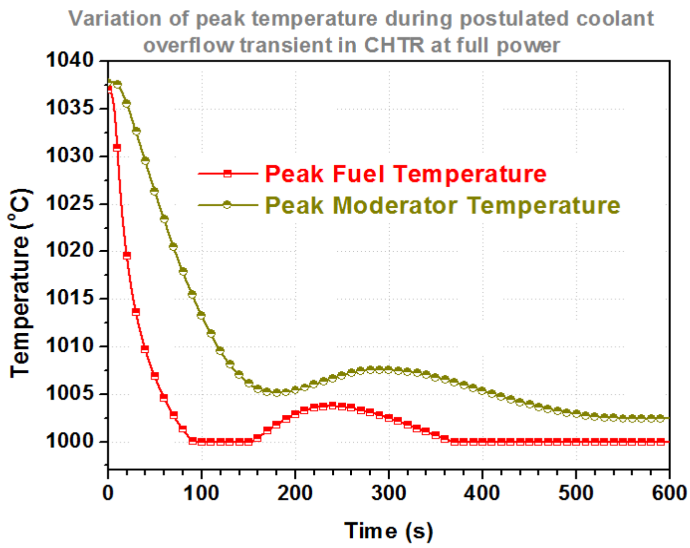

Figure-5.21: Variation of peak temperatures in the fuel and moderator during the transient

The increase in mass flow rate in the channels consequently increases the heat removal rate from the core, which is resulting in temperature reductions of core materials (Figure-5.21). The reductions in fuel and moderator temperature during the transient introduce positive reactivity in the core as feedbacks (Figure-5.22), and nuclear fission power started rising, as shown in Figure-5.23. The rising nuclear power stated more heating in the core and core temperature started rising to compensate for the positive reactivity introduced earlier as feedbacks. Therefore, after a few oscillations, the nuclear power stabilizes at a higher level, i.e. power production will be equal to removal in the core. The net reactivity after transient becomes zero for a critical condition with different temperature distribution in the core.

These postulated transients of unprotected coolant blockage and overflow in CHTR at full power condition have been investigated to assess the intrinsic-safety and stability features of the core neutronics design. The study shows that the physics design is inherently safe during thermal-hydraulics initiated perturbations in the core. However, core heat in CHTR is designed to be passively removed by natural circulation of LBE coolant in the coupled channels.

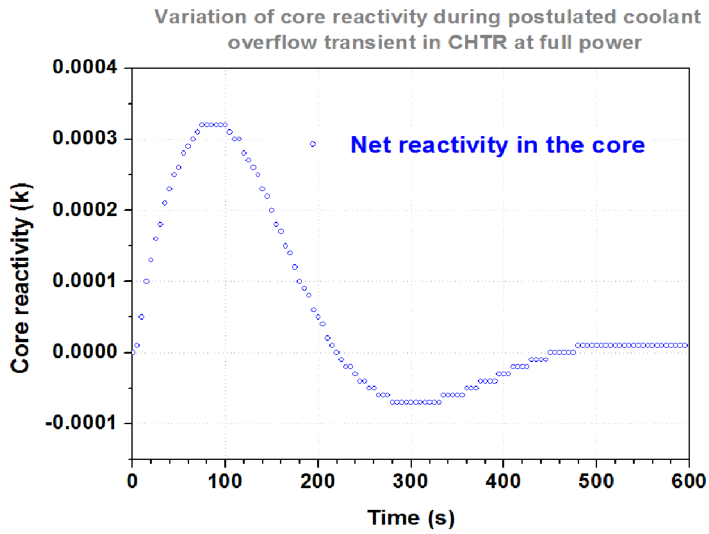

Figure-5.22: The core reactivity during the transient of postulated overflow

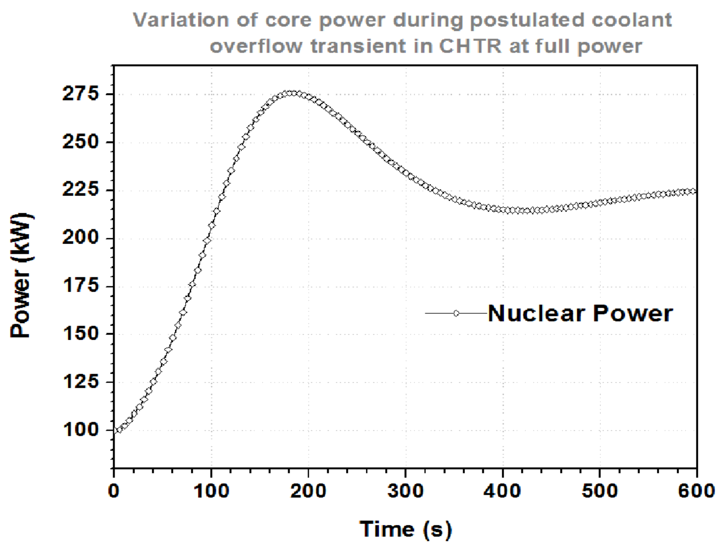

Figure-5.23: The variation in core due to postulated overflow in CHTR

Further investigations of core design and safety in CHTR have been carried out under the natural circulation of the coolant. The analyses of CHTR transients presented till this section have been investigated with temperature-dependent thermo-physical properties of the LBE coolant only, and the other core materials' temperature dependences have been ignored. However, after this section, analyses of CHTR transients have been carried out with considerations of temperature-dependent thermo-physical properties of the fuel, moderator and coolant as discussed in Chapter 3.

5.6. LORA without scram under natural circulation of coolant at full power

After the successful development and validation of TH module of code ARCH-TH for the natural circulation capability, the inadvertent withdrawal of single control rod (i.e. LORA) scenario in CHTR at full power condition has been investigated with explicit consideration of coolant natural-circulation (Dwivedi et al., 2018). In this analysis, the LBE coolant flow in coupled channels of CHTR is considered under natural circulation. In natural circulation cooled CHTR, the core average mass flow rate and outlet temperature of coolant have been estimated at different power levels assuming inlet temperature at 900°C (Figure-5.24). The mass flow rate in the core is found to be about 6.7 kg/s at full power. The coolant is entering in the 19 coupled channels of CHTR with given inlet temperature and taking out heat to the upper plenum under natural circulation (Figure-1.2). The core heat is being transferred to the secondary side using high-temperature heat pipes inserted in downcomers at the upper plenum. The coolant is returning from upper plenum to lower plenum by 18 down-comers. All the channels have different power as well as thermal-hydraulic conditions. However, it is considered that all the down-comers have the same conditions.

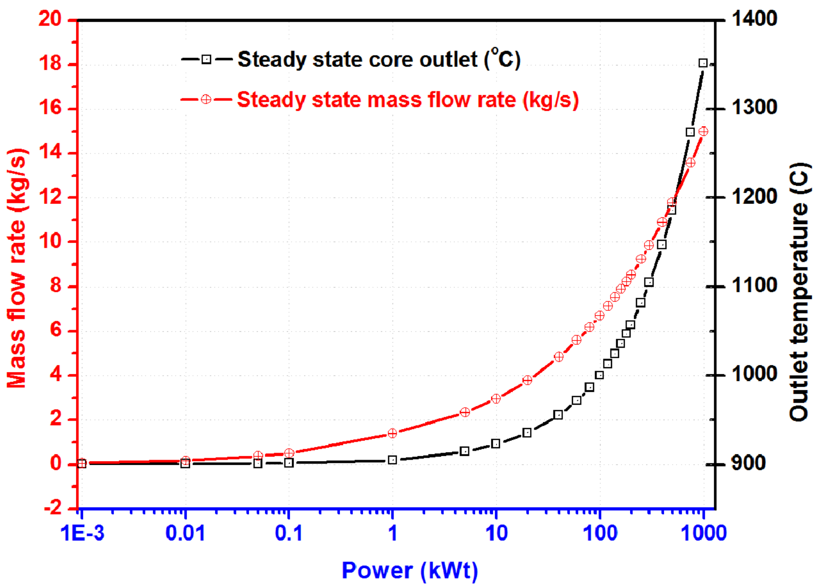

Figure-5.24: The steady-state mass flow rate and outlet temperatures at different power

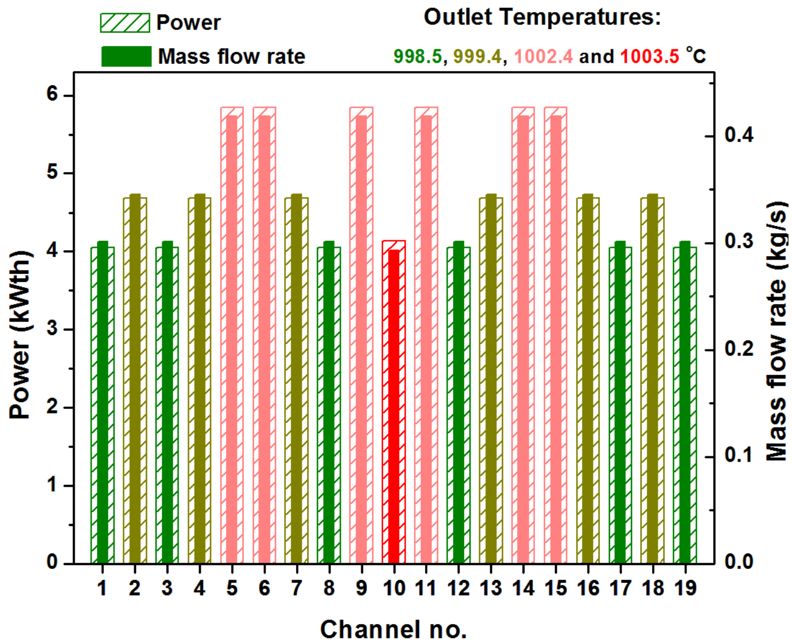

Figure-5.25: Steady-state channel power, mass flow rate and outlet temperature at full power

In the analysis, about 91.4% of thermal heat generated in the core is considered to be removed by coolant flowing in the channels. The rest of the heat is assumed to be deposited/transferred out regions of the core as heat loss. The thermal power, mass flow rate, as well as outlet temperature in the channels of CHTR at full power, have been predicted in natural circulation condition as shown in Figure-5.25.

In case of unprotected withdrawal of control rod transient, +1.04mk reactivity is introduced in the core within 2.3 s. It is assumed that shutdown systems are not being activated for the trip (i.e. ATWS). The rising power and temperature in the core, are being passively controlled by reactivity feedbacks from the change in temperatures of the fuel, moderator and LBE coolant. The transient has been simulated for 1800 s. The core power, coolant outlet enthalpy (Figure-5.26), reactivity (Figure-5.27), channel pressure drop (Figure-5.28) as well as peak fuel, moderator and coolant outlet temperatures (Figure-5.29) during the transient have been predicted by code ARCH-TH. The variations in coolant outlet temperature and mass flow rate in all the channels of CHTR during the transient, are shown in Figure-5.30 and Figure-5.31.

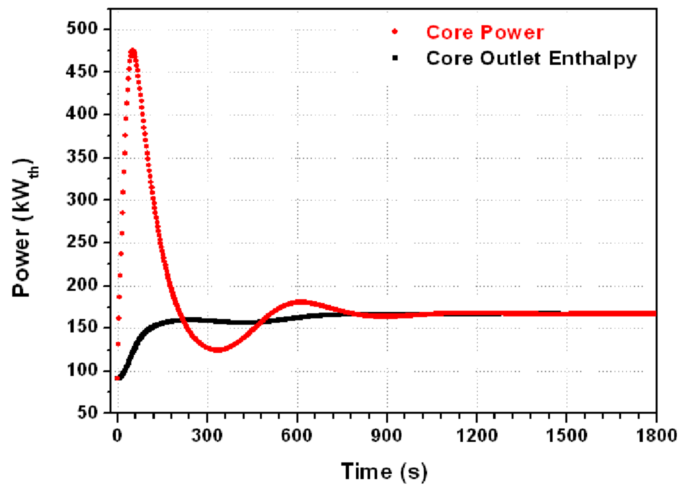

Figure-5.26: Core thermal power from fission and change in coolant outlet enthalpy

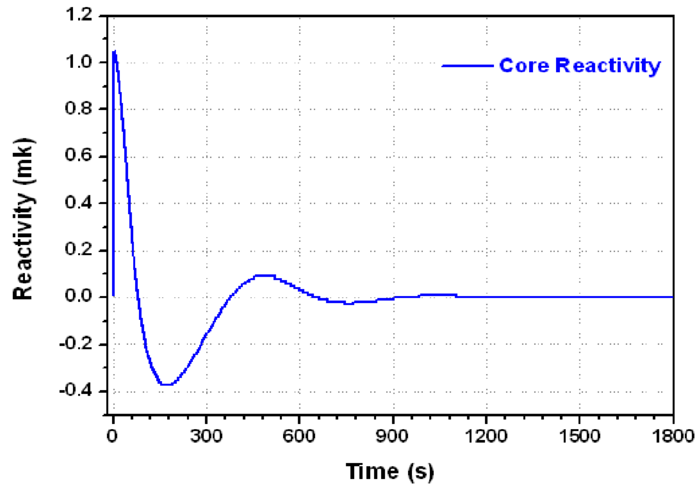

Figure-5.27: The core reactivity during the transient under natural circulation condition

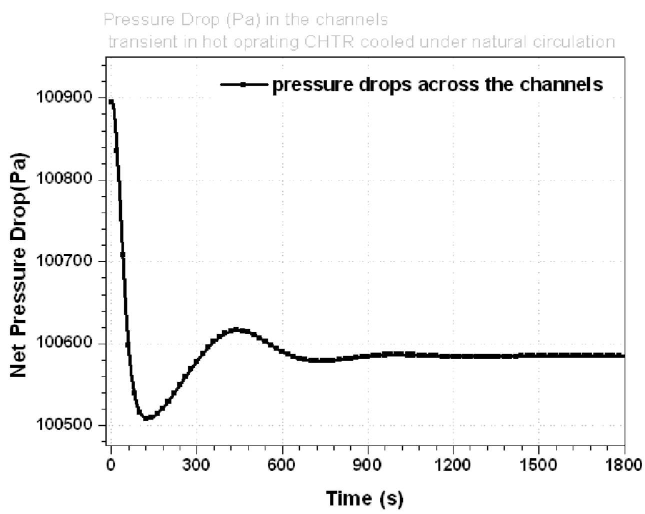

Figure-5.28: Variation of pressure drop across the channels of CHTR

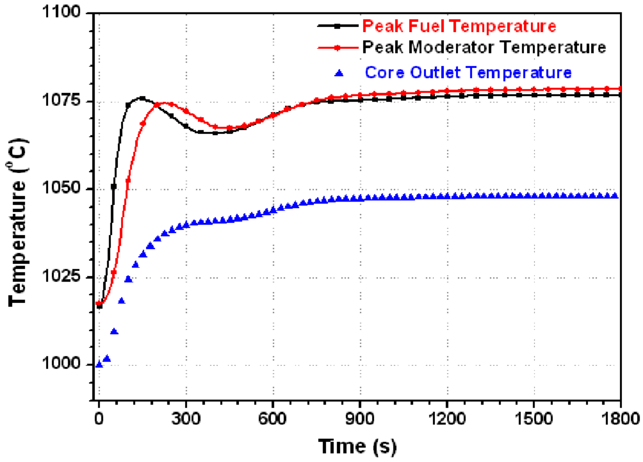

Figure-5.29: Variation of peak temperatures of fuel, moderator and coolant outlet

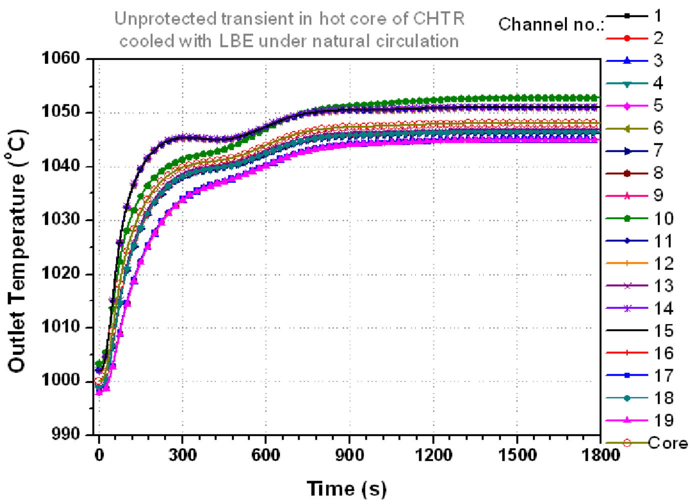

Figure-5.30: Variation of outlet temperature of the channels

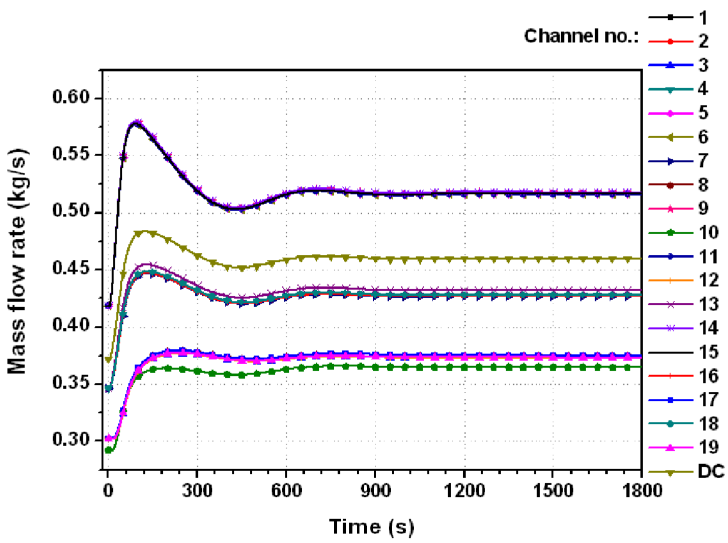

Figure-5.31: Variation of coolant mass flow rate in the channels

The core power is observed to be initially rising to about 5.0 times in 52 s (Figure-5.26) and then coming down and stabilizing at about 1.8 times of its initial value due to self-controlling temperature feedbacks from fuel and moderator (Figure-5.27). The core mass flow rate is observed to be increasing and finally stabilising at 1.24 times of the initial value with the average core outlet temperature around 1048°C (Figure-5.29 and Figure-5.31). It is predicted that the peak temperature of the fuel stays far below the safety limit of 1600°C for TRISO particles in the core. Due to increase in the mass flow rate during such overpower transient under natural circulation, the outlet temperatures in the channels are observed to be rising lower as compared to the case of no change in flow rate in the transient discussed in section-5.4. Even in the steady-state operation under natural circulation, the mass flow rates in peak powered channels are higher (Figure-5.25) and consequently their lower outlet temperatures in comparison of the transient study with average mass flow considered in all the channels. Thus natural circulation in CHTR is observed to be resulting in even more safe conditions and limiting factor in the fuel and coolant temperature rise during such over-power transients.

5.7. Conclusion

The proto-type 100kWt core of CHTR is being designed as a technology demonstrator for Indian HTR programme. The core has been assessed for reactivity initiated transients with 3D multi-physics code ARCH-TH. The cases of inadvertent withdrawal of control rod (i.e. loss of regulation or LORA) in various core conditions have been studied to predict the core safety response during overpower transients. The cases have been investigated with and without scram, i.e. in protected and unprotected scenarios. The study shows that in the transient during core start-up without scram, the rise in peak fuel temperature is far below the safety limit of TRISO fuel due to negative feedback from the fuel temperature. However, during LORA at full power condition, analysis shows that the effect of feedback reactivity is not considerable (in low power reactor) when scram is activated at 110% of the initial power.

Therefore, the unprotected control rod withdrawal case has been investigated further with the given mass flow as well as under natural circulation of the coolant. The study shows that the feedback of the BeO moderator temperature in CHTR is very significant and could be considered as a major passive safety feature. This novel observation of BeO temperature feedback in the high-temperature core has been published (Dwivedi et al., 2017). The differential effect of the fuel, moderator and coolant temperature feedbacks during CHTR transients have been studied in detail and results are presented in the international conferences. The natural circulation in CHTR, which is an inherent safety design feature, could limit the rise in peak temperatures passively by increasing heat removal during overpower transients as confirmed in the study. The natural circulation in coupled multi-channel of CHTR results in higher mass flow rates in the more heated/ powered channels, consequently lesser radial temperature peaking in the core. The core neutronics of CHTR has also been assessed for its safety response during thermal-hydraulics perturbations like postulated loss of flow and increase in the flow (i.e. overflow) of coolant. The negative reactivity coefficients in CHTR could passively control the transient temperatures within safety limits. These analyses confirm the passive safety design features of the core for high-temperature operation.

CHAPTER 6

ANALYSES OF LOSS OF HEAT SINK ACCIDENT IN COMPACT HIGH TEMPERATURE REACTOR

6.1. Introduction

The design of 100 kWt Compact High Temperature Reactor (CHTR), which is envisaged as a technology demonstrator for Indian HTR programme, consists of several inherent safety features. The core neutronics is designed with negative reactivity feedback coefficients for stable reactor operations. The core heat removal during normal-operation is based on the natural circulation of LBE coolant in multiple vertical channels between the two plenums (Dwivedi et al., 2018). A set of sodium heat pipes placed in the downcomers at the upper plenum passively transfer core heat to the secondary side (Panda et al., 2017 and Dulera et al., 2017). Durability, reliability and robust functioning of these heat pipes are essential for the safe and efficient operation of the reactor (Mylavarapu et al., 2012 and Yan et al., 2020) because the failure of these pipes disrupts the core heat transfer to the secondary side and result in the loss of heat sink accident. Therefore, the scenario of unprotected loss of heat sink accident (ULOHSA) in the operating condition of the CHTR at the beginning of the life cycle has been investigated with multi-physics code ARCH-TH (Dwivedi et al., 2020). The consequence of reactivity feedbacks has been assessed on the core power production during the transient. Since the loss of heat sink drastically reduces the natural circulation of LBE, the phenomena of reverse flow in low powered channels during transient are also investigated. The flow reversal in the low powered channels indicates that these channels could also act as downcomers during such transients. The phenomena of flow reversal in low powered channels have been the first time predicted in natural circulation cooled high-temperature core design. The flow reversal would degrade the performance of equipment and cause significant hammer-effect (Radaideh et al., 2019; Czyszczewski, 2017). Despite the peak fuel and coolant temperatures stay much below the safety limits during the transient, the core design modifications are investigated to suppress the predicted coolant flow reversal.

Several coupled/ integrated N-TH studies on loss of heat sink accident for LBE or lead cooled reactor concepts have been reported in the literature. In 1996, Zaki and Sekimoto reported the unprotected loss of heat sink (ULOHS) transient study in small safe long-life fast reactor cooled with lead or lead-bismuth under forced circulation (Zaki and Sekimoto, 1996). It was reported that the safety margin is small for these designs for fuel rod with cladding during such severe transients. It was also found that the LBE coolant possesses better thermal-hydraulics. The loss of heat sink analysis without scram in natural circulation lead cooled fast reactor coupled with supercritical carbon dioxide Brayton cycle was published by Moisseytsev and Sienicki (2008). In the article, the whole-plant response during the ULOHSA was predicted with point kinetics to confirm the passive safety features of the reactor. The ULOHSA in natural circulation LBE-cooled 10MWt fast reactor had also been investigated by Gu et al., (2015). The investigation found out that the fuel and cladding temperatures stay below the safety limits and the reactor shut itself down due to negative feedbacks. It was pointed out that the mass flow rate decreases during the transient, but the variation of coolant mass flow rates in the channels were not described. They had also compared the scenario of LOHSA in the fast reactor to ADS system and mentioned that the fast reactor has a better safety advantage under LOHS transient (Wang et al., 2015). In the literature, various other core concepts have also been assessed for loss of heat sink transients and published. These include PBWFR (Wei et al., 2018), VVER-1000 using RELAP5/MOD3.2 (Abbasi and Hadad, 2012), MTR (El-Khatib et al., 2013), LBE cooled ADS (Sugawara et al., 2013), the MSR and FHR (Guo et al., 2013 and 2016).

The analytical and experimental studies on stability and flow reversal in natural circulation (NC) systems, have been published by several researchers in the past years (Misale, 2014; Gartia et al., 2006; Mousavian et al., 2004; Linzer and Walter, 2003; Takeda et al. 1987; Zvirin, 1986; Bau et al., 1981; IAEA-TECDOC-1474, 2005). Criteria to avoid flow reversal was reported by Linzer and Walter (2003) for asymmetrically heated risers connected to a common downcomer in the NC loop. The paper gives emphasis that in the case of NC system with coupled multi-channel, a critical heat absorption ratio exists which is dependent on the geometry and materials of risers and the overall heating conditions. Heating conditions which exceed this critical value lead to the possibility of flow reversal or almost flow stagnation in coupled low powered riser/ channel. The range of stable operation can be extended, i.e. the condition of flow reversal can be suppressed by modification of the flow resistance in the heated channels. It was also emphasized that the possibility of flow reversal cannot be completely eliminated in coupled multi-channel systems with common downcomers (Linzer and Walter 2003). Therefore, to suppress the condition of flow reversal during ULOHSA in CHTR, the transient has also been analysed with modifications in the design such as reducing the core radial power peaking, adjusting the flow resistance in the channels and both of these together. The analyses indicate that these modifications consequently delay the flow reversal in low powered channels, i.e. the occurrences of flow reversal are observed at even lower power during the ULOHSA. These analyses in natural circulation cooled CHTR have been performed with integrated neutronics and thermal-hydraulics in code ARCH-TH and studies are presented in the following sections.

6.2. Investigation of unprotected loss of heat sink accident in the designed core

The unprotected loss of heat sink accident (ULOHSA) in the CHTR during the initial core-life cycle, has been investigated with 3D multi-physics code ARCH-TH (Dwivedi et al., 2020). It has been considered that the core was operated initially at 100kWt power in steady-state conditions with coolant inlet temperature 900ºC. In the core about 91.4 % of thermal heat generated in the fuel is being removed ultimately by the LBE coolant under natural circulation (NC). The rest of the thermal heat has been assumed to be deposited outside the core region, i.e. basically to compensate the loss through outer surfaces as well as radiation leakage. The investigation has been carried out using integrated neutronics− thermal-hydraulics in the code considering temperature feedbacks from fuel, moderator and coolant. The moderator temperature feedback in the core is found to be strongly negative and play a very significant role during the transient. The comparative effect of reactivity feedbacks of the temperatures and the delayed neutron parameters of the reactor have already been discussed in Chapter 5. The steady-state power, mass flow rates and outlet coolant temperatures of the channels are predicted and found to be as presented in the Figure-5.25. The core cross-sectional schematic depicting the channel's number and its closed-loop model for coolant dynamics simulation is presented in Figure-6.1.

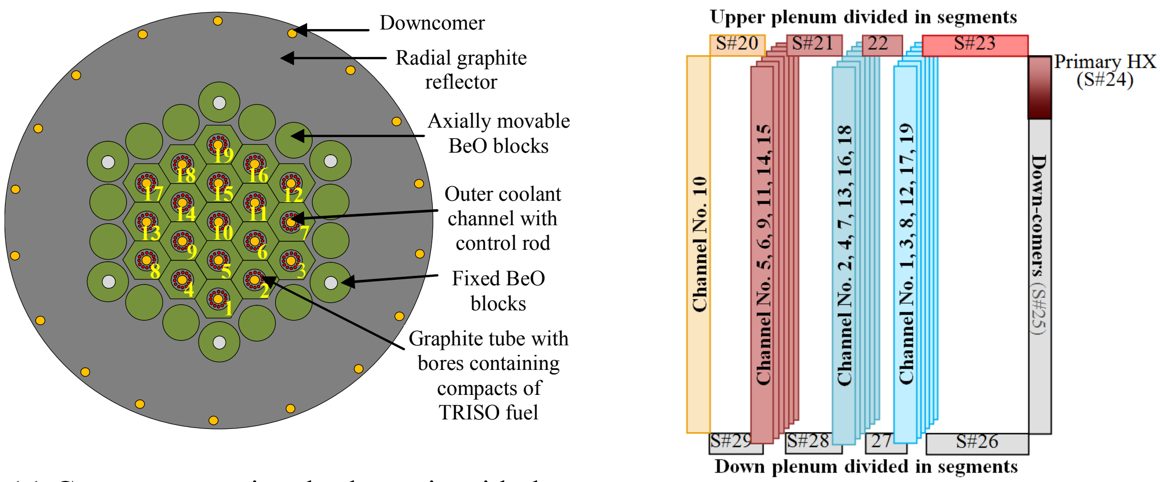

(a) Core cross-sectional schematic with the number index of the channels

(b) close-loop model for coolant dynamics

Figure-6.1: CHTR core with (a) number index of the channels and (b) close loop model for coolant dynamic simulation

In CHTR design, the coolant is returning from the upper plenum to the lower plenum through the 18 downcomers. The channels are asymmetrically heated as the core radial power peaking is approximately 1.21, and so are their mass flow rates and outlet temperatures (Figure-5.25). However, channel# 5, 6, 9, 11, 14 and 15 (in Figure-6.1) are observed to be peak powered channels with equal mass flow rates and outlet temperatures. Symmetrically, the six side-channels of the outer ring (channel# 2, 4, 7, 13, 16 and 18) are also having equal power, mass flow rates and outlet temperatures. Similarly, channel# 1, 3, 8, 12, 17 and 19, i.e. the corner assemblies of the outer ring (Figure-6.1), have same neutronics and thermal-hydraulics conditions. It is earlier discussed that the central channel in CHTR has gadolinium mixed with the fuel and it has no absorber rod partially inside unlike other channels. The central channel (#10) is observed to be producing lesser power but with the hottest outlet temperature due to least mass flow rate as observed in the steady-state simulation at the full power.

The initial steady-state operation in the core has been simulated for some duration without any perturbation in the core. Then the transient is considered to be initiated (i.e. at t=0 s shown in the results) due to total failure of the primary heat exchanger/ heat pipes (Figure-6.2). The transient is simulated with temperature feedbacks from the fuel, the moderator and the coolant. The unprotected loss of heat sink disrupts the heat transfer to the secondary side and leads to a rise in the coolant temperature firstly in the downcomers. The heating of the coolant reduces the pressure drops along the downcomers immediately, then it is followed by the channels (Figure-6.3). The heating of coolant in the downcomers reduces the density differences between the downcomers and the heated channels. This phenomenon leads to a decrease in the driving force, which consequently reduces the natural circulation flow in the channels (Figure-6.4). The interruption in natural circulation results in a rapid fall in the core outlet power/ coolant enthalpy. As there is no heat removal from the primary circuit, the rise in the core temperature occurs with higher peak fuel and moderator temperature (Figure-6.5).

The rising temperatures of the fuel and the moderator in the core introduce negative reactivity (Figure-6.6). Hence, there is a reduction in the fission rate and the core power (Figure-6.2). The coolant temperature (including density) feedback is also considered along with the fuel and moderator feedbacks. However, it has a negligible effect in CHTR (Dwivedi et al., 2017). The analyzed transient has been followed for about 30 minutes.

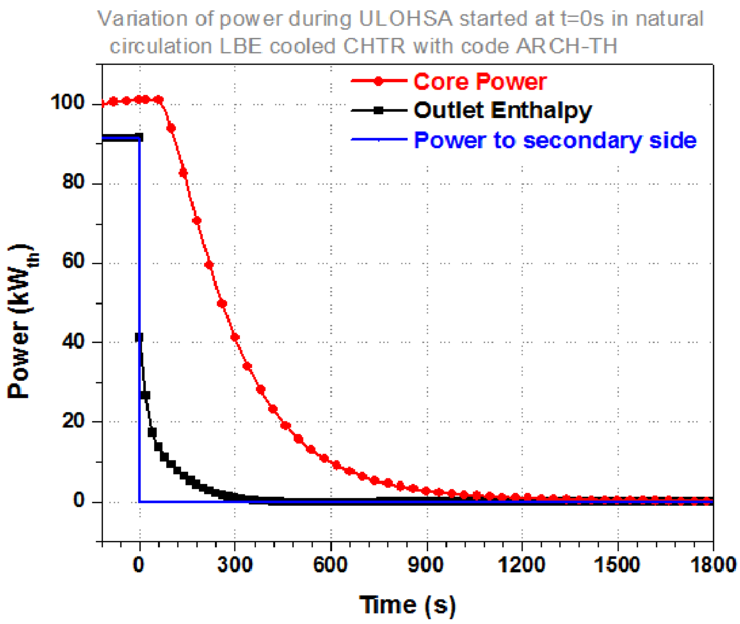

Figure-6.2: The core power and outlet coolant enthalpy during the ULOHSA in CHTR

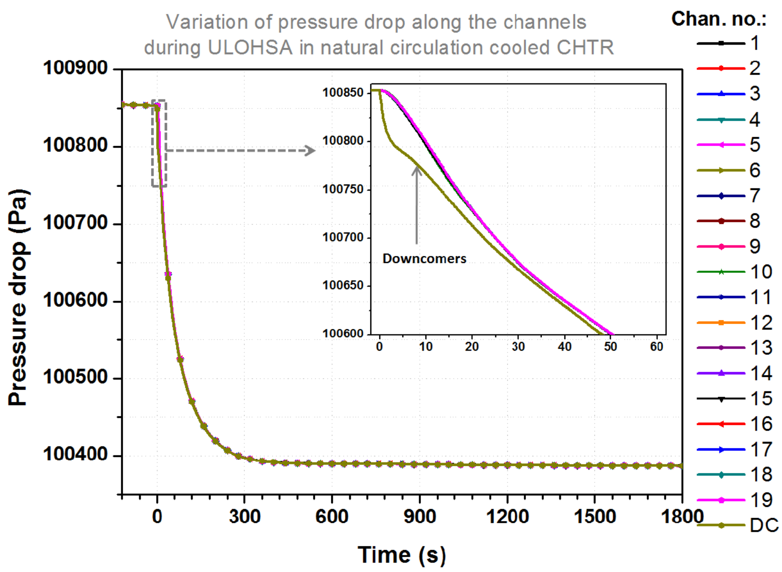

Figure-6.3: Estimated pressure drops along the channels during the transient

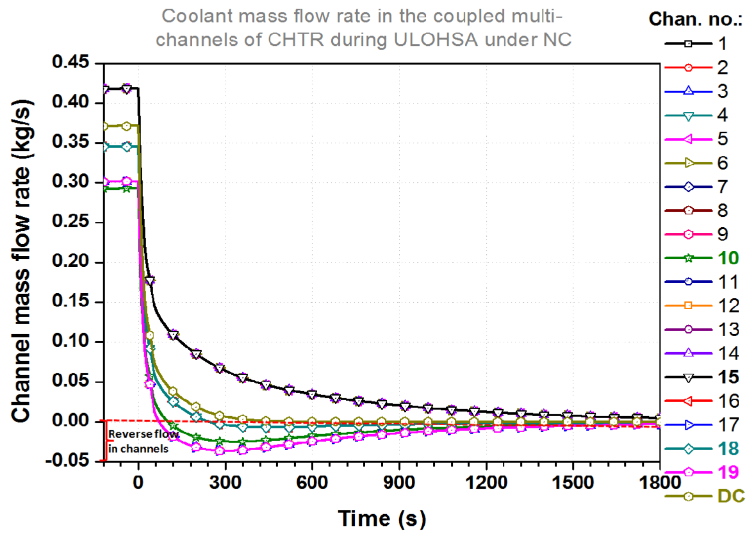

Figure-6.4: Mass flow rate evolution in the channels during the transient

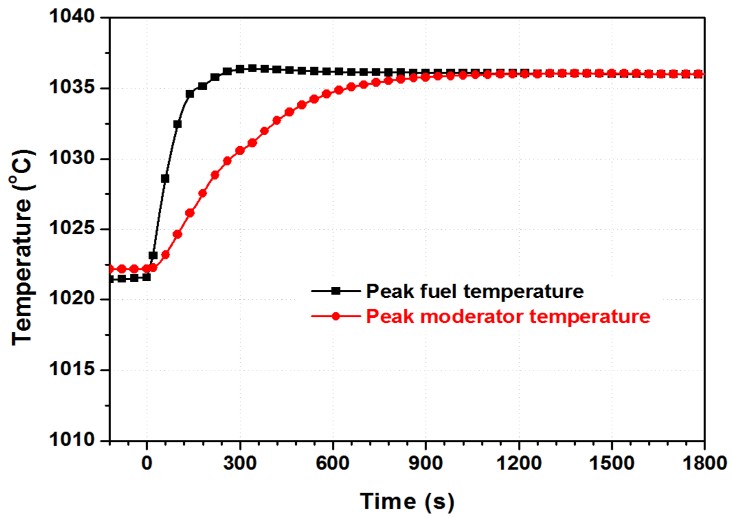

Figure-6.5: The peak temperatures in fuel and moderator during the ULOHSA

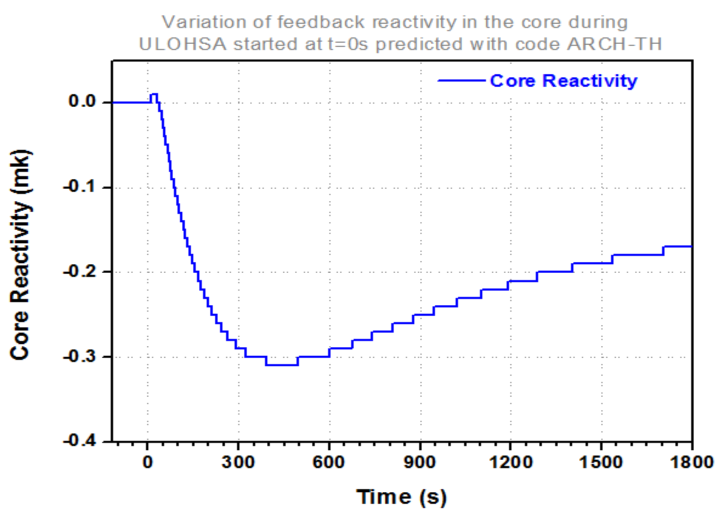

Figure-6.6: The feedback reactivity in the core during the ULOHSA

The investigation indicates that the reactor core shuts down passively due to temperature feedbacks during the transient (Figure-6.2 and Figure-6.6). The core then stabilizes with higher temperature profile and the eventual rise in the peak fuel temperature (~1040ºC) is found to be far below the leak-tightness limit (~1600ºC) of TRISO fuel particles in the core (Figure-6.5). The variations of the axial temperature profile in the fuel and the coolant of the peak powered channels are also simulated during the transient and presented in Figure-6.7 and Figure-6.8, respectively. The Figure-6.8 also shows that the inlet coolant temperature rises in the channel due to ULOHSA. The variation of the radial temperature profile in the central axial mesh of peak powered channel (Figure-6.9) indicates that the rise in the coolant temperature is maximum from its initial values as compared to the fuel and the moderator. It is mainly due to the drastic reduction in mass flow rate under natural circulation during ULOHSA. After about 20 minutes of the transient, all the radial regions in the mesh almost achieve the same temperature (Figure-6.9). The Figure-6.10 presents the variation of the core integral power and shows that the core is producing negligible heat in the passive shutdown state after about 20 minutes of the transient. The other means of heat removal from the core after the shutdown, such as heat conduction, convection at the outer-adiabatic surfaces and radiation from the heated core-materials are ignored in the current analysis.

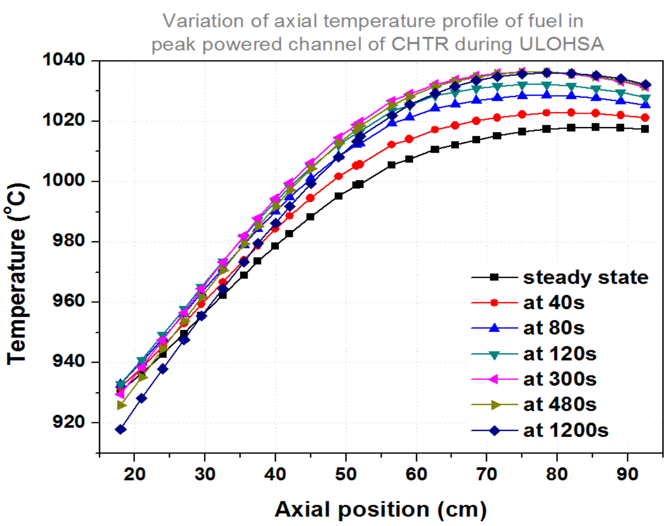

Figure-6.7: Axial temperature profile in the fuel of peak powered assembly during ULHOSA

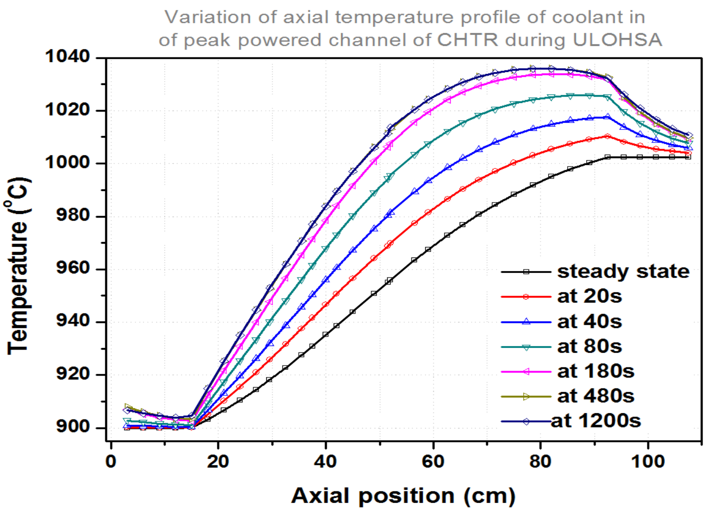

Figure-6.8: Axial coolant temperature in the peak powered assembly

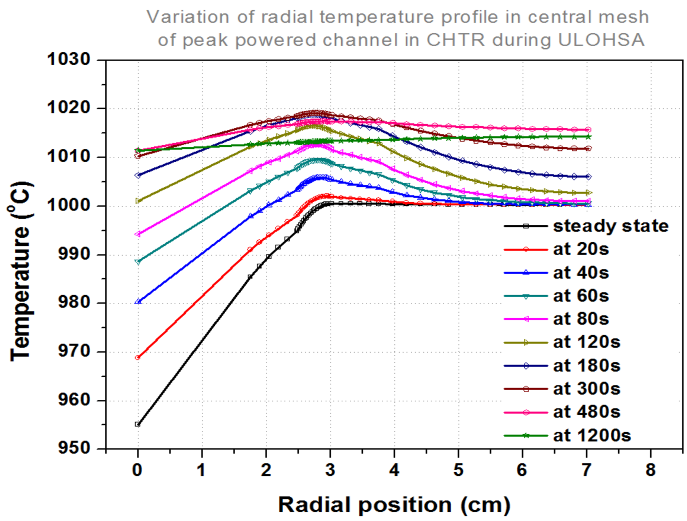

Figure-6.9: Radial temperature profile in the central axial mesh of the peak powered channel

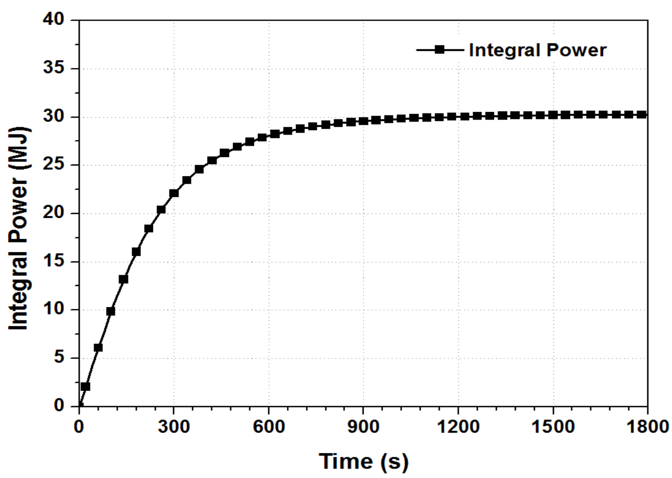

Figure-6.10: The variation of integral core power during the transient

The Figure-6.4 shows that the mass flow rates in the channels and downcomers are reducing simultaneously at the beginning of the loss of heat sink. The positive sign of mass flow rates in the channels indicates to upward flow, whereas, negative is for downward flow (or reverse flow). However, in the case of the downcomer, the downward mass flow rate is represented with positive signs. In the Figure-6.4, the flow reversal in the least powered channels (# 1, 3, 8, 12, 17 and 19) occur first at about 73 s of the transient, i.e. at about 96% of the initial core power in the present configuration. The reverse flow in the central channel (#10) is observed to be next occurring at about 103 s of the transient. These phenomena have been found to be also occurring in the rest of the outer channels (# 2, 4, 7, 13, 16 and 18) at about 247 s. The phenomena of reverse flow are found to have occurred in all the 13 low powered channels under the natural circulation of LBE coolant during the ULOHSA in CHTR. The core is found to be shutting down passively with the almost stagnant flow in the primary coolant circuit after 20 minutes of the ULOHSA. The peak temperature (~1040ºC) of the coolant stays far below the boiling point (1670ºC) of the LBE (Figure-6.8).

It is noticeable that the occurrences of flow reversal in the low powered channels have been observed only in case of complete loss of the primary heat sink, i.e. simultaneous failure of all the heat pipes in the present core design. The phenomena have not been observed in the case of reactivity initiated overpower transient in the core with a heat sink, which is discussed in Chapter 5 (Dwivedi et al., 2018). Although the peak temperatures of the fuel and the coolant are observed to stay much below the safety limits during ULOHSA in the present core design, the transient is further investigated with the following design modifications to pacify the flow reversal;

a) Reducing the radial power peaking in the core,

b) Adjusting the flow resistance in the channels and,

c) Both of these modifications together.

The reduction in the radial power peaking in CHTR has been achieved with re-distribution of burnable poison (gadolinium) in more fuel assemblies. However, the flow resistances in low powered channels (i.e. except # 5, 6, 9, 11, 14 and 15) have been enhanced by slightly increasing the outer diameter of the carbon composite guide tubes for control rods in the channels near top reflector zone. In this case, the flow area in the segment of the downcomers with heat pipes is also slightly adjusted accordingly to keep the core mass flow rate almost unchanged for the desired outlet temperature (~1000°C). The individual, as well as combined consequences of these modifications on flow reversal during ULOHSA in CHTR, are discussed briefly in the following sections.

6.3. Analysis of ULOHSA in the core with reduced radial power peaking

The ULOHSA has been first simulated in the modified core design of CHTR with reduced radial peaking (Dwivedi et al., 2020). The lower radial power peaking (~1.04) has been achieved with more flat power profile after re-distribution of burnable poison in the more fuel assemblies keeping initial excess reactivity almost unchanged.

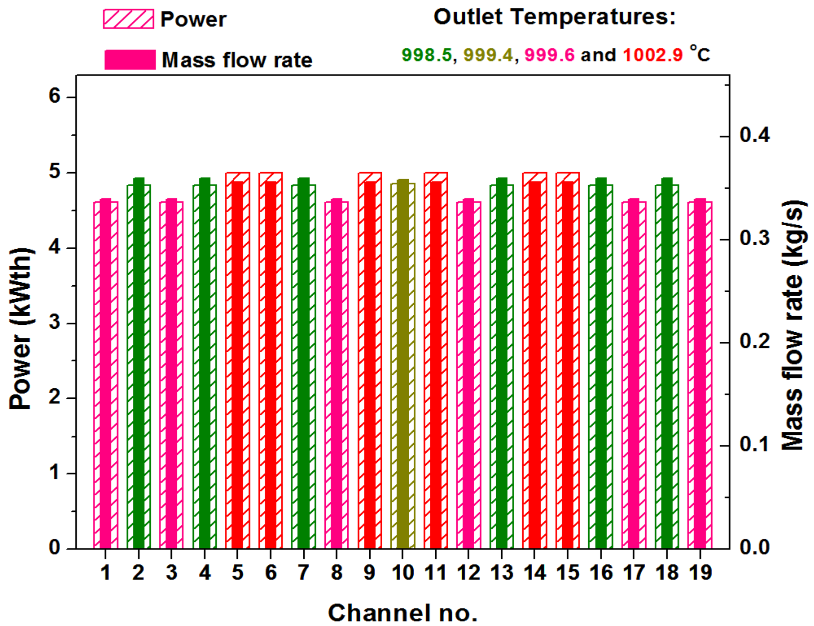

Figure-6.11: Steady-state power, mass flow rate and outlet temperature of the channels in the core with reduced radial power peaking

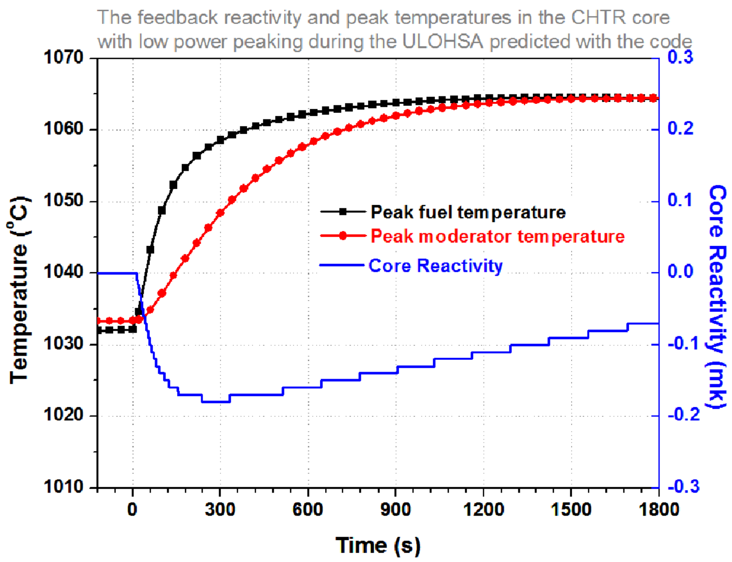

Figure-6.12: The peak temperatures and feedback reactivity during transient in the core design with reduced radial power peaking

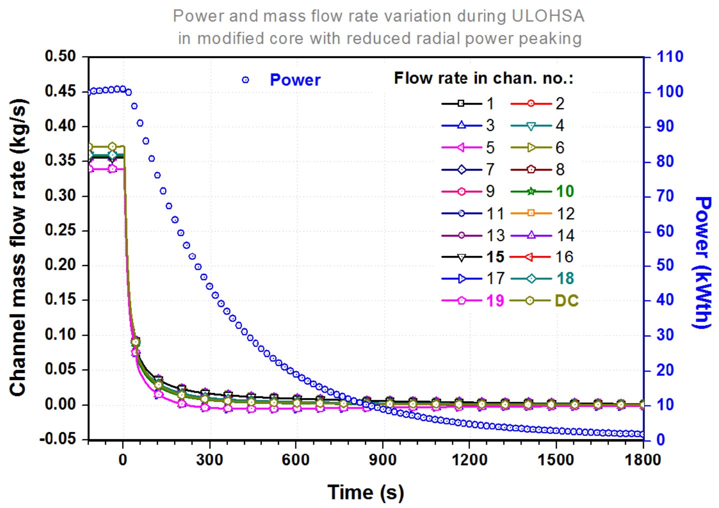

Figure-6.13: The core power and the channel mass flow rates during ULOHSA in the core design with reduced radial power peaking

The steady-state operation of the modified core has been simulated, and channel power, mass flow rates and outlet temperatures are shown in Figure-6.11. The variation of peak fuel temperature and total feedback reactivity in the modified core during the ULHOSA is shown in Figure-6.12. In this case, the first occurrence of flow reversal is predicted after 220 s of the transient at about 56% of the initial core power level (Figure-6.13). Therefore, reduction in the radial power peaking of the core pacifies the condition for reverse flow and delays its occurrence during the ULOHSA. The peak fuel temperature is found to be rising to ~1065°C in this design. The higher rise in peak temperature is observed due to less negative fuel temperature feedback coefficient after mixing of more gadolinium in the fuel (Figure-6.12).

6.4. Analysis of ULOHSA after adjusting the flow resistance in the coolant channels

In the second option of modification, only the flow resistances in the low powered channels of the CHTR are increased slightly by increasing the outer diameter of the guide tubes near top reflector zone (Dwivedi et al., 2020). The absorber rod inserted through a guide tube at the top reflector zone of the central channel (#10) is also considered, which was absent in the earlier design. After these modifications in the coolant channels, the case of ULOHSA has been simulated keeping radial power profile unchanged (i.e. peaking about 1.21).

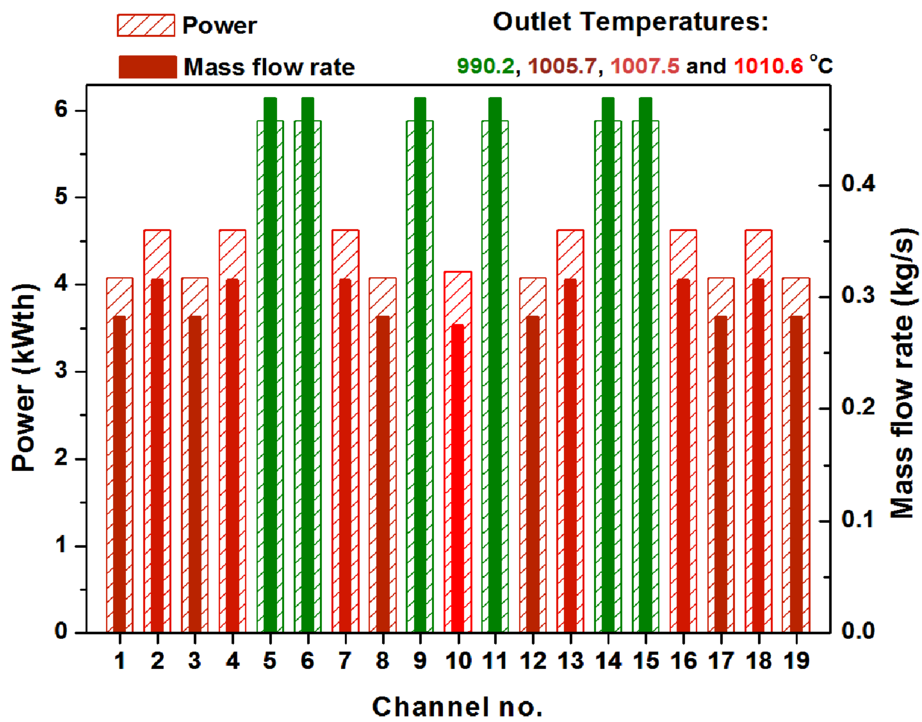

Figure-6.14: Steady-state power, mass flow rate and outlet temperature of the channels after adjusting the flow resistance in the channels

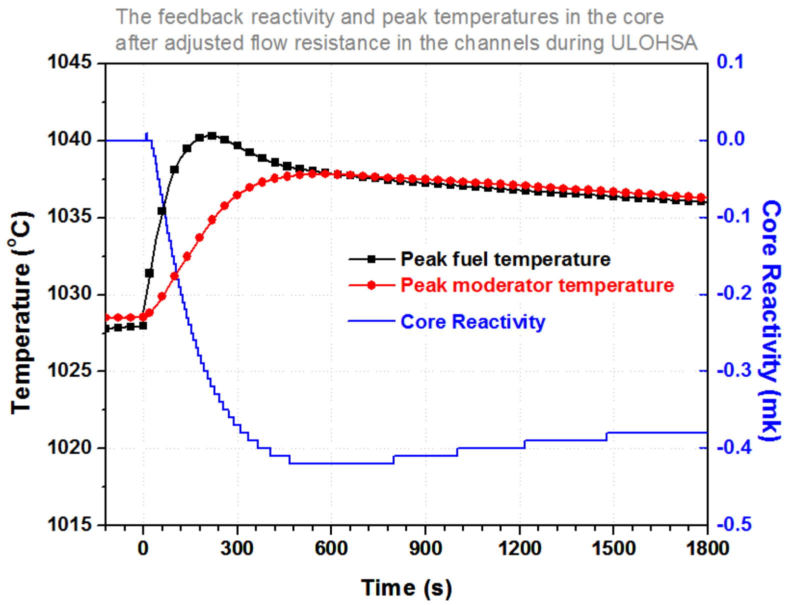

Figure-6.15: The peak temperatures and feedback reactivity during transient in the core design with adjusted flow resistance in the channels

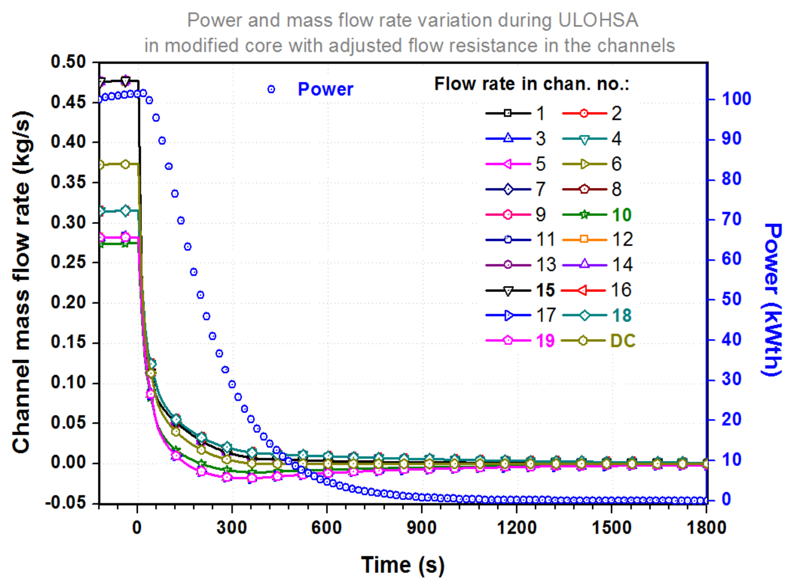

Figure-6.16: The core power and the channel mass flow rates during ULOHSA in the core design with adjusted flow resistance in the channels

The steady-state of the modified core has been simulated. The estimated parameters, such as power, mass flow rates, as well as outlet temperatures of the channels, are found to be as shown in Figure-6.14. After this design modification, the case of ULOHSA has been investigated and predicted peak fuel temperature and total feedback reactivity in the core are found to be as shown in Figure-6.15. The first occurrence of flow reversal is predicted after 151 s of the transient, i.e. at about 66% of the initial power level in the core (Figure-6.16). Therefore, increasing the flow resistances in the low powered channels also pacifies the condition for flow reversal and results in the delay of its occurrence during the ULOHSA. In this case, the peak fuel temperature is found to be rising to ~1040^{o}C during the transient.

6.5. Analysis of ULOHSA with reduced power peaking and adjusted flow resistance

In the third option for modification in the core design, the reduction in power peaking (~1.04) as well as enhanced flow resistance in the low powered channels, are considered together (Dwivedi et al., 2020). In this case, the channel power, mass flow rates and outlet temperatures are predicted under steady-state operation as shown in Figure-6.17.

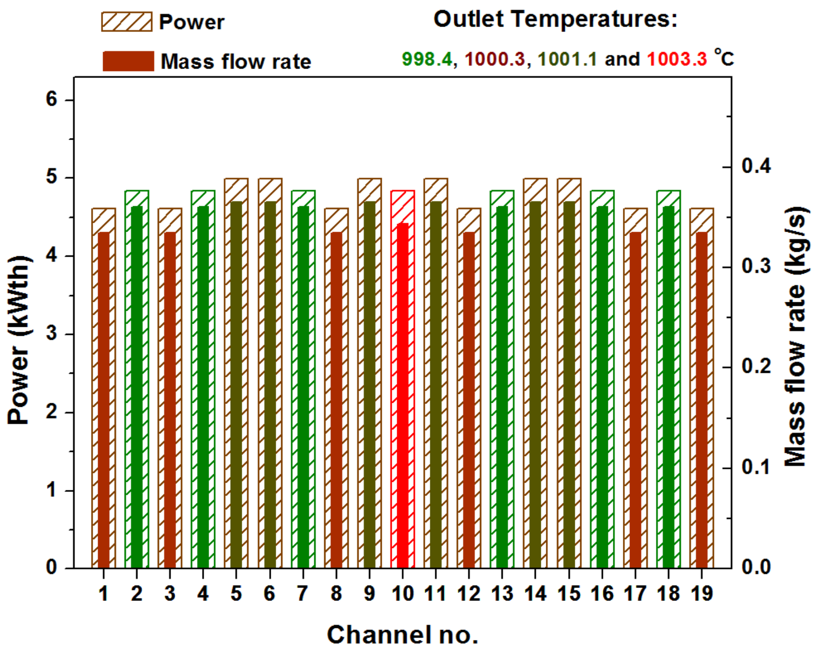

Figure-6.17: Steady-state power, mass flow rate and outlet temperature of the channels in the core with reduced radial peaking and adjusted flow resistance in the channels

In the modified core design the case of ULOHSA has been investigated. The peak fuel temperature and total feedback reactivity in the core are estimated to be varying as in given

Figure-6.18. The flow reversal is observed first at after 448 s from starting of the ULOHSA, i.e. at about 30% of the initial power level in the core (Figure-6.19). Therefore, the occurrence of flow reversal in the transient was found to be most delayed in this case. The peak fuel temperature is observed to be rising to ~1066ºC during the transient.

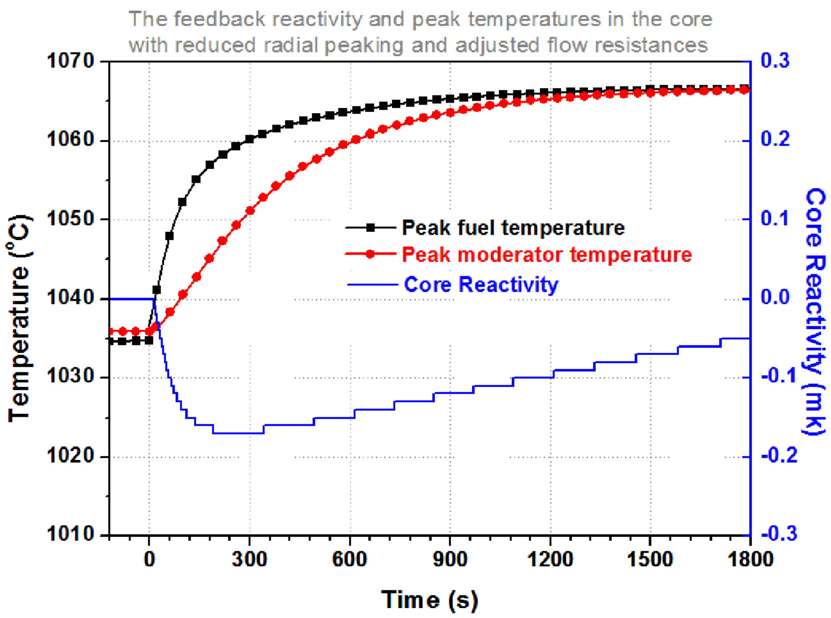

Figure-6.18: The peak temperatures and feedback reactivity during transient in the core design with adjusted flow resistance in the channels

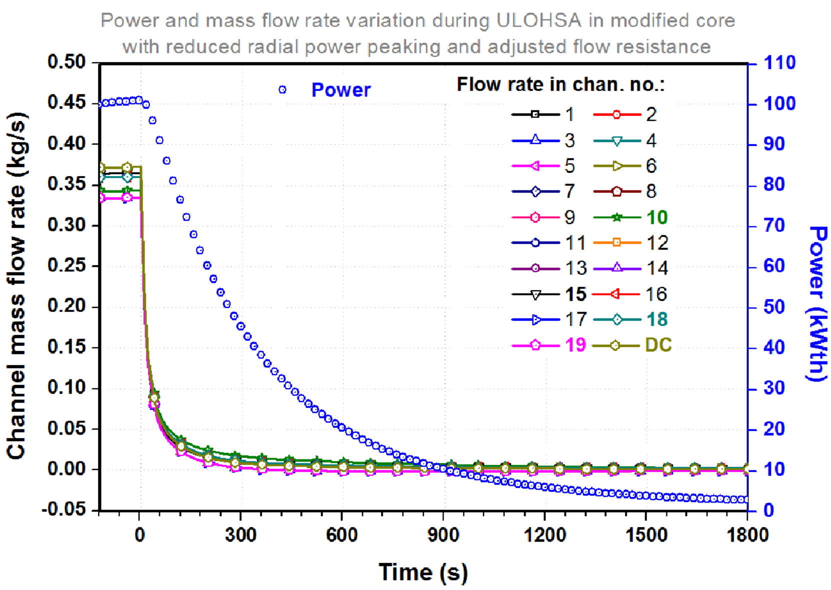

Figure-6.19: The core power and the channel mass flow rates during ULOHSA in the design with reduced radial power peaking and adjusted flow resistance

Although all these design modifications pacify the condition of flow reversal during ULHOSA, and the peak temperatures of the fuel and the coolant are found to stay well below the safety limits. In case of reduction in the core radial power peaking, the mixing of gadolinium in the fuel of more assemblies consequently makes the fuel temperature coefficient less negative. It leads to a higher rise in the fuel temperature and the relatively slow shutdown of the core (Figure-6.13 and Figure-6.19). However, the radial power peaking factor would also reduce during the life cycle of the core without reshuffling. Therefore, the design modification by adjusting the flow resistance in the channels is preferable in this context.

6.6. Conclusion

The design and safety of the prototype 100kWt CHTR core necessitate comprehensive, integrated neutronics-thermal hydraulics analyses of the anticipated transients and accidents. Therefore, unprotected loss of heat sink accident (ULOHSA) in the core has been investigated with the indigenously developed 3D multi-physics code ARCH-TH. The steady-state of CHTR core at full power has been simulated for the initial mass flow rate and outlet temperature of the channels. The total failure of the primary heat exchanger/ heat pipes is considered during the loss of heat sink accident in CHTR. The reactivity feedbacks from the fuel, moderator and coolant temperatures have been considered in the simulation under the natural circulation of LBE. The predicted automatic shutdown in the analysis due to temperature feedbacks after the transient proves the passive safety feature of the core. The phenomena of flow reversal in the low powered channels have also been predicted for the transients. Even though, the peak temperatures in the fuel and the coolant stay far below the failure limit (~1600ºC) of TRISO particles and boiling point (1670ºC) of LBE, the design modifications have also been studied to suppress the condition of flow reversal during such transients. The study indicates that the occurrence of flow reversal can be delayed by reducing radial power peaking and also by adjusting the flow resistance in the channels. These modifications are also resulting in lower mass flow rates in the channels during flow reversals. These could have more significant safety implications if employed in similar designs of high power HTR or power-reactors. However, the mixing of more gadolinium in the fuel for reducing radial power peaking makes the fuel temperature coefficient less negative. Therefore, the modified design with adjusting the flow resistance in the channels to pacify the condition of flow reversal during the ULOHSA is preferred.

CHAPTER 7

CONCLUSION AND SUMMARY

A comprehensive HTR programme is being pursued in India for enabling high-temperature applications of nuclear energy such as hydrogen production through the thermo-chemical splitting of water. The high-temperature core design imposes several challenges such as the choice of core and structural materials, core reactivity management, control and safety during operation in addition to materials compatibility at high-temperature configurations with deep fuel burnup. The performance of safety analyses of core transients is the essential aspects of the design and operation of advance nuclear reactor concepts of the next generation. Accurate and efficient core simulations are vital to these analyses, but require capabilities and tools for the study of multi-physics phenomena in such nuclear systems. The neutronics and thermal-hydraulics of HTRs are designed with several inherent safety features for safe, stable and economical operations at high temperature. The 100 kWt power Compact High Temperature Reactor (CHTR) is envisaged as a technology demonstrator for Indian HTRs. The CHTR design consists of additional safety features such as core heat removal by natural circulation of LBE during normal operations, passive heat transfer to the secondary side using high-temperature heat-pipes, negative reactivity coefficients in thorium fuelled core with long core-life-cycle etc.

The thesis emphasizes the indigenous development of 3D multi-physics code ARCH-TH for high fidelity simulations to study the nuclear fission power and safety transients in high-temperature reactors. The new development of TH modules in the code also include the capability for simulation of steady-state and transient natural circulation in coupled multi-channel based high-temperature cores. The neutronics and thermal-hydraulics capabilities in the code have been meticulously validated with reactor transient-benchmarks and also with experimental data obtained from LBE natural circulation loop. The validation results confirm the correctness and viability of the code for design and safety analyses of HTR designs. The code is being extensively used for the multi-physics studies of Indian design of HTR, i.e. CHTR. Some of the new findings have been reported in the literature.

The anticipated transients of inadvertent withdrawal of control rod without scram (i.e. ATWS) in CHTR have been investigated with various TH feedback considerations using the code. The studies have been reported in the literature highlighting the new finding that the thermally coupled BeO moderator if used in the high-temperature reactor, could provide vital temperature feedback during unprotected transients in the core. The assessments of the designed core during unprotected reactivity as well as flow initiated transients show that the fuel and coolant temperatures stay well below the safety limits.

The unprotected loss of heat sink accident (ULOHSA) in CHTR has also been investigated for the postulated failure of primary heat exchanger/ heat pipes at full power condition. The possibility of flow reversal in the natural circulation cooled high-temperature core is predicted for the first time using the indigenously developed multi-physics code. The temperatures in the reactor core are observed to be varying much below the safety limits for leak-tightness of TRISO fuel (~1600ºC) and boiling point of LBE coolant (i.e. 1670ºC). The negative reactivity feedbacks are resulting in core shut-down passively during the transient.

The scope of design modifications in natural circulation cooled high-temperature core has been evaluated for the first time to suppress the flow reversal during the ULOHSA. The research asserts that the flow reversal during such transients occurs due to asymmetrical thermal-hydraulic conditions in the coupled multi-channel system, which can be pacified through adjustments of flow resistance in the channels and more flat radial power production in the core.

These safety transients in the proto-type high-temperature concept of CHTR have been carried out with the newly developed and validated multi-physics tool to predict and confirm the designed passive safety features in the core. The research emphasizes that CHTR is a safe and stable core design even in case of postulated transients and accidents without scram during high-temperature operation.

The scope of future development in multi-physics code ARCH-TH is also under consideration. It is planned to enhance the heat transfer model of the developed TH module to simulate even more complex heating in the core of HTRs such as heat losses at high temperature through the outer surfaces of the prismatic assemblies and ex-core components of the primary coolant circuit. The secondary side heat balance equations are planned to be solved in simulation with proper modelling. The axial heat conduction in the LBE coolant will also be assumed, which is more relevant in case of flow stagnant conditions. For the post-shutdown analysis of HTRs, the development of the appropriate model for the decay heat production is also under consideration. The TH capability in code ARCH-TH is also intended to extend for pebble bed HTRs as well as water and molten salt cooled Indian concepts of the advance reactors.

The operational transients of CHTR such as core start-up from low power to full power, power setbacks through the action of control rods, are also being considered for investigations with multi-physics capability. The more severe transients of reactivity, such as ULOHSA after the inadvertent withdrawal of control rod accident, loss of coolant after the breach in the primary coolant circuit, i.e. downcomers etc. would also be studied in future.

The neutronics and thermal-hydraulics capabilities in code ARCH-TH have been well qualified with the suitable benchmark problems. The best available input data for CHTR is taken for the transient analyses reported in the thesis. The predictions of these transients at the nominal power configuration of CHTR is not expected to change significantly for small uncertainty in the considered thermo-physical properties and correlations. It is due to the low power density in the designed core consisting of ceramic materials of high heat capacity. However, for more accurate perditions of the safety parameters such as peak temperatures in the TRISO fuel compacts and the LBE coolant, experiments and related research are needed under realistic TH conditions similar to CHTR core operations. Therefore, these correlations and thermo-physical properties of core materials such as thorium-based TRISO fuel compacts, BeO moderator, graphite tube and LBE coolant can be concurrently updated in the code if obtained in future.

The developed code can also be validated with coupled 3D neutronics - thermal-hydraulics transient benchmark case particularly of natural-circulation HTR design, if and when available to us. The in-house transport-theory based deterministic code for full core could also be considered for similar coupling/ integration with the TH modules for higher accuracy in predictions of multi-physics phenomena in high-temperature core designs.

Abbasi, S., Hadad, K., (2012). Analysis of the loss of heat sink transients in the secondary circuit of a VVER-1000 using RELAP5/MOD3.2. *Annals of Nuclear Energy, vol. 47. pp. 28–37.*

Aghaie et al., (2012). Coupled neutronic thermal–hydraulic transient analysis of accidents in PWRs. *Annals of Nuclear Energy 50, 158–166.*

Agrawal, S.K., Chauhan , A., Mishra, A. (2006). The VVERs at KudanKulam. *Nuclear Engineering and Design, vol. 236, pp. 812–835.*

Alemberti et al., (2020). Lead-cooled Fast Reactor (LFR) System Safety Assessment. *www.gen-4.org/gif/upload/docs/application/pdf/2020-06/gif_lfr_ssa_june_2020 _2020-06-09_17-26-41_202.pdf, GIF.*

Askew et al., (1966). A general description of lattice code WIMSD4. *J. Br. Nucl. Energy Soc., 5 (1966), pp. 564.*

ASTM (2014). Standard for Testing Graphite and Boronated Graphite Material for High Temperature Gas-Cooled Nuclear Reactor Components. *Std. Procedure C781-08.*

ATHLET, (2003). ATHLET Mod 2.0 Cycle A, Input Data Description, *GRS-P-1/Vol. 1, Rev.3, Gesellschaft für Anlagen- und Reaktorsicherheit (GRS) mbH, Germany, 2003.*

Aufiero et al. (2011). Development of a single-channel multi-physics model for lead fast reactors. *In: 20th Int. Conf. Nuclear Energy for New Europe, Slovenia.*

Avramova et al., (2015). Multi-physics and multi-scale benchmarking and uncertainty quantification within OECD/NEA framework. *Annals of Nuclear Energy 84, Pages 178-196.*

Badwal et al., (2013). Hydrogen production via solid electrolytic routes. *WIREs Energy and Environment, vol. 2(5), pp.473-487.*

Bajaj, S.S. and Gore, A.R. (2006). The Indian PHWR. *Nuc. Engg.& Des.,236, pp.701-722.*

Balestra et al. (2016). Simulation of AER-DYN-002 and AER-DYN-003 Control Rod Ejection Benchmarks by RELAP5-3D/PHISICS Coupled Codes. *Nuclear Technology, vol. 193:1, pp. 175-182.*

Balestra et al., (2020). Modular high temperature gas reactor core modeling with RELAP5-3D/PHISICS–Optimization schemes for load following. *Nuclear Engineering and Design 362, 110526.*

Banerjee et al. (2007). Studies on sulfur-iodine thermo-chemical cycle for hydrogen production. *BARC Newsletter Issue no. 285, pp. 67-70.*

Banerjee, S. and Gupta, H.P. (2017). The evolution of the Indian nuclear power programme. *Progress in Nuclear Energy, vol.-101, pp. 4-18.*

Bau, H.H. and Torrance K.E., (1981). On the stability and flow reversal of an asymmetrically heated open convection loop. *Journal of Fluid Mechanics. Vol. 109. pp. 417-433.*

Bell and Glasstone (1970). Book on Nuclear Reactor Theory. *ISBN: 10 : 0442206844.*

Bhabha, H.J. and Prasad, N.B. (1958). A study of the contribution of atomic energy to a power programme in India. In: *Proceedings of 2nd UN International Conference on 'Peaceful Uses of Atomic Energy' Geneva, September 1-13, vol. 1, pp. 89-101.*

Boer et al., (2008). Coupled neutronics / thermal hydraulics calculations for High Temperature Reactors with the DALTON - THERMIX code system. *International Conference on the Physics of Reactors, "Nuclear Power: A Sustainable Resource". Casino-Kursaal Conference Center, Interlaken, Switzerland, September 14-19.*

Bonifetto et al., (2013). A full-core coupled neutronic/thermal–hydraulic code for the modeling of lead-cooled nuclear fast reactors. *Nuclear Engineering and Design 261, pp. 85-94.*

Borgohain, A., Maheshwari, N. K., Vijayan, P. K., Sinha, R. K., (2011). CFD analysis on heat transfer in low Prandtl number fluid flows. *NURETH14, 457.*

Borgohain et al., (2016). Natural circulation studies in a LBE loop for a wide range of temperature. *Nuclear Engineering and Design, vol. 300, pp. 358–375.*

Brook, B.W., Alonso, A., Meneley, D.A., Misak, J., Blees, T., van Erp, J.B. (2014). Why nuclear energy is sustainable and has to be part of the energy mix. *Sustainable Mater Technol., vol.-1, pp. 8-16, 10.1016/j.susmat.2014.11.001.*

Chapin et al., (2004). The Very High Temperature Reactor: A Technical Summary. *MPR Associates, Inc.*

Cheng, X., Tak, N.-i., (2006). Investigation on turbulent heat transfer to lead–bismuth eutectic flows in circular tubes for nuclear applications. *Nuc. Engg and Design 236, 385–393.*

Chetal et al. (2006). The design of the Prototype Fast Breeder Reactor. *Nuclear Engineering and Design, vol. 236, pp. 852–860.*

Choi et al. (2018). Namjae Choi, Junsu Kang, and Han-gyu Joo. (2018). Massively Parallel Method of Characteristics Neutron Transport Calculation with Anisotropic Scattering Treatment on GPUs. *In. Proceedings of the International Conference on High Performance Computing in Asia-Pacific Region, HPC Asia 2018. ACM, New York, NY, USA, 148–158. doi.org/10.1145/3149457.3149460.*

Czyszczewski, M.F. (2017). How to Prevent Circulating Water Flow Reversal. *Power Magazine*, June-*2017, pp. 1-7*

D'Angelo, A. and Gabrielli, F., (2003). Benchmark on Beam Interruptions in an Accelerator-driven System – Final Report on Phase I Calculations. *OECD Nuclear Energy Agency, NEA/NSC/DOC(2003)17, ISBN 92-64-02138-8.*

D'Angelo, A. and Gabrielli, F., (2004). Benchmark on Beam Interruptions in an Accelerator-driven System – Final Report on Phase II Calculations. *OECD Nuclear Energy Agency, NEA/NSC/DOC(2004)7, ISBN 92-64-02072-1.*

D'Auria and Lanfredini (2019). V&V&C in nuclear reactor thermal-hydraulics. Nuclear Engineering and Design, vol. 354,1101622.

Demaziere, Christophe (2020). Modelling of Nuclear Reactor Multi-physics. *Acadmic Press, Elsevier. 2020.*

Devan et al., (2011). Approach to equilibrium fuelling scheme of 500 MWe PFBR based on 3-D core burnup modeling. *Nuclear Engineering and Design 241(5), pp. 1596-1605.*

Downar (2006). PARCS n2.7 US NRC Core Neutronics Simulator. *School of Nuclear Engineering, Purdue University, W. Lafayette, Indiana.*

Duderstadt, J.J. and Hamilton, L.J. (1976). Nuclear reactor analysis. *Wiley, New York.*

Dulera, I.V., Sinha, R.K., Rama Rao, A., Patel, R.J. (2017). High temperature reactor technology development in India. *Progress in Nuclear Energy, vol. 101, pp. 82-99.*

Dulera I.V. and Sinha R.K. (2007). The Indian high temperature reactor programme. *IAEA-CN-152-20, IAEA Proceedings Series (2009): 85-93.*

Dwivedi, D.K., Gupta, A., Krishnani, P.D. (2010). Challenges in core reactivity management and control optimization in physics design of Compact High Temperature Reactor. *BARC Newsletter 317, 22–28.*

Dwivedi, D.K., Gupta, A., Srivastava, A.K., Krishnani, P.D., (2013). Incorporation of Improved Quasi Static (IQS) scheme module in 3-D space-time analysis codeARCH. In: *Proceedings of ARP-2013, Mumbai, India, October 23–25.*

Dwivedi, D.K. and Gupta, Anurag (2015). Development of adiabatic Doppler feedback model in 3D space time analysis code ARCH. *Life Cycle Reliability and Safety Engineering, 2015, 4(4), pp. 22-28.*

Dwivedi, D. K., Gupta, A., Krishnani, P. D. (2015[b]). Significance of moderator temperature feedback in 3D space time safety analysis of Compact High Temperature Reactor (CHTR). *In. Proceedings of CANSAS - 2015 (CANDU Safety Association for Sustainability) & NRTHS - 2015 (New Horizons in Nuclear Reactor Thermal-Hydraulics and Safety), Mumbai, Dec. 8 - 11, 2015.*

Dwivedi, D. K., Gupta, A., Krishnani, P. D. (2016). In. *Proceedings of '36th Annual Conference of the Canadian Nuclear Society and 40th Annual CNS/CNA Student Conference', vol-2, pp-1170-1177, Toronto, ON, Canada, June 19-22, 2016. ISBN: 978-1-5108-3649-5.*

Dwivedi, D. K., Gupta, A., Kannan, U. (2016[b]). Analyses of postulated case of coolant blockage and over-flow accidents in CHTR with 3D space-time code ARCH-IQS. report no. *RPDD/HTR/75/2016.*

Dwivedi, D.K., Gupta, Anurag, Kannan, U., (2017). 3D Space-Time Analysis of ATWS in Compact High Temperature Reactor with Integrated Thermal-Hydraulic model in code ARCH-TH. *Annals of Nuclear Energy 110, 306-316.*

Dwivedi, D.K., Gupta, Anurag, Kannan, U. (2017[b]). Analysis of coolant blockage in Compact High Temperature Reactor with 3D space-time code ARCH-TH. In. *Proceedings of DAE-BRNS National Symposium on 'Advances in Reactor Physics', page 275-278, Mumbai, December 06-09, 2017.*

Dwivedi, D.K., Gupta, A. and K., Umasankari (2018). Transient simulation of LBE cooled CHTR under natural circulation with 3D multi-physics code ARCH. *IUSSTF, Nuclear Safety Symposium, at IITB, Mumbai, December 15-19, 2018. https://newprairiepress.org/asemot/2018/fullprogram/20/*

Dwivedi, D.K., Gupta, A. and Krishnani, P.D. (2019). 3D space time analysis of anticipated transient analyses in CHTR with Fuel Temperature feedback. *In: Nayak A., Sehgal B. (eds) Thorium—Energy for the Future. Springer, Singapore. https://doi.org/10.1007/978-981-13-2658-5_31*

Dwivedi, D.K., Gupta, Anurag, Kannan, U. (2020). Analysis of unprotected loss of heat sink accident in compact high temperature reactor cooled under natural circulation of LBE coolant. *Nuclear Engineering and Design, 2020, 370, 110881.*

El-Khatib et al., (2013). Modeling and simulation of loss of the ultimate heat sink in a typical material testing reactor. *Annals of Nuclear Energy, vol. 51, pp. 156–166.*

Ellis et al. (2013). Progress in the development of an implicit steady state solution in the coupled code TRACE/PARCS. *Prog. Nucl. Energ., 66, pp. 1-12.*

Fermi, E. (1946). The development of the first chain reacting pile. Proc. Am. Philos. Soc., 90(1), pp. 20-24

Fernando, M.P.S. (2018). Coupling of 3D Space Time Neutronics with Thermal Hydraulics for Safety Analysis of Large PHWRs. *Symposium on Advanced Sensors and Modeling Techniques for Nuclear Reactor Safety*.

Folsom et al., (2015). Experimental measurement and numerical modeling of the effective thermal conductivity of TRISO fuel compacts. *J. of Nuc. Mat., v.458, pp.198–205.*

Fowler, (1999). Citation-LDI2 Nuclear Reactor Core Analysis System. *CCC 643, Oak Ridge National Laboratory, Oak Ridge, Tennessee.*

Gammi et al. (2011). A multi-physics modelling approach to the dynamics of Molten Salt Reactors. Ann. Nucl. *Energy, 38 (2011), pp. 1356-1372.*

Gartia, M.R., Pilkhwal, D.S., Vijayan, P.K. and Saha, D., (2006). Analysis of metastable regimes in a parallel channel single phase natural circulation system with RELAP5/MOD3.2. *International J. of Thermal Sciences, vol. 46, pp. 1064–1074.*

Gaston et al., (2015). MOOSE: A parallel computational framework for coupled systems of nonlinear equations. *Nucl. Eng. Des. 239, 1768–1778.*

Gaston et al., (2015). Physics-based multiscale coupling for full core nuclear reactor simulation. *Annals of Nuclear Energy 84, Pages 45-54.*

Gerwin, H, Scherer, W., Teuchert, E., (1989). The TINTE Modular Code System for Computational Simulation of Transient Processes in the Primary Circuit of a Pebble-Bed High-Temperature Gas-Cooled Reactor. *Nucl. Sci. and Engg. 103, pp 302-312.*

GIF (2020). The Generation IV International Forum. webpage: accessed on 09 Nov. 2020 *www.gen-4.org/gif/jcms/c_59461/generation-iv-systems.*

Glasstone and Sesonske (1994). Book on 'Nuclear Reactor Engineering: Reactor Design Basics', *Fourth edition (vol-1), Chapman & Hall, Inc., NY, ISBN: 81–239–0647–1.*

Goldberg, S.M. and Rosner, R. (2011). " Nuclear Reactors: Generation to Generation", *American Academy of Arts and Sciences, ISBN: 0-87724-090-6.*

Gougar, H.D. (2006). The Application of the PEBBED Code Suite to the PBMR-400 Coupled Code Benchmark – FY 2006. *Annual Report. INL/EXT-06-11842.*

Gu, Z., et al., (2015). Transient analyses on loss of heat sink and overpower transient of natural circulation LBE-cooled fast reactor. *Progress in Nuclear Energy, vol. 81, pp. 60-66.*

Guo et al., (2013). Simulations of unprotected loss of heat sink and combination of events accidents for a molten salt reactor. *Annals of Nuclear Energy, vol. 53, pp. 309–319.*

Guo et al., (2016). Development of the FHR advanced natural circulation analysis code and application to FHR safety analysis. *Progress in Nuclear Energy, vol. 91, pp. 56-6.7*

Gupta, A., Kumar, A., Dwivedi, D.K., Krishnani, P.D., (2008). Physics design of Compact High Temperature Reactor (CHTR). Proceedings of International conference on Physics of Reactors (PHYSOR-08), Interlaken, Switzerland, Sept 14-19, 2008.

Gupta, Anurag (2012). ARCH: a 3D space–time analysis code in cartesian and hexagonal geometries. In: *Proceedings of NSRP 19, Mamallapuram, TN, 12–14 Dec 2012.*

Gupta et al., (2013). Architecture of integrated neutronics and thermal–hydraulics code system ARCH+RELAP5 for the analysis of anticipated transients in AHWR. In: *Severe accident analysis and management (SAAM-2013), IIT Kanpur, India.*

Gupta and Kannan, (2017). An overview on neutronic simulation schemes for reactor transient and safety analysis. *SRESA's Int J Life Cycle Reliab Saf Eng 6:83–98.*

Gupta, Anurag (2017). ARCH- A 3-D core simulations tool. In. *Proceedings of 3rd DAE-BRNS Symposium on Advances in Reactor Physics (ARP-2017), Anushakti Nagar, Mumbai, India, Dec 06-09, 2017.*

Grundmann, U., Rossendorf, FZ, (2000). AER Benchmark Specification Sheet- Test ID: AER-DYN-002. *http://aerbench.kfki.hu/aerbench/Dyn002.pdf* .

Grundmann et al., (2000). DYN3D – three-dimensional core model for steady-state and transient analysis of thermal reactors. *In: Proc. PHYSOR 2000, Pittsburgh, Pennsylvania, USA.*

Haubenreich, P.N. and Engel, J.R. (1970). Experience with the Molten-Salt Reactor Experiment. *Nuc. Application and Tech., 8:2, 118-136, DOI: 10.13182/NT8-2-118.*

HTRE, (1959). Summary report of HTRE NO. 3 Nuclear Excursion. United States: N. p., 1965. *Report no. APEX-509, osti_4643464, web. doi:10.2172/4643464.*

IAEA (2005). TECDOC-1474. Natural circulation in water cooled nuclear power plants: Phenomena, models, and methodology for system reliability assessments. *ISBN 92–0–110605–X, ISSN 1011–4289.*

IAEA (2020). Nuclear Power Reactors in the World. Reference data series no. 2, *ISBN 978–92–0–114820–9, ISSN 1011–2642 & www.iaea.org/newscenter/news/ exploring-research-reactors-and-their-use,* accessed on 09 Nov-2020.

IAEA-THPH, (2008). Thermophysical Properties of Materials For Nuclear Engineering: *A Tutorial and Collection of Data. ISBN 978–92–0–106508–7.*

Ikeda, Hideaki and Takeda, Toshikazu (2001). Development and Verification of an Efficient Spatial Neutron Kinetics Method for Reactivity-Initiated Event Analyses. *J. of Nuc. Sci. and Tech., 38:7, 492-502. 10.1080/18811248.2001.9715059.*

Jain, V.K., (1989). Point-kinetics model with one-dimensional (radial) heat conduction formalism. report no. *BARC-1452*.

Jérôme et al. (2014). The molten salt reactor (MSR) in generation IV: Overview and perspectives. *Progress in Nuclear Energy, vol. 77, pp. 308-319.*

Joo et al., (1998). PARCS, A Multi-dimensional Two- group Reactor Kinetics Code based on the Nonlinear Analytic Nodal Method, *PU/NE-98-26, Purdue University*.

Kannan, U. and Krishnani, P. D. (2013). Energy from thorium—An Indian perspective. *Sadhana, Vol. 38 (5), pp. 817–837.*

Kasselmann et al., (2018). Verification of the HTR code package (HCP) as a comprehensive HTR steady state and transient safety analysis framework. Nuclear Engineering and Design 329, 167–176.

Katiyar, S.C., and Bajaj, S.S. (2006). Tarapur Atomic Power Station Units-1 and 2 Design features, operating experience and license renewal. *Nuclear Engineering and Design, vol. 236, pp. 881–893* .

Keresztúri, A., et al. (1992). A Three-Dimensional Hexagonal Kinetic Benchmark Problem. *2nd AER Symposium , Paks Hungary*

Keresztúri, A., et al.(2000). AER benchmark Specification Sheet. *accessed on 09-Nov-2020. aerbench.kfki.hu/aerbench/Dyn001.doc*

Kereszturi, A., et al., (2009). http://aerbench.kfki.hu/aerbench/dyn002_solaeki.txt. *accessed on 09-Nov-2020* .

Kim, Y., Kim, K., Noh, J.M., (2005). Reactivity-Equivalent Physical Transformation for Homogenization of Double-Heterogeneous Fuels. *Transactions of the Korean Nuclear Society Autumn Meeting, Busan, Korea, October 27-28, 2005.*

Kliem et al., (2007). DYN3D/ATHLET and ANSYS CFX calculations of the OECD VVER-1000 collant transient benchmark. *In: The Fifth International Conference: Safety Assurance of NPP with WWER, Russia.*

Krepel et al. (2007). DYN3D-MSR spatial dynamics code for molten salt reactors. *Annals Nuclear Energy, 34, pp. 449-462.*

Krishnani, P.D., (1982). CLUB-A multi group integral transport theory code for analysis of cluster lattices. *Annals of Nuclear Energy, vol. 9, pp. 255–260.*

Kubo et al. (2004). A demonstration study on a closed-cycle hydrogen production by the thermochemical water-splitting iodine–sulfur process. *Nuclear Engineering and Design, vol. 233, Issues 1–3, pp. 347-354.*

Lemaire et al., (2017). Multi-physics steady-state analysis of OECD/NEA modular high temperature gas-cooled reactor MHTGR-350. *J. Nuc. Sci. and Tech. 54:6, 668-680.*

Linzer, W. and Walter, H., (2003). Flow reversal in natural circulation systems. *Applied Thermal Engineering, vol. 23, pp. 2363–2372.*

Magedanz et al., (2015). High-fidelity multi-physics system TORT-TD/CTF/FRAPTRAN for light water reactor analysis. *Annals of Nuclear Energy 84, Pages 234-243.*

Mahadeven and Ragusa, (2007). Coupling Schemes for Multiphysics Reactor Simulation. *INL/EXT-07-13490, Idaho National Laboratory, Idaho.*

Majumdar et al., (2020). Preparation and Characterization of Nb-1Zr-0.1C Alloy Suitable for Liquid Metal Coolant Channels of High Temperature Reactors. *ASME J of Nuclear Rad Sci. doi: https://doi.org/10.1115/1.4047919*

Maschek et al., (2005). SIMMER-III and SIMMER-IV Safety Code Development for Reactors with Transmutation Capability. In: *Mathematics and Computation, Supercomputing, Reactor Physics and Biological Applications, Palais des Papes, Avignon, France, September 12–15, 2005.*

McEligot et al., (2016). Thermal Properties of G-348 Graphite. *INL/EXT-16-3824 (Rev.-0), Idaho National Laboratory.*

Merle-Lucotte and Heuer et al., (2008). "Introduction of the Physics of Molten Salt Reactor", *Materials Issues for Generation IV Systems, NATO Science for Peace and Security Series B, Editions Springer, pp. 501-52, ISBN 978-1-4020-8422 -5* .

Mirji et al., (2016). Technological Challenges in Extractive Metallurgy and Refining of Nb, Ta and Preparation of their Compounds & Alloys. *Mat. Today: Proc.3, 3151.*

Misale, M., (2014). Overview on single-phase natural circulation loops. In. *Proc. of the International conference MAE 2014, ISBN: 978-1-63248-022-4.*

Mkhabela, Peter. (2010). Optimization of coupled multiphysics methodology for safety analysis of pebble bed modular reactor. *PhD thesis.*

Moisseytsev, A., Sienicki, J.J., (2008). Transient accident analysis of a supercritical carbon dioxide Brayton cycle energy converter coupled to an autonomous lead-cooled fast reactor. *Nuclear Engineering and Design, vol. 238, pp. 2094–2105.*

Mollick et al., (2015). Deposition of diversely textured buffer pyrolytic carbon layer in TRISO coated particle by controlled manipulation of spouted bed hydrodynamics. *Chemical Engineering Science, vol. 128, pp. 44–53*.

Mousavian, S.K., Misale, M., D'Auria, F. and Salehi, M.A., (2004).Transient and stability analysis in single-phase natural circulation. *Annals of Nuclear Energy, vol. 31, pp. 1177–1198.*

Mylavarapu et al., (2012). Fabrication and design aspects of high-temperature compact diffusion bonded heat exchangers. *Nuclear Engineering and Design, vol. 249, pp. 49– 56.*

Mylonakis et al., (2014). Multi-physics and multi-scale methods used in nuclear reactor analysis. *Annals of Nuclear Energy 72, 104–119.*

Naterer et al. (2008). Recent Canadian advances in nuclear-based hydrogen production and the thermochemical Cu–Cl cycle. *Int. J. of Hydrogen Energy 34, pp.2901–2917.*

NPCIL (2017). Nuclear Power Corporation of India Limited (NPCIL) webpage. *www.npcil.nic.in/content/328_1_AboutNPCIL.aspx* accessed on 09 Nov-2020.

Oberkampf and Trucano (2008). Verification and validation benchmarks. *Nuclear Engineering and Design, vol. 238(3), pp. 716-743.*

OECD/NEA, (2005). PBMR Coupled Neutronics/Thermal Hydraulics Transient Benchmark the PBMR-400 core design - First Workshop. *NEA/NSC/DOC(2005)13.*

OECD/NEA, (2007). Nuclear Science Committee, Working Group on Lead-Bismuth Eutectic,. Handbook on Lead-Bismuth Eutectic Alloy and Lead Properties, Materials Compatibility, Thermal hydraulics and Technologies, *ISBN 978- 92-64-99002-9.*

OECD/NEA, (2015). Handbook on Lead-bismuth Eutectic Alloy and Lead Properties, Materials Compatibility, Thermal-hydraulics and Technologies. 2015 edition. *OECD/NEA No. 7268, Paris, France.*

OECD/NEA, (2017). 'Benchmark of the Modular High-Temperature Gas-Cooled Reactor-350 MW Core Design Volumes I and II'. *NEA/NSC/R(2017)4.*

OECD/NEA, (2019). Coupled Neutronic/Thermal-Fluid Benchmark of the MHTGR-350 MW Core Design: Results for Phase I Exercise 1. *NEA/NSC/R(2019)5.*

Ortensi, J., Pope, M.A., Strydom G., et al., (2011). 'Prismatic core coupled transient benchmark'. *Idaho National Laboratory. 2011. (No. INL/CON-11-20811).*

Ott, K.O., Meneley, D.A., (1969). Accuracy of the quasistatic treatment of spatial reactor kinetics. *Nuclear Science and Engineering 36, 402–411.*

Panda, K.K., Dulera, I.V., Basak, A., (2017). Numerical simulation of high temperature sodium heat pipe for passive heat removal in nuclear reactors. *Nuclear Engineering and Design, vol. 323, pp. 376-385.*

Pioro, I., Duffey, R. B., Kirillov, P. L., Pioro, R., Zvorykin, A., and Machrafi, R. (2019). Current Status and Future Developments in Nuclear-Power Industry of the World. *ASME J of Nuc. Engg. and Rad. Sci.; 5(2):024001. 10.1115/1.4042194.*

Pioro, I. and Duffey, R.B. (2019). Current status of electricity generation in the world and future of nuclear power industry. *In book: Managing Global Warming (pp.67-114). 10.1016/B978-0-12-814104-5.00003-X.*

Puthiyavinayagam et al., (2017). Development of fast breeder reactor technology in India. *Progress in Nuclear Energy. vol.-101, pp.19-42.*

Radaideh et al., (2019). Loss of coolant accident analysis under restriction of reverse flow. *Nuclear Engineering and Technology vol.-51, pp.1532-1539.*

Ragusa et al., (2010). Neutronic / thermalhydraulic coupling techniques for sodium cooled fast reactor simulations. *NERI Final Progress Report, DE-FC07-07ID14837*.

Ravnik et al. (2008). CORD-2 Core Design system for PWR Type reactors, *report. Institute Jozef Stefan, Slovenia.*

Reitsma, Frederik Ivanov, Kostadin, Downar, Tom, Han de Haas and Gougar Hans D (2006). The OECD/NEA/NSC PBMR Coupled Neutronics/Thermal Hydraulics Transient Benchmark: The PBMR-400 Core Design. *PHYSOR-2006, ANS Topical Meeting on Reactor Physics Organized and hosted by the Canadian Nuclear Society. Vancouver, BC, Canada. 2006 September 10-14.*

Revankar (2019). Chapter Four - Nuclear Hydrogen Production. In Book: *'Storage and Hybridization of Nuclear Energy', Ac. Press, pp. 49-117, ISBN 9780128139752.*

Rohde et al., (2012). Development and verification of the coupled 3D neutron kinetics/thermal-hydraulics code DYN3D-HTR for the simulation of transients in block-type HTGR. *Nuclear Engineering and Design 251. 412– 422*

Saad, Y (1996). Iterative methods for sparse linear system. *PWS, Boston.*

Sawa et al., (2001). Safety criteria and quality control of HTTR fuel, *Nuclear Engineering and Design 208(3), pp. 305.*

Seker, V., Downar, T.J. (2007). Multiphysics Methods Development for High Temperature Gas Cooled Reactor analysis. *International Conference on Emerging Nuclear Energy Systems (ICENES-2007), Istanbul, TURKEY, June 3 – 8 2007.*

Shaposhnik et al., (2010). The effect of radial distribution of coolant density on the multiplication factor. *In: Proc. of IYNC, Cape Town, South Africa.*

Singh, I., Gupta, A. and Krishnani, P.D. (2013). Coolant Void Reactivity Coefficient of FliBe with (Th-^{233}U)O_2 and Enriched UO_2 Fuel in Pebble of IHTR-600MWth. *Proceedings of Conference on Molten Salts in Nuclear Technology, Mumbai* .

Sinha, R.K. and Kakodkar, A. (2006). Design and development of the AHWR—the Indian thorium fuelled innovative nuclear reactor. *Nuclear Engineering and Design, vol. 236, pp.683-700.*

Sinha, R.K. (2011). Advanced Nuclear Reactor Systems – An Indian Perspective. *Energy Procedia, vol-7 , pp. 34–50.*

Sinha, R.K., Chellapandi, P., Srinivasan, G., Dulera, I., Vijayan, P.K., (2016). Generation-IV Concepts: India. In. *Handbook of Generation IV Nuclear Reactors. Woodhead Publishing Series in Energy, pp. 413-452.*

Spore et al., (1992). TRAC-PF1/MOD2. Programmer's Guide, Los Alamos National Lab., *Tech. Report, US Nuclear Regulatory Commission Report NUREG/CR-5673-V3.*

Srivastava, A.K.,Dwivedi, D.K., Gupta, A., Krishnani, P.D., (2013). In: *Proceedings of ARP-2013, Mumbai, India, October 23–25.*

Srivastava et al., (2021). Development of a Python Module "SARRA" for Refuelling Analysis of MSR Using DRAGON Code. *In: Bose M., Modi A. (eds), Proceedings of the 7th International Conference on Advances in Energy Research, Springer Proceedings in Energy. p.1513-1519, ICAER-2019, Dec-2019, IIT-B, Mumbai*

Stacy W.M. (2007). Nuclear Reactor Physics. *WILEY-VCH Verlag GmbH & Co. KGaA, Weinheim, ISBN978-3-527-40679-1, ISBN: 9783527611041.*

Stainsby et al., (2011). The Generation IV Gas-cooled Fast Reactor. *Proceedings of ICAPP 2011, Nice, France, May 2-5, 2011.*

Strydom et al., (2010). The OECD/NEA/NSC PBMR 400 MW Coupled Neutronics Thermal Hydraulics Transient Benchmark: Transient Results. *PHYSOR 2010 – Advances in Reactor Physics to Power the Nuclear Renaissance Pittsburgh,* *Pennsylvania, USA, May 9-14, 2010, on CD-ROM, American Nuclear Society, LaGrange Park, IL (2010).*

Strydom et al., (2016). Comparison of the PHISICS/RELAP5-3D Ring and Block Model Results for Phase I of the OECD/NEA MHTGR-350 Benchmark. *INL/JOU-14-33637*

Strydom, G., (2018). IAEA Coordinated Research Project on HTGR Physics, Thermal-Hydraulics, and Depletion Uncertainty Analysis, Prismatic HTGR Benchmark Specification: Phase II. *INL/EXT-18-44815 Rev.0.*

Suetomi E and Sekimoto, H (1991). Conjugate gradient like methods and their application to eigenvalue problems for neutron diffusion equations. *Annals of Nuclear Energy 18(4), pp. 205–227.*

Sugawara, T., Nishihara, K., Tsujimoto, K., (2013). Transient analyses for lead–bismuth cooled accelerator-driven system. *Annals of Nuclear Energy, vol. 55, pp. 238–247.*

Takeda, T., Kawamura, H. and Seki, M., (1987). Natural circulation in parallel vertical channels with different heat inputs. *Nucl. Engg. and Design., vol. 104, pp. 133-143 .*

Tewari et al. (2011). Development of Nb-1% Zr-0.1%C Alloy as Structural Components for CHTR. *BARC Report- BARC/2011/E/020, 2011.*

Todreas, N.E., and Ferroni, Paolo (2009). Enhancing reactor core thermal performance through inverted fuel design. *NURETH-13: Proceedings of the 13th international topical meeting on nuclear reactor thermal hydraulics, (p. 4617). Japan.*

Todreas and Kazimi (2012). Nuclear Systems: Thermal Hydraulic Fundamentals, volume1, second edition, *CRC Press, Taylor & Fracis Group, ISBN:978-1-4398-0887-0.*

Trkov, (2008). GNOMER – Multigroup 3-Dimensional Neutron Diffusion Nodal Code with Thermohydraulic Feedbacks. *Institute Jozef Stefan, Ljubljana, Slovenia, IJS- DP-6688.*

Trkov and Ravnik, (1994). CORD-2 package for PWR nuclear core design calculations. In: *Proceedings of the International Conference on Reactor Physics and Reactor Computations, Tel-Aviv, Ben-Gurion University of the Negev Press, 23–26 January.*

Van der Vorst, H. (2002) Iterative Krylov methods for large linear systems. *Cambridge Press, Cambridge.*

Vijayan et al., (2015). Conceptual design of Indian molten salt breeder reactor. *Pramana – J. Phys., Vol. 85, No. 3, pp. 539–554.*

Vijayan, P.K. , Shivakumar, V., Basu, S., Sinha, R.K. (2017). Role of thorium in the Indian nuclear power programme. *Progress in Nuclear Energy. vol.-101, pp.43-52.*

Wang et al., (2015). Comparison of transient analysis of LBE-cooled fast reactor and ADS under loss of heat sink accident. *Annals of Nuclear Energy, vol. 85, pp. 494–500*.

Wang et al., (2020). Review on neutronic/thermal-hydraulic coupling simulation methods for nuclear reactor analysis. *Annals of Nuclear Energy 137, 107165.*

Wei et al., (2018). Transient thermal-hydraulic evaluation of lead-bismuth fast reactor by coupling sub-channel and system analysis codes. *Nuc. Engg. and Desg., vol. 337, pp. 228–235.*

WNA (2020). World Nuclear Association webpage on 'World Energy Needs and Nuclear Power'. *www.world-nuclear.org/information-library/current-and-future-generation world-energy-needs-and-nuclear-power.aspx* accessed on 09 Nov-2020.

Wu et al., (2016). A tightly coupled scheme for neutronics and thermal–hydraulics using open-source software. *Annals of Nuclear Energy 87, pp. 16–22.*

Yan (2016). Very high-temperature reactor. In. *Handbook of Generation IV Nuclear Reactors Woodhead Publishing Series in Energy, pp. 55-89.*

Yan, B.H., Wang, C., Li, L.G., (2020). The technology of micro heat pipe cooled reactor: A review. Annals of Nuclear Energy, vol. 135, 106948.

Zaki, S., Sekimoto, H., (1996). Accident analysis of lead or lead-bismuth cooled small safe long-life fast reactor using metallic or nitride fuel. *Nucl. Engg. and Des., vol.162, pp. 205-222.*

Zvirin, Y., (1986). The onset of flows and instabilities in a thermosyphon with parallel loops. *Nuclear Engineering and Design, vol. 92, pp. 217-226.*